ENVIRONMENTAL ENGINEERING
ASSOCIATION OF THAILAND

THAI ENVIRONMENTAL ENGINEERING JOURNAL

Vol. 36 No. 2 May – August 2022
ISSN (PRINT) : 1686 - 2961
ISSN (ONLINE) : 2673 - 0359

Thai Environmental Engineering Journal

Thai Environmental Engineering Journal

Vol. 36 No. 2 May – August 2022

ISSN (PRINT) : 1686 - 2961
ISSN (ONLINE) : 2673 - 0359

Thai Environmental Engineering Journal Vol. 36 No. 2 (2022) : 1-8
www.eeat.or.th

Removal of Turbidity, COD and Coliform Bacteria in Duck-Pond Water by Hydroponic Water Convolvulus Gardening

Sreyneang Sim[1], Chompoonut Sinlawatpongsakul[2], Nantiwat Somngam[2], Phumin Phunumkhang[2] and Petch Pengchai[2*]

[1]LUMA System Co., Ltd. UYFC Phnom Penh headquarter in Chroy Changvar, Fine Arts Street, Sangkat Prek Leap, Khan Chroy Changvar, Phnom Penh, Cambodia, 12112
[2]Environmental Engineering Laboratory, Circular Resources and Environmental Protection Technology Research Unit (CREPT), Faculty of engineering, Mahasarakham University, Mahasarakham 44150, Thailand
[*]E-mail : petch.p@msu.ac.th

Abstract

The objective of this research is to investigate the performance of hydroponic water convolvulus gardening in the removal of turbidity, COD, and coliform bacteria from duck-pond water. The experiment was done using 2 hydroponic gardening sets in the condition of 5-day HRT and 7-day HRT separately for a 42-day operation. The results showed that removal efficiencies were 89.39 ± 7.73% for turbidity and 77.48 ± 11.25% for COD at the 5-day HRT, and were 91.79 ± 6% for turbidity and 75.01 ± 18.41% for COD for the 7-day HRT. And removal efficiencies of total coliform bacteria and E. coli were 87.0 ± 15.3% and 94.5 ± 13.6% for 5-day HRT operation, and 81.5 ± 11.7% and 99.8 ± 0.5% for 7-day HRT operation. According to t-test results at the confidence level of 95%, the system showed no difference in removal efficiencies at both HRTs. The effluent from the systems had turbidity and COD in ranges of 5.52-40.10 NTU and 4.77-81.60 mg/L, respectively which passed the quality standard of effluent from the domestic wastewater treatment. Due to the surface water quality standard, total coliform bacteria and E. coli concentrations of the effluent were in the range of 0-31.8 CFU/100ml which could be used for full-body contact. However, the water convolvulus grown in the hydroponic systems should be well washed and inspected for residual bacteria before eating due to its high level of fecal coliforms (240 to 930 MPN/g).

Keywords : Hydroponic; Water convolvulus; Turbidity; COD; Coliform Bacteria; E. coli

Introduction

It has been the age-long tradition for Thailand to raise ducks in rice-developing regions [1]. As ducks prefer water [2], raising ducks require a pond, and this often conduces duck farmers to a water pollution problem. Due to natural inputs of duck manure, duck food waste, soil, plankton, microorganisms, etc. into the pond, the pond water can become turbid with high Chemical Oxygen Demand (COD) content or even become green in a eutrophication state with high concentrations of nitrogen and phosphorus compounds [3].

Phytoremediation is one of the economical wastewater treatment methods that can feasibly remove pollution from water and soil by cultivating plants [4]. The pollutants, such as organic matter, heavy metals, and certain toxic compounds were removed from wastewater and soil that present around the plant roots through several mechanisms, i.e., phytodegradation, rhizofiltration, phyto-stimulation, phytorestoration, and phytovolatilization, [4]. Lu et al. (2008) observed that water hyacinth planted in their constructed wetland system removed 64.44% of COD, 21.78% of Total Nitrogen (TN), and 23.02% of Total Phosphorus (TP) from duck-farm wastewater [5]. Pongthornpruek (2017) succeeded in removing 61.87-75.36% of COD, 66.11-75.74% of Total Kedah Nitrogen (TKN), 95.18-96.53% of TP from swine wastewater using constructed wetland planted with vetiver grass [6]. Interestingly, water convolvulus, a fast-growing vegetable that can be grown in all regions of Thailand in all seasons with a short harvest time [7] was proven possible to grow and treat sewage at the same time [8, 9]. Fahim et al. (2017) found that water convolvulus planted in floating-bed wetland achieved high performance in the removal of TN and TP with average removal efficiencies of 75.9, and 94.3%, respectively [8]. However, there is a possible disadvantage of applying plants directly in the polluted duck pond as an in situ constructed wetland since dead leaves and roots of the floating plants can fall and accumulate in the bottom of the pond. Recently, several researchers gave a trial to use the hydroponic system, another form of phytoremediation, in wastewater treatment. Nguyen et al. (2018) reported that water convolvulus planted in a pilot-plant hydroponic system can achieve the removal of 65% Suspended Solid (SS), 74% COD, 90% ammonium, 30% nitrate, and 86% phosphate from municipal wastewater [9]. This result suggested hydroponic water convolvulus gardening as a promising method to treat polluted duck ponds as well as to grow water convolvulus for sale. However, the ability of water convolvulus in coliform bacteria removal as well as the amount of residual coliform bacteria in hydroponic water convolvulus is still unclear. Additionally, design criteria, e.g., hydraulic retention time (HRT) for the hydroponic gardening system in wastewater treatment is unidentified. To provide more information for the construction and performance of the hydroponic water convolvulus gardening system, 2 sets of hydroponic water convolvulus gardening systems were constructed in this study. Polluted duck-pond water was applied to the hydroponic systems using 2 different HRTs. The removal of coliform bacteria, turbidity, and COD, as well as the growth of cultivated water convolvulus, were monitored throughout the experiment. The harvested water convolvulus was also analyzed for residual coliform bacteria.

Materials and Methods

Construction of the hydroponic systems

The authors constructed 2 sets of hydroponic water convolvulus gardening systems. Each one system composed of 4 cultivation vessels made from a 5.08-cm diameter pipes with total length of 504 cm. Each cultivation vessel contained 6 holes with 5.5-cm diameter. Therefore, totally 24 holes per 1 set were available for the plant cultivation as shown in Figure 1.

Figure 1 Experimental apparatus

Preparation of water convolvulus

Approximately 300 water convolvulus seeds were wrapped with cloth and put in water for one night. Bad seeds which were floating in the water were then removed. Selected good seeds (1-2 seeds per sheet) were planted in small foam sheets soaked in water and put in the shade at room temperature. After 5 days the seedlings were ready to plant in the hydroponic system.

Experimental setup

Each hydroponic gardening set contained 12-L duck-pond water which was loaded into 50-L tank and circularly pumped up to the 4 cultivation pipes (100% recirculation all days and nights) before being collected and released at the end of each HRT cycle. This setting provided HRT of 5 days for the 5-d HRT hydroponic set, and 7 days for the 7-d HRT hydroponic set.

Five water convolvulus seeds were put inside sponges (2×2 cm) before placing them inside each hole of the gardening systems.

System operation

On the 1st day of each operation cycle, raw duck-pond water samples were collected and analyzed for turbidity, COD, and coliform bacteria. At the end of each operation cycle, i.e., day 5th for the 5-d HRT hydroponic set, day 7th for the 7-d HRT hydroponic set, treated duck-pond water samples were collected at the 50L-tank using grab sampling method and analyzed for turbidity, COD, and coliform bacteria. Stem length, root length, and weight of water convolvulus inside each hole were also measured on every sampling day to confirm the viability of the plants. Water convolvulus plants were harvested at the end of the experiment which was day 42nd when the 5-d HRT hydroponic set completed 8 operation cycles and the 7-d HRT hydroponic set completed 6 operation cycles. The whole surviving plants including roots, stems and leaves were collected for the residual bacteria analysis.

Analytical methods

Water samples were analyzed according to verified methods, i.e. Nephelometry [10] for turbidity analysis, Closed reflux, titrimetric method [11] for COD analysis, Compact dry EC method [12] for total coliform bacteria, and Escherichia coli (E. coli) analysis in the unit of CFU/100ml. Additionally, the Presumptive test stated in Bacteriological Analytical Manual (BAM) [13] was used for fecal coliform analysis in the unit of MPN/100ml. Wastewater treatment capability of the hydroponic gardening sets was considered from removal efficiencies calculated by equation (1) where C_0 is pollutant concentration (turbidity, COD, total coliform bacteria, E. coli) in raw duck-pond water and C is pollutant concentration in treated duck-pond water. Paired two-sample Student's t-Test with one-side 95% confidence interval was used for removal- capability comparison between the 7-d- HRT hydroponic set and the 5-d HRT hydroponic set.

$$\% \text{ removal} = (C_0\text{-}C)\times 100/C_0 \qquad (1)$$

Results and Discussions

Turbidity removal efficiencies

The result revealed that both hydroponic gardening sets can treat raw duck-pond water. For a 5-d HRT hydroponic set, turbidity values of 121.30-395.00 NTU in raw duck-pond water reduced to 10.28-40.10 NTU at the end of the operation cycles as shown in Figure 2. Turbidity removal efficiencies ranged from 70.94 to 94.94% with the mean ± standard deviation of 89.39 ± 7.73%.

In the case of the 7-d HRT hydroponic set, turbidity values of 94.70-424.00 NTU in raw duck-pond water were reduced to 5.52-24.8 NTU at the end of the operation cycles as shown in Figure 3. Turbidity removal efficiencies ranged from 80.64 to 96.86% with the mean ± standard deviation of 91.79 ± 6.00%. According to the t-test result, turbidity removal efficiencies of the 2 hydroponic sets were not significantly different (P-value = 0.109).

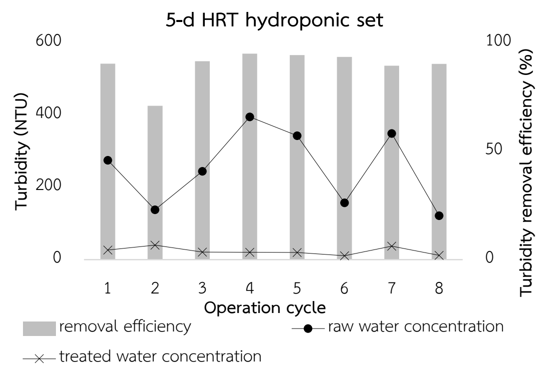

Figure 2 Turbidity concentrations and removal efficiencies of 5-d HRT hydroponic set

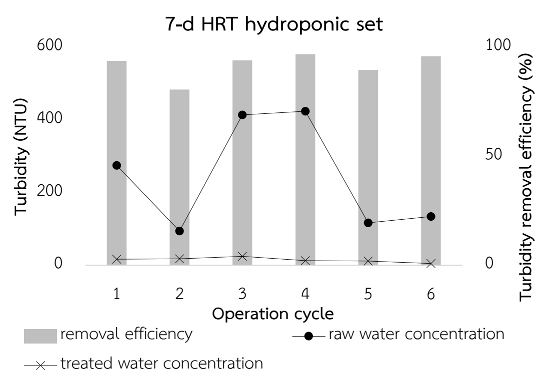

Figure 3 Turbidity concentrations and removal efficiencies of 7-d HRT hydroponic set

Turbidity removal in this study probably occurred due to the clinging of colloidal and suspended solids onto the water convolvulus root. Sedimentation [9] at the bottom of the hydroponic pipes, and biodegradation [9] of the bacteria living on the surface of water convolvulus root were also possible.

COD removal efficiencies

For COD treatment, the 5-d HRT hydroponic set was able to reduce COD concentrations from 85.88-159.12 mg/L to 4.77-50.22 mg/L as shown in Figure 4 with COD removal efficiencies ranging from 64.51 to 97.00% while the 7-d HRT hydroponic set was able to reduce COD concentrations from 112.00-190.08 mg/L to 9.08-81.60 mg/L with COD removal efficiencies ranged from 40.51 to 95.22% (77.48 ± 11.25%) as shown in Figure 5.

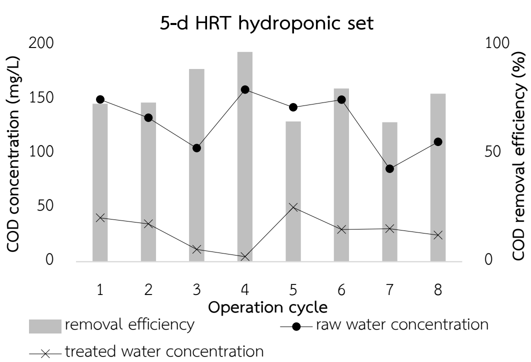

Figure 4 COD concentrations and removal efficiencies of 5-d HRT hydroponic set

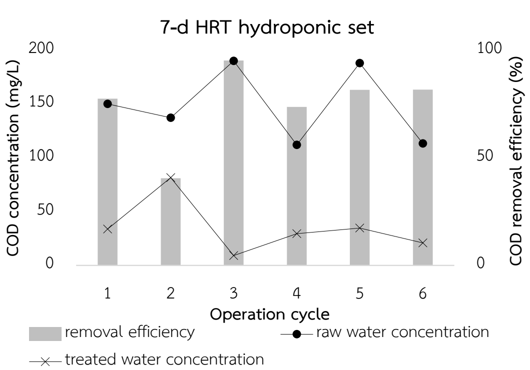

Figure 5 COD concentrations and removal efficiencies of 7-d HRT hydroponic set

The main COD removal mechanism in this study should be the organic-matter degradation caused by microbes living on the surface of water convolvulus root as suggested by Nguyen et al. (2018) [9]. Comparing mean COD removal efficiencies of the 5-d HRT hydroponic set (77.48 ± 11.25%) with the 7-d HRT hydroponic set (75.01 ± 18.41%) based on the t-test result (P-value = 0.342), there was no significant difference between both sets.

Bacteria removal efficiencies

As shown in Figure 6-9, both hydroponic gardening sets were able to reduce total coliforms bacteria and E. coli.

For total coliforms bacteria (Figure 6-7), the concentrations of 127-709 CFU/100ml were reduced to 0-75.23 CFU/100ml with removal efficiencies between 55.49 and 100% (87.0 ± 15.3%) for the 5-d HRT hydroponic set.

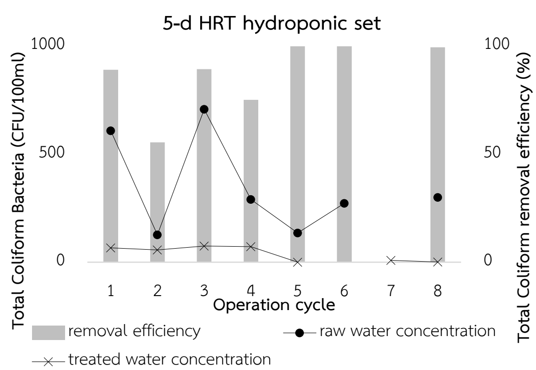

Figure 6 Total coliforms bacteria concentrations and removal efficiencies of 5-d HRT hydroponic set

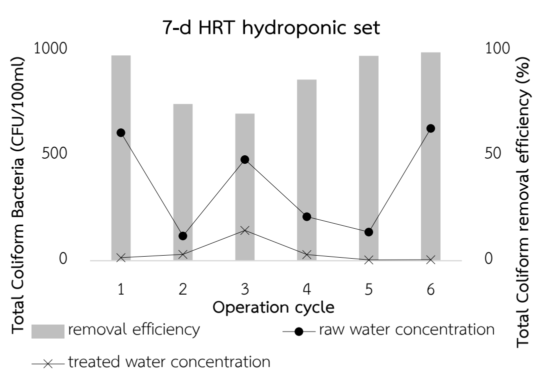

Figure 7 Total coliforms bacteria concentrations and removal efficiencies of 7-d HRT hydroponic set

In the 7-d HRT hydroponic set, total coliforms bacteria of 118-630 CFU/100ml were reduced to 3.33-144.71 CFU/100ml with removal efficiencies ranging from 69.98 to 99.21% (81.5 ± 11.7%). The t-test results showed no significant difference in total coliform removal efficiencies between both hydroponic sets (P-value = 0.321).

For E. coli reduction, concentration values of E. coli in untreated water were in ranges of 64-713 CFU/100ml (Figure 8) and 73-499 CFU/100ml (Figure 9) which were reduced to 0-31.8 CFU/100ml and 0-5.11 CFU/100ml by 5-d HRT hydroponic set and 7-d HRT hydroponic set, respectively. E. coli removal efficiencies, in this case, ranged from 61.22-100% (94.5 ± 13.6%) for the 5-d HRT hydroponic set and 98.66-100% (99.8 ± 0.5%) for the 7-d HRT hydroponic set. However, the t-test results (P-value = 0.196) indicated no significant difference between both sets.

The decline of bacteria after being treated by the hydroponic systems could occur due to natural UV radiation during the experiment, attachment or adherence of bacteria such as E. coli on roots of the plants or biofilms formed on the plant material [14], antimicrobial compounds produced by roots of aquatic plants which reduce the survival of pathogens [14], oxygen supplied through roots of aquatic plants which is crucial for the activity and metabolism of microorganisms such as bacteria, and viruses [14].

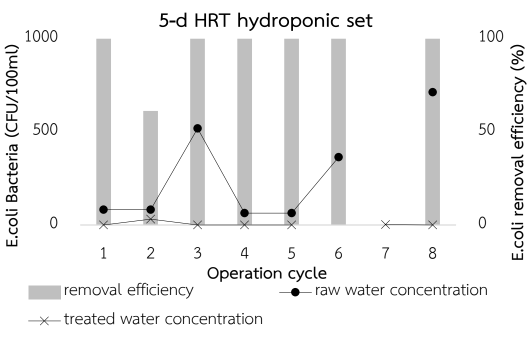

Figure 8 E. coli concentrations and removal efficiencies of 5-d HRT hydroponic set

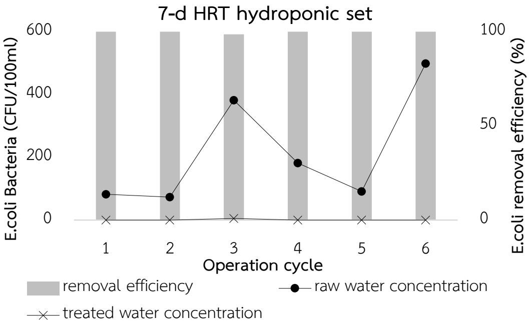

Figure 9 E. coli concentrations and removal efficiencies of 7-d HRT hydroponic set

Since mean concentrations of E. coli in treated water of both hydroponic sets were 4.8 ± 11.0 CFU/100ml and 0.85 ± 1.9 CFU/100ml which were less than 126 CFU/100ml, the suitable level for full-body contact defined in Bacterial Water Quality Standards for Recreational Waters of USEPA (EPA-823-R-03-008) stated in the work of Sanders et al. (2013) [15], the hydroponic systems could be one of the possible methods for water reclamation.

On the last day of the operation, fecal coliforms were detected in the treated water samples, i.e., 13 MPN/100ml for the 5-d HRT hydroponic set and 17 MPN/100ml for the 7-d HRT hydroponic set. Based on these fecal coliform concentrations and Thailand surface water quality standards [16], the treated water can be classified as a category 2 water resource that was allowed to be used for fisheries and water sports.

It was noted that the standard deviations of removal efficiencies derived in this study varied between 0.5% and 15% in spite of the large fluctuation of raw water quality. This result implied stability of the hydroponic sets for wastewater treatment.

Plant growth

Plant growth (Figure 10-12) was monitored through three parameters including plant height, root length, and plant weight. As shown in Figure 10-11, the growth of water convolvulus mostly increased due to the operation time in both hydroponic sets.

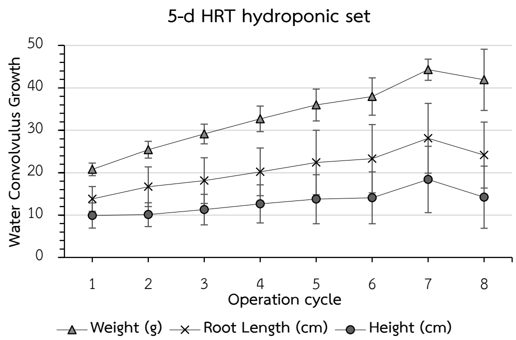

Figure 10 Water convolvulus growth at 5-d HRT hydroponic set

In the case of a 5-d HRT hydroponic set, average plant heights ranged from 3.92 to 9.95 cm; mean values of plant roots length ranged from 9.91 to 18.40 cm, and plant weights ranged between 6.95 and 17.94 g. The decrease of plant growth from the 7th to 8th operation cycle occurred due to the rot on plants. For the 7-d HRT hydroponic set, the mean values of plant heights were 10.75-19.95 cm, average root lengths were 9.88-17.93 cm and plant weights were 6.95-17.74 g.

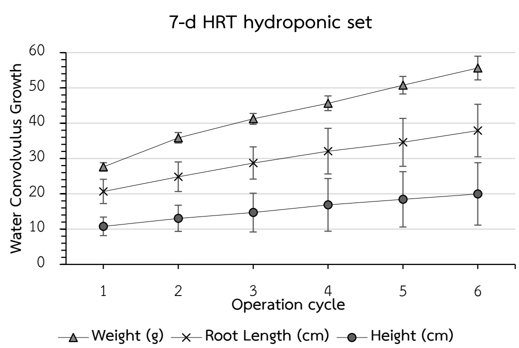

Figure 11 Water convolvulus growth at 7-d HRT hydroponic set

Figure 12 water convolvulus plants during the operation

According to the t-test result, the mass of water convolvulus grown in the 7-d HRT hydroponic set was significantly greater than that of the 5-d hydroponic set (P-value = 0.0224).

Residual coliform bacteria in water convolvulus

Total coliform bacteria, which all were fecal coliforms, were detected in water convolvulus plants grown in the hydroponic sets. With the fecal coliforms of 240 MPN/g for the 5-day HRT set, and 930 MPN/g for the 7-day HRT set exceeded the recommended levels by WHO and International Commission on Microbiological Specifications for Food (ICMSF) standards (10-100 coliforms/g, 10 fecal coliforms/g) [17], the harvested water convolvulus plants were considered not ready to eat. Well-washing followed by the inspection of residual bacteria is required for good hygiene before cooking or sending the vegetable for sale.

Conclusion

By circulating duck-pond water in hydroponic water convolvulus gardening sets at hydraulic retention time (HRT) of 5 and 7 days, turbidity, COD, and coliform bacteria in the water were removed. The removal efficiencies were 89.39 ± 7.73% for turbidity, 77.48 ± 11.25% for COD, 87.0 ± 15.3% for total coliform bacteria, and 94.5 ± 13.6% for E. coli at the 5-day HRT operation. In terms of 7-day HRT operation, the efficiencies were relatively high, i.e. 91.79 ± 6% for turbidity, 75.01 ± 18.41% for COD, 81.5 ± 11.7% for total coliform bacteria 69.98-99.21%, and 99.8 ± 0.5% for E. coli. However, no significant difference between removal efficiencies of 7-day HRT operation and 5-day HRT operation was approved by statistical analysis. The effluent quality of both hydroponic systems showed 5.52-40.10 NTU turbidity and 4.77-81.60 mg/L COD which passed the quality standard of effluent from the domestic wastewater treatment. In the viewpoint of bacterial contamination, the effluent from the 2 systems with E. coli of 0-31.8 CFU/100ml satisfied the water quality standard for full-body contact. However, the water convolvulus plant grown in the hydroponic systems were not ready to eat due to their high level of fecal coliforms (240 to 930 MPN/g) which exceeded the acceptable level (10 MPN/g). Based on these findings, hydroponic gardening at a 5-day or 7-day hydraulic retention time is not only the method for growing vegetables, such as water convolvulus plants but also the cost-effective method for wastewater treatment which duck farmers can easily install and operate in their farms. For pilot-scale operation, the farmers can install a long-pipe hydroponic system near or surrounding their duck ponds. The duck-pond water should be directly pumped up and continuously feed to the hydroponic system using a low flow-rate water pump to arrange the sufficient HRT. The effluent of the system can be directly discharged to the duck pond. Better water quality of the duck pond could be expected during a long operation period. However, the aspect of bacterial contamination in harvested vegetables is still left for further improvement.

Acknowledgment

We extend our sincere thanks to all those who provide us the possibility to complete this research. We appreciated Mr. Khajornsak Saeteng for devoting his farm area, pond water, and electricity to support our experiments. In the last, we would like to thank Mahasarakham University for supporting this research study.

References

[1] Chankaew, P. 2021. Unleash the ducks! Thai drought worries threaten farming tradition," Reuters, 2020 Accessed: Apr. 18, 2021 [Online]. Available: https://www.reuters.com/article/thailand-ducks/unleash-the-ducks-thai-drought-worries-threaten-farming-tradition-idINKBN26610S.

[2] Waitt, C., Jones, T. and M. Dawkins. 2009. Behaviour, synchrony and welfare of Pekin ducks in relation to water use. Applied Animal Behaviour Science. 121(3): 184-189.

[3] Soliman, K.A., El-Horbeety, A.A.A., Essa, M.A.R., Kosba, A.M. and Kariony, A.I. 2000. Effects of introducing ducks into fish ponds on water quality, natural productivity and fish production together with the economic evaluation of the integrated and non-integrated systems. Aquaculture International. 8(4): 315-326.

[4] Sri Lakshmi, K., Hema Sailaja, V. and Anji Reddy, M. 2017. Phytoremediation - A Promising Technique in Waste Water Treatment. International Journal of Scientific Research and Management (IJSRM). 5(6): 5480-5489.

[5] Lu, J., Fu, Z. and Yin, Z. 2008. Performance of a water hyacinth (Eichhornia crassipes) system in the treatment of wastewater from a duck farm and the effects of using water hyacinth as duck feed. Journal of Environmental Sciences. 20(5): 513-519.

[6] Pongthornpruek, S. 2017. Swine Farm Wastewater Treatment by Constructed Wetland Planted with Vetiver Grass. Environment and Natural Resources Journal. 15(2): 13-20.

[7] Thailand Regional Environmental Office 5. 2021. The water convolvulus management manual. Accessed: Nov. 26, 2021 [Online]. Available: http://lib.mnre.go.th/book/paktob.pdf.

[8] Fahim, R., Lu, X., Jilani, G., Hussain, J. and Hussain, I. 2019. Comparison of floating-bed wetland and gravel filter amended with limestone and sawdust for sewage treatment. Environmental Science and Pollution Research. 26(20): 20400-20410.

[9] Nguyen, T.V.D., Huynh, H.N.T., Nguyen, M.N.H. and Ngo, T.V. 2018. The use of water spinach (Ipomoea aquatica) in domestic wastewater treatment. The Journal of Agriculture and Development. 17(3): 49-54.

[10] U.S. Environmental Protection Agency (EPA). 1993. Method 180.1 Determination of Turbidity by Nephelometry. Accessed: Nov. 26, 2021 [Online]. Available: https://www.epa.gov/sites/default/files/2015-08/documents/method_180-1_1993.pdf.

[11] U.S. Environmental Protection Agency (EPA). 1978. Method 410.3: Chemical Oxygen Demand (Titrimetric, High Level for Saline Waters) by Titration). Accessed:

Nov. 26, 2021 [Online]. Available: https://www.epa.gov/sites/default/files/2015-08/documents/method_410-3_1978.pdf.

[12] Mizuochi, S., Nelson, M., Baylis, C., Jewell, K., Green, B., Limbum, R., Fernandez, M.C., Salfinger, Y. and Chen, Y. 2016. Matrix Extension Study: Validation of the Compact Dry EC Method for Enumeration of Escherichia coli and non-E. coli Coliform Bacteria in Selected Foods. Journal of AOAC International. 99(2): 451-450.

[13] Food and Drug Administration (FDA). 2020. Chapter 4: Enumeration of Escherichia coli and the Coliform Bacteria. Bacteriological Analytical Manual (BAM), October 2020. Accessed: Nov. 26, 2021 [Online]. Available: https://www.fda.gov/food/laboratory-methods-food/bam-chapter-4-enumeration-escherichia-coli-and-coliform-bacteria.

[14] Dhir, B. 2020. Effective control of waterborne pathogens by aquatic plants. Waterborne Pathogens. 2020: 339-361. Accessed: June. 5, 2022 [Online]. Available: https://www.ncbi.nlm.nih.gov/pmc/articles/PMC7173607/pdf/main.pdf.

[15] Sanders, E.C. and Yuan, Y. 2013. Fecal Coliform and E. coli Concentrations in Effluent-Dominated Streams of the Upper Santa Cruz Watershed. Water 2013. 5(1): 243-261.

[16] Thai Government. 1994. Notification of Thailand National Environmental Board, No. 8, B.E. 2537 (1994). Royal Thai Government Gazette. 111 Part 16: B.E. 2537.

[17] Benti, G., Kebede, A. and Menkir, S. 2014. Assessment of bacteriological contaminants of some vegetables irrigated with Awash River water in selected farms around Adama town, Ethiopia. Journal of Microbiology and Antimicrobials. 6(2): 37-42.

Thai Environmental Engineering Journal Vol. 36 No. 2 (2022) : 9-23
www.eeat.or.th

Design Strategies to Lead Thailand's Building Sector toward Net-Zero Greenhouse Gas Emissions: A Review

Rataphong Rahong and Trakarn Prapaspongsa*

Graduate Program in Environmental and Water Resources Engineering,
Department of Civil and Environmental Engineering, Faculty of Engineering,
Mahidol University, Nakhon Pathom 73170, Thailand
*E-mail : trakarn.pra@mahidol.ac.th

Abstract

The building sector is one of the intensive greenhouse gas (GHG) emitters in Thailand. Furthermore, Thailand also aims to reach net-zero GHG emissions by 2065. This study therefore aims to evaluate whether the current design strategies are adequate to lead the building sector to net-zero emissions. The study initially finds that the embodied and operational phases have equal chances of becoming hotspot of buildings as the emissions from each phase can be influenced by choice of material, choice of energy-saving retrofits, and electricity grid profiles. Since either phase could become the hotspot of buildings, this study reviews two international and national green-building guidelines each to identify the design strategies used for buildings' GHG mitigation. The review highlights five main strategies: to substitute low-carbon materials for carbon-intensive materials, to improve structural performances of carbon-intensive materials, to increase the circularity of buildings; as well as, to use passive and active energy-saving retrofits. Afterward, the efficiencies and limitations of the aforesaid strategies are assessed through 46 Life Cycle Assessment (LCA) studies and relevant documents such as reports by Thailand's government, building code, etc. The assessment indicates that, in theory, the aforesaid strategies show great potential on leading Thailand's building sector to net-zero GHG emissions, given a condition that all buildings use renewable energy-based on-site electricity generators on a large scale. However, in reality, there are various limitations preventing this ideal situation to arise. Thus, this study posts five possible research improvements and a hands-on management strategy as a means to provide practical benefits and push forward Thailand's building sector toward the net-zero GHG emissions goal ultimately.

Keywords : building sector; design strategies; net-zero; greenhouse gas; review

Introduction

From a life cycle perspective, buildings emit GHG during their operational and embodied phases. The former is the period when buildings are used. Meanwhile, the latter is the period before and after buildings are used. The latter includes raw-material extraction, material production, transportation, construction, maintenance, demolition, and waste management. In 2021, Thailand's building sector consumed about 97,265 GWh of electricity through their operations such as cooling, lighting, etc. [1]. This caused the sector to release about 42 million tons of GHG, representing 17% of the nation's total GHG emissions [1]. Furthermore, the sector also emits GHG during their embodied phase [2]. Nonetheless, the embodied GHG were normally included within the transportation and industrial sectors [2], making them account for 71.5 and 70.6 million tonnes of GHG in the year 2021 respectively [1]. However, if one were to extract the embodied emissions hidden within the aforesaid two sectors and sum them with the operational emissions, one would thus safely find that the GHG emissions contributed by Thailand's building sector may well be around 49 million tonnes, representing 20% the nation's total GHG emissions. In response to the GHG level, Thailand's Ministry of Energy (MOE) has established Energy Efficient Plans [3, 4] as a means to make all economy sectors less energy intensive. For the building sector, this plan specifically suggests designers to apply design strategies advised by international and national standards while designing buildings. Given that this plan is well executed, the MOE has projected that the building sector will contribute to about 9,718 ktoe of energy saving [3, 4]. This saving will then contribute to the nation's total energy reduction of 49,064 ktoe; and thus, leading Thailand to achieve 20-25% GHG emission reduction by 2030 [3-5]. Despite the projected achievement of the 2030 goal, the MOE has forecasted that the country's final energy consumption will reach 126,867 ktoe by 2037, with the building sector being one of the main energy consumers [4]. This issue thus raises an academic and a practical concern of whether the building sector can and will achieve net-zero GHG emission by 2065 as planned in [6]. Following this concern, this study has established three-fold goals: (1) to indicate buildings' hot-spots and their factors, (2) to identify design strategies and their efficiencies to mitigate the GHG emissions, (3) to evaluate the adequacies of the design strategies on leading Thailand's building sector to become a net-zero GHG emission sector; and highlighting future research needs and suggestions.

Methodology

As buildings are intensive GHG emitters throughout their lifetime, this study thereby chose to review LCA-related studies which allowed the authors to analyze the environmental performances of buildings holistically [7, 8]. This study firstly conducted an online search through Scopus database for LCA studies of buildings with alterations of electricity grid supplies and energy-saving retrofits. The time restriction for the publication was between 2015 and 2022, while the language was limited to English. The keywords were LCA, buildings, different locations and different electricity grid mixes. The journal studies that holistically assessed buildings with both alterations of electricity supplies and energy-saving retrofits were included. On the contrary, the journal studies (1) that assessed buildings with only one of the aforesaid alterations, and (2) that assessed buildings either at embodied or at operational phase were excluded. Through the search method shown in Figure 1, 13 journal studies were selected to assess building hotspots when electricity grids and retrofits are altered. Secondly, this study reviewed Thailand's long-term plans [3, 4, 9, 10] in order to identify the international and national standards for building designs. Through the review, four guidelines [11-14] were identified. Further review was then conducted on [11-14] to identify design strategies for GHG mitigation. Afterward, five design strategies were identified: to substitute low-carbon materials for carbon-intensive materials, to improve structural performance of carbon-intensive materials, to increase the circularity of buildings, and to use passive and active measures. Thirdly, this study searched through Scopus database under the previously mentioned restrictions for LCA studies of buildings that apply the aforesaid design strategies. The keywords searched included LCA, buildings, concrete, steel, timber, hollow, lightweight, high-strength, design for disassembly, orientation, vegetation, envelope, bioclimatic, ventilation, solar-cell, air condition and heating. Through the search for studies related to materials, journal studies that performed LCA on alternative and conventional materials in term of structural materials were included. Contrariwise, the journal studies (1) that performed LCA analysis on alternative materials in term of non-structural materials, (2) that performed LCA analysis on buildings equipped with dissimilar retrofits, and (3) that performed LCA analysis on floor elements without considering their supporting elements were excluded. Likewise, through the search for studies related to energy-saving retrofits, journal studies which performed LCA analysis on buildings that are equipped with both passive and active measures were included. Whereas the journal studies which performed LCA on buildings that are equipped with only one of the aforesaid measures were excluded. Fourthly, this study collected journal studies which performed LCA on buildings in Thailand. Through the search method shown in Figure 1, 46 studies were collected. This study lastly collected relevant documents [15-18] to evaluate the adequacies of the design strategies on leading Thailand's building sector to net-zero GHG emissions goal and to highlight potential research improvements.

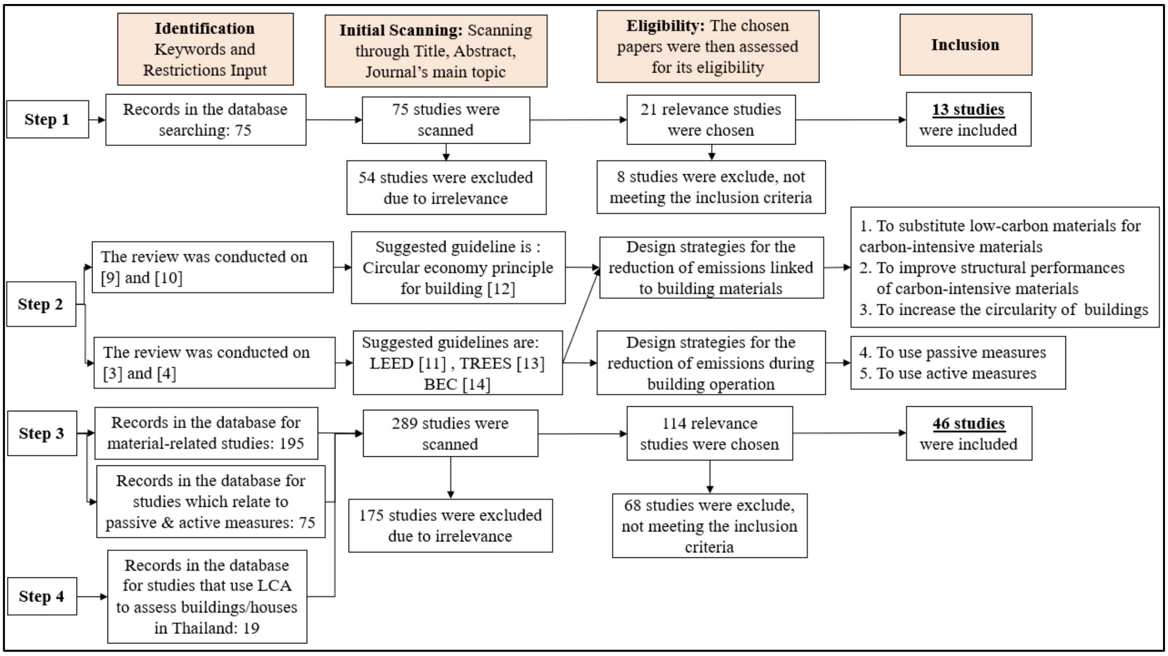

Figure 1 The schematic diagram on reference searching (from step 1 to 4)

Results and Discussion

Hotspots for building and their influencing factors

The embodied and operational phases have equal chances of becoming the hotspot of buildings as the emissions in each phase are linked to design-related and policy-related factors. The former is the choice of energy-saving materials and devices, so called retrofits. The latter is the profile of electricity grid [19-31]. Generally, when a building is supplied by fossil-fuel based grid and is not equipped with any retrofits, the operational emissions (OEs) will accumulate and overtime surpass the embodied emissions (EEs). Thus, the operational phase becomes the hotspot of buildings [7, 8, 19-31]. However, Table 1 shows that the replacement of fossil fuels by renewable energies in grid profile can reduce the amount of carbon emitted per kWh electricity generated. This thereby results in reduction of the OEs and total life cycle emissions (TLEs). Likewise, Table 2 illustrates that the use of retrofits can make buildings less energy intensive. This in turn reduces the OEs and TLEs, despite the additional EEs associated with the retrofits. Nonetheless, success in reducing the OEs leads to the embodied phase becoming significant, and in some cases become the hotspot of buildings. This issue is shown in Table 1 and 2, where the share of EEs-to-TLEs increases when the OEs are cut. For Thailand, the 2021 national grid profile comprised of 55% natural gas, 18% coal & lignite, 14% imported electricity, 12% renewable energy, and 0.4% oil [1]. This profile caused the grid to emit about 0.442 kg of carbon per kWh electricity generated. Nonetheless, by 2037, Thailand's Ministry of Energy aims to reduce the carbon emitted per electricity generated to 0.271 kg via reduction of fossil fuels to 11% and increasing the renewable energy up to 30%, whereas the natural gas will remain about the same [17]. This suggests that Thailand's grid is moving toward a more sustainable composition; and thus, the importance of the embodied and operational phases will incline and decline simultaneously and respectively [28-31]. With this regard, it is advisable for designers to not only consider the OEs, but also the EEs whilst designing buildings. This is because the retrofits will become less effective as the grid is decarbonized; thus, an excessive use of the retrofits can intensify the EEs and can potentially increase the TLEs [23, 29, 31]. For example, Table 3 shows that in a lesser sustainable grid, the use of PV and heat-pump reduces the OEs by 85%; and reduces the TLEs by almost half. Meanwhile, the same devices provide 86% reduction for the OEs in a more sustainable grid, but they only provide 23% reduction for the TLEs. This example demonstrates that the embodied phase plays an important role in a decarbonized grid and without consideration of both the OEs and EEs while designing buildings, one could potentially end up using retrofits such that the add-on EEs are larger than the reduced OEs resulting in larger TLEs for the buildings. It is thereby necessary for designers especially in Thailand where the grid is being decarbonized [17], to consider the EEs and OEs during the design stage. Doing so will improve the designers' decisions on the choice of retrofit, ultimately helping the designers to obtain truly GHG-less building.

Table 1 Influence of grid-profile variation on EEs, OEs, and TLEs

Reference	Country	Type & Area (m^2)	System Boundary	Use phase (years)	Electricity Grid Supply	EEs ($kgCO_2$ eq/m^2)	OEs ($kgCO_2$ eq/m^2)	TLEs ($kgCO_2$ eq/m^2)	% of EEs to TLEs
[20]	New Zealand	Office 5,841	Cradle-to-Grave	50	FF 34% , RE 66%	1,000	37,500	38,500	2.6%
					FF 26% , RE 74%	1,000	35,000	36,000	2.8%
					FF 19% , RE 81%	1,000	27,500	28,500	3.5%
[21]	Northern Ireland	Resident 187.1	Cradle-to-Grave	60	FF 59% , RE 41%	354	2,077	2,431	15%
					FF 40% , RE 60%	354	1,628	1,982	18%
					FF 30% , RE 70%	354	1,571	1,925	18.4%
					FF 20% , RE 80%	354	1,540	1,894	19%
[22]	Singapore	Office 420	Cradle-to-Grave	20	NG 77% , PP 20%	51	1,155	1205	4.2%
					NG 84% , PP 13%	51	1,046	1097	4.6%
					NG 95% , PP 1%	51	913	964	5.3%

Note. This table represents buildings subjected to the variations of electricity grid mix under a fixed retrofit scenario (the least retrofit). Abbreviations are Cradle: raw-material extraction, Grave: Disposal, FF: Fossil Fuel, RE: Renewable Energy, PP: Petroleum Products, NG: Natural Gas (more environmentally friendly compared to PP), EEs: Embodied Emissions, OEs: Operational Emissions, TLEs: Total Life Cycle Emissions

Table 2 Influence of energy-saving retrofits variation on EEs, OEs, and TLEs

Reference	Country / Type of Building /Areas	Use Phase (years)/ System Boundary	Grid Supply	Retrofit Scenarios	EEs ($kgCO_2$ eq/m^2)	OEs ($kgCO_2$ eq/m^2)	TLEs ($kgCO_2$ eq/m^2)	% of EEs to TLEs
[20]	New Zealand Office , 5841 m^2	50 Cradle-to-Grave	FF 34% , RE 66%	S:1 Baseline	1,000	37,500	38,500	3%
				S2: improved Enve, HVAC	7,000	15,500	22,500	31%
[21]	Northern Ireland Resident 187.1 m^2	60 Cradle-to-Grave	FF 59% RE 41%	S1: Baseline	354	2,077	2,431	15%
				S2: floor insulation, PV	430	1,750	2,180	20%
				S3: improve Enve, HVAC	351	1,362	1,713	21%
				S4: improve Enve, HVAC, DHW	366	1,017	1,383	26%
[22]	Singapore Office , 420 m^2	20 Cradle-to-Grave	NG 77% , PP 20%	S1: Baseline	51	1,155	1,205	4.2%
				S2: improve HVAC	53	757	811	6.6%

Note: This table represents buildings subjected to the variations of energy-saving retrofits under a fixed electricity-grid scenario (the most fossil fuels). Abbreviations are Cradle: raw-material extraction, Grave: Disposal, FF: Fossil Fuel, RE: Renewable Energy, PP: Petroleum Products, NG: Natural Gas (more environmentally friendly compared to PP), Enve: Building Envelope, HVAC: Heating /Ventilation / Air-Condition, DHW: Domestic Hot Water, PV: photovoltaic (solar-cell) panels, EEs: Embodied Emissions, OEs: Operational emissions, TLEs: Total Life cycle Emissions

Table 3 Influence of grid-profile and energy-saving variation on EEs, OEs, and TLEs

Reference	Country / Type of Building /Areas	Use Phase (years)/ System Boundary	Grid Supply	Retrofit Scenarios	EEs ($kgCO_2$ eq/m^2)	OEs ($kgCO_2$ eq/m^2)	TLEs ($kgCO_2$ eq/m^2)	Different in TLEs
[23]	Spain Office , 2782 m^2	50 Cradle-to-Grave	FF 61% RE 39%	S1: Baseline (improve Enve)	220	780	1,000	-
				S2: Baseline , improve HVAC, PV	440	110	550	45%
			FF 26% RE 74%	S1: Baseline (improve Enve)	220	430	650	-
				S2: Baseline , improve HVAC, PV	440	60	500	23%

Note. This table represents buildings subjected to the variations of energy-saving retrofits and electricity-grid mix. Abbreviations are Cradle: raw-material extraction, Grave: Disposal, FF: Fossil Fuel, RE: Renewable Energy , Enve: Building Envelope, HVAC: Heating / Ventilation / Air-Condition, PV: photovoltaic (solar-cell) panels, EEs: Embodied Emissions, OEs: Operational emissions, TLEs: Total Life cycle Emissions

Design strategies and their effectiveness to mitigate the life cycle GHG emissions

1. Substitution of carbon-intensive materials with low-carbon materials

Substitution of carbon-intensive materials with low-carbon materials is a strategy advised by [11]. According to Table 4, the substitution of concrete and steel with timber helps to mitigate the EEs of buildings. This mitigation occurs because timber is a natural resource which can be regarded either as low-carbon materials [32-34], carbon-neutral materials [32, 35-39], or carbon-storage materials [40]. Moreover, timber residues and wastes from the production and End-Of-Life (EOL) stages can also be employed in energy generation instead of fossil fuels. This ultimately results in further drop of EEs in buildings [34, 36, 38, 41, 47]. Besides timber, Table 4 shows that composite and innovative materials could be substituted for concrete and steel. This approach yields reduction in EEs

Table 4 Substitution of carbon-intensive materials with timber, composite, and novel materials

Reference	Country	type	Area (m^2)	Cast Studies	System Boundary	EE	Difference in EEs
[32]	USA	Parking Garage	13,300	Steel (0% recycle)	Cradle-to-Gate	107	-
			13,300	Steel (93% recycle)		41	-62%
			12,300	PC (0%SCM)		80	-25%
			12,300	PC (50%SCM)		52	-51%
			19,900	Timber (CN)		37	-65%
			19,900	Timber (LC)		67	-47%
[33]	UK	Residential	2,250	Steel Frame	Cradle-to-Grave	486	-
				Concrete Frame		420	-14%
				Timber (LC)		178	-63%
[34]	Australia	Residential	603	Concrete (concrete landfill, steel recycle)	Cradle-to-Grave	312	-
				Steel (recycle)		237	-24%
				Mature Hardwood (LC, energy recovery)		80	-74%
[35]	EU, China, North America, Australia	Resident, Office, Commercials, Parking Lots	1,140 - 29,100	RC	Cradle-to-Gate	average difference of 216	
				Timber (CN)			
[36]	UK	Not Specified	Not Specified	Steel (recycle)	Cradle-to-Grave	228	-
				RC (landfill & recycle steel bar)		185	-19%
				Timber (CN / landfill)		119	-48%
[37]	Portugal	House	56	Concrete	Cradle-to-Gate	7143	-
				Steel		5714	-20%
				Timber (CN)		4464	-38%
[38]	U.S	Office	10,702	Concrete building	Cradle-to-Site	450	-
				Hybrid CLT with fireproofing (CN)		333	-26%
[39]	Switzerland	Residential	1,100	Concrete Hollow Block	Cradle-to-Site	160	-
				Bamboo (CN)		80	-50%
[40]	China	Nursing Home	4,297	Concrete Frame	Cradle-to-Grave	360	-
				Timber Frame (CS)		215	-40%
[41]	Thailand	Residential	112	Steel Modular (recycle where possible)	Cradle-to-Grave	641	-
				Timber Modular (recycle where possible)		381	-41%
[42]	Australia	Commercial	50,000	Concrete Slab	Cradle-to-Grave	29.4	-
				Concrete with SCMs slab		25	-15%
				Timber-Concrete slab		29	-1%
				Steel-Concrete slab		37	+26%
[43]	China	residential	357	RC Frame	Cradle-to-Grave	535	-
				Steel-Bamboo composite Frame		482	-10%
[44]	Malaysia	residential	119	block system	Cradle-to-Grave	273	-
				precast system		102	-63%
				steel system		203	-26%
				timber system		17	-94%
				Glued laminated timber & steel supports		53	-81%
				laminated veneer lumber & steel supports		49	-82%
[45]	China	residential	3,248	Bricks Structure	Cradle-to-Grave	628	-
				RC block masonry structure		506	-19%
[46]	Potugal	residential	N.S.	Brick	Cradle-to-Gate	29	-
				Glass fiber - insulation - glass fiber		11.65	-60%

Note. This table extracts only embodied emissions. Also, if there are multiple scenarios representing timber buildings with the same assumption, this table only considers the scenario with the largest EEs (the worst performance by timber). The abbreviations are: Cradle: raw-material extraction, Gate: manufacturing process, Site: construction activities, Grave: disposal, CN: Carbon Neutral materials, LC: Low Carbon emitted materials, CS: Carbon Storage Materials, RC: Reinforce Concrete, PC: Precast Concrete, SCM: Supplementary Cement Materials, EEs: Embodied Emissions (kgCO_2 eq/m^2). The negative and positive signs represent the reduction and increase in EEs relative to the baseline case respectively.

because it allows designers to not only develop composite materials by combining traditional carbon-intensive materials with traditional low-carbon materials [38, 42-46], but also to develop greener solutions from novel materials [46]. Apart from substituting alternative materials for concrete and steel, another approach that can reduce the EEs embedded within concrete and steel is to use low-carbon ingredients in their productions. To produce concrete, various industrial byproducts, so called Supplementary Cement Materials (SCMs) can be used to reduce the cement content required in concrete mixes [48-52]. Likewise, steel scraps could be employed as a raw material for the production of steel. Doing so will avoid the need for virgin materials and their associated processes; hence, a corresponded reduction in embodied energy and emissions [32]. Despite the aforesaid benefits, designers are tasked to assure that the proposed solutions are structurally viable [11] and the TLEs of the proposed solutions are lower than the TLEs of the baseline solution [11, 42]. The former can be assured through ASTM test or equivalent [11]. Meanwhile, the latter can be assured through LCA tool [11]; the assessment which tasks designers to consider the OEs and TLEs of the buildings. For example, [42] shows that although the concrete-steel composite slab provides highest EEs among all solutions, this solution offers the least heat transfer through the slab during building's operation. This thereby yields a substantially low OEs which later-on leads the solution to provide a lower TLEs compared to baseline (concrete) slab.

2. Improvement of materials' structural performances

Improvement of materials' structural performances is suggested to lessen the need of materials required in buildings, whilst ensuring that buildings still perform at the same level of structural service [11, 12]. Doing so will subsequentially dematerialize the buildings; thus, reducing the needs for natural and carbon-intensive resources and preventing wastes associated with buildings' lifecycle [11, 12]. This results in a drop of the EEs ultimately. According to Table 5, this strategy could be executed by three main techniques. The first is to develop and use lightweight materials such as hollow floor. The advantageous characteristic of these materials is its lightness, as it allows designer to downsize the dimensions of the corresponded support elements; hence, a drop in the EEs [53-55]. The second is to develop and use high-strength materials such as high-strength concrete, and concrete reinforced with carbon fiber reinforced polymer. Although high-strength materials are more carbon intensive during their production compared to normal-strength materials, the durability associated with the high-strength materials allows designers to cutdown materials required in building designs to an extent that the carbon induced during materials' production are offset by the cut-off carbon from the reduction of required materials [56, 57]. Nonetheless, it is essential for designers to assure that the carbon induced are offset by the carbon cut-off, or else, the overall EEs will increase as shown in [56]. The third is to adjust the structural design of buildings in a way that the buildings require smaller amount of materials but have sufficiently structural performance. This technique could be achieved by various methods such as reducing thickness of structural elements, rearranging the structural configurations, and choosing systems that requires minimal carbon-intensive materials and construction equipment [58-61]. By applying such methods, designers are allowed to cutdown materials required in buildings which subsequentially reduces the needs for raw-materials extraction, transportation, construction activities, construction equipment, and wastes generated throughout the lifecycle of buildings. This third technique, thus, results in a reduction of the EEs correspondingly.

Table 5 Improvement of materials' structural performances

Reference	Country	Type	Area (m^2)	Case Studies	System boundary	EEs	Difference in EEs
[53]	Spain	Housing project	500	CIP RC slab with insulation slab	Cradle-to-Grave	230	-
				CIP RC slab		223	-3%
				Prestress hollow RC slab		136	-41%
				Precast hollow RC slab		179	-22%
[54]	South Korea	Commercial	13,487	RC slab with beams	Cradle -to-Site	242	-
				RC flat slab		234	-3%
				RC voided slab		218	-10%
[55]	South Korea	Commercial	N.S.	RC slab with beams	Cradle-to-Site	196	-
				RC voided slab		171	-13%
[56]	Brazil	Office	3,600	Slab built from RC25	Cradle-to-Grave	100%	-
				Slab built from RC50		91%	-9%
				Slab built from RC75		98%	-2%
[57]	Germany	Bridge	45	Reinforce Concrete	Cradle-to-Gate	150%	-
				Steel Bridge		150%	0%
				Carbon Fiber Reinforced Polymer Concrete		100%	-33%
[58]	Hong Kong	Apartment	39,501	Hybrid CIP and Precast system	Cradle -to-Site	561	-
				Increase Precast rate by 35%		553	-1.4%
				Reduce thickness of walls		551	-2%
[59]	Not Specify	Not Specify	3,600	Outrigger Steel	Cradle -to-Site	30	-
				Diagrid Steel		23	-23
				Braced Tube Steel		28	-7
				Braced Tube Concrete		15	-50
				Tube-in-Tube Concrete		18	-40
[60]	U.K.	Residential	4,356	Slab thickness of 0.275m, 12 Columns with the size of 0.2mx0.8m Column Grid-X (m): 7.33, 7.33, 7.33 Column Grid-y (m): 7.33, 7.33, 7.33	Cradle -to-Site	210	-
				Slab thickness of 0.25m, 14 Columns with the size of 1.2m x0.35m Column Grid-X (m): 5,6,5,6 Column Grid-y (m): 7,7,8		183	-12%
[61]	Hong Kong	Residential	310,000	CIP system	Cradle -to-Site	92.7*	-
				Increase Precast rate by 35%		74.9*	-19%

Note. This table extracts only the embodied emissions. The abbreviations are Cradle: raw-material extraction, Gate: manufacturing process, Site: construction activities, Grave: disposal, EE: Embodied Emissions ($kgCO_2$ eq/m^2), CIP: Cast-In-Place, RC: Reinforce Concrete. The negative sign represents the reduction in EEs relative to the baseline case. * represents that the unit is endpoint.

3. Adaptation of design-for-disassembly (DfD) and sustainable waste management

Table 6 portrays that adaptation of DfD principle in buildings, suggested by [11, 12, 62], can reduce the EEs of buildings. This reduction occurs considering that the principle allows parts of buildings to be disassembled and reused at the building's EOL [63-67]. Reflecting on the results shown in [65], one can observe that reusing the materials can offset the additional EEs associated with the DfD structure. Moreover, [66-68] show that reusing and recycling the construction wastes can improve the environmental performance of building compared to landfilling. This reflection agrees with [69] which suggests one to sustainably manage the wastes via reusing (applicable for steel and timber), recycling (applicable for concrete, steel, and timber), and energy recovery (applicable for timber). To summarize, the DfD design principle and the sustainable waste management can lessen the demands for virgin materials and for material productions, hence enhancing the circularity for the buildings whilst decreasing the EEs simultaneously.

Table 6 Adaptation of DfD principle, reusing, and recycling strategies

Reference	Country	Type	Area (m^2)	Cast Studies	System Boundary	EEs	Difference in EEs
[63]	Denmark	Residential	150	Conventional Built House	Cradle-to-Grave	800	-
				DfD Built House		667	-17%
[64]	Denmark	Office	37,839	Reinforce Concrete	Cradle-to-Grave	226	-
				PC Concrete built with DfD (reused 1 time)		190	-16%
				PC Concrete built with DfD (reused 2 times)		180	-20%
[65]	USA	N.S.	N.S.	Steel-Concrete Composite Floor	Cradle-to-Grave	125	-
				PC DfD Floor with Mechanical Connectors (reuse 0)		140	+12%
				PC DfD Floor with Mechanical Connectors (reuse 1)		75	-40%
				PC DfD Floor with Mechanical Connectors (reuse 2)		50	-60%
				PC DfD Floor with Mechanical Connectors (reuse 3)		40	-68%
[66]	Brazil	Pavilion	4133	DfD steel: 1st life, 100% recycle, Disposal	Cradle-to-Grave	1,621	-
				DfD steel: 1st life, 64%recycle & 36%reuse, 2nd life, Disposal		1,354	-16%
				DfD steel: 1st life, 100%reuse, 2nd life, Disposal		1,016	-37%
[67]	Italy	Residential	130	CIP Concrete (99% recycle, 1% landfill)	Cradle-to-Grave	1,250	-
				Steel Modular (87.5% recycle, 12.5% landfill)		1,213	-3%
				CIP Concrete (99% recycle, 0.8% reuse, 0.2% landfill)		853	-32%
				Steel Modular (79.3% recycle, 16.3% reuse, 2.5% landfill)		512	-59%
[68]	Thailand	Industrial	14,938	Landfill all materials	Cradle-to-Grave	616	-
				Recycle all materials that are eligible		436	29%

Note. This table only extracts the embodied emissions. The abbreviation is EEs: Embodied Emissions (kg CO2/ m^2), Cradle: raw-material extraction, Grave: Disposal, DfD: Design-for-Disassembly, PC: Precast Concrete, CIP: Cast-In-Place. The negative and positive signs represent the reduction and increase in EEs relative to the baseline case respectively.

4. Use of passive and active measures

Table 7 shows that the use of passive and active measures, suggested by [11-14], contributes to mitigation in GHGs, despite the additional EEs associated with employment of retrofits. The table also depicts that the use of active measures results in greater mitigation of the OEs and TLEs compared to the practice of passive measures [68, 70-79]. The main reason behind this is: the active principle involves the use of advanced technologies (such as photovoltaic PV solar-cell panels, LEDs, improving HVAC, etc.) to produce and distribute the energy required for the occupants' thermal and lighting comforts; whereas, the passive principle aims to improve and maximize the properties of building envelopes (such as the use of insulation, the reduction in Window-to-Wall Ratio, etc.) as a means to achieve thermal and lighting comforts for occupants.

Evaluation of the strategies' adequacies on reaching net-zero GHGs emission goal

The previous section indicates that the EEs can be reduced by substituting low-carbon materials for carbon-intensive materials, by improving structural performance of the materials, and by increasing the circularity of buildings. Nonetheless, the EEs cannot be cut to an absolute zero due to the limitations presented in Table 8. Apart from the EEs, the previous section also shows that the use of passive and active measures can result in reduction of OEs for the buildings. Furthermore, the use of PV solar-cell panels is a unique design strategy because it is capable of reducing and compensating the OEs and EEs, whereas the other strategies are only capable of reducing either OEs or EEs. In depth details, [68, 70, 76] demonstrate that the PV solar-cell panels can diminish the demands for the national grid electricity and can provide electricity surplus which can be fed to the national grid. This in turn results in the buildings to gain negative OEs that can compensate for the EEs. As a result of the compensation, the buildings then achieve the net-zero GHGs emission ultimately. The described performance of PV solar-cell is illustrated in Figure 2. Through the figure, one can find that the use of PV solar-cells not only reduces the OEs to zero [70], but also provides negative OEs that can compensate for the EEs; thus, leading to the TLEs of buildings to achieve net-zero and net-negative emissions [68,76]. Due to the described performance, one can thus safely accept, based on the life cycle principle, that the use of PV solar-cell panels is the key for buildings to achieve the net-zero emission, whereas the use of the other strategies helps to accelerate the performance of PV and shortens the time for buildings to achieve net-zero GHGs emissions by cutting-down the EEs and OEs. From this finding and based on the life cycle principle, the study concludes that: in theory, the presented design strategies demonstrate great potential on leading Thailand's building sector towards the net-zero GHG emissions goal given the condition that all buildings in Thailand are equipped with renewable energy-based on-site electricity self-generator (such as PV solar panels) on a large scale. However, this conclusion is theoretical, idealized, and solely based on the principle of life cycle. In reality, there is a wide range of practical limitations that prevents PV solar-cell panels from being used extensively such as financial viability of the building owners [18], locations of the buildings, available spaces for the PV installation, the electricity fed-back limit [17], etc. Thus, these limitations prevent Thailand's building sector to attain the net-zero emissions through the use of the design strategies. This finding thus calls for action from the supply side (such as a decarbonization of grid, an implementation of financial incentive policies, etc.) [9, 17, 18], and the demand side which are to: improve and deploy energy-saving materials and devices together with other design strategies [18]. In response to the need of the latter, this study highlights five possible research improvements and one management strategy as means to add practical values for the design strategies and to promote Thailand's building sector towards the net-zero emissions goal.

Table 7 Embodied and operational emissions via the use of passive and active measures

Reference	Country / Type/ Area	SB / use-phase	Scenario	EEs ($kgCO_2$ eq/m^2)	OEs ($kgCO_2$ eq/m^2)	TLEs ($kgCO_2$ eq/m^2)	Difference in TLEs
[68]	Thailand, Industrial 14,938 m^2	Cradle-to-Grave 20 years	S1: Baseline (lighting, natural airflow)	616	264	880	-
			S2: improved PV	871	-1171	-300	-134%
[70]	Norway Office 2,940 m^2	Cradle-to-Grave 60 years	S1: Baseline	311	1021	1,332	-
			S2: slightly improved Enve , baseline HVAC	362	323	685	-49%
			S3: slightly improved Enve , improved HVAC	350	283	633	-52%
			S4: largely improved Enve , baseline HVAC	373.8	327	700	-47%
			S5: largely improved Enve , improved HVAC	358	277	635	-52%
			S6: largely improved Enve , improved HVAC, PV	416.7	0	416.7	-69%
[71]	London Residential 123.2 m^2	Cradle-to-Use 60 years	S1: Baseline	0	4,623	4,623	-
			S2: slightly improved Enve , HVAC , DHW	15	2,541	2,556	-45%
			S3: medium improved Enve , HVAC , DHW	79	1,513	1,592	-66%
			S4: deeply improved Enve, HVAC, DWH , PV	175	896	1,071	-77%
[72]	USA University 130,993 m^2	Cradle-to-Grave 100 years	S1: Baseline	496	305	802	-83%
			S2: improved HVAC	504	229	733	-84%
			S3: improved HVAC, lighting	504	191	695	-85%
			S4: improved HVAC, lighting, Enve	573	76	649	-86%
[73]	Portugal Residential 100 m^2	Cradle-to-Use 30 years	S1: Baseline , gas boiler for DHW	0	271,800	271,800	-
			S2: improved Enve , HVAC, solar collector for DHW	1,000	137,900	138,900	-49%
			S3: improved Enve , HVAC, VTC for DHW	1,200	42,600	43,800	-84%
			S4: improved Enve , HVAC, VTC for DHW, PV	3,500	12,910	16,410	-94%
[74]	Sweden Residential 2822 m^2	Cradle-to-Grave 50 years	S1: Baseline , baseline HVAC temp setting at 22.7	65	298	363	-
			S2: improved Enve , baseline HVAC	104	223	327	-10%
			S3: improved Enve , improved HVAC temp at 21	118	181	299	-18%
			S4: improved HVAC temp at 21	72	230	302	-17%
			S5: improved HVAC temp at 22.7	72	255	327	-10%
[75]	Turkey Residential 573 m^2	Cradle-to-Use 30 years	S1: Baseline	100%	100%	100%	-
			S2: improved Enve , PV	105%	70%	81%	-19%
[76]	Thailand Residential 141.4 m^2	Cradle-to-Grave 50 years	S1: Baseline	406	3,119	3,525	-
			S2: improve Enve , HVAC , DHW , PV 30 m^2	578	654	1,232	-65%
			S3: improve Enve , HVAC , DHW , PV 44 m^2	612	47	659	-82%
			S4: improve Enve , HVAC , DHW , PV 85 m^2	733	-1,763	-1,030	-129%

Note. [71,73] assumed that the model building is already existant; hence, the baseline EEs are zero, and the EEs in improved scenarios represent additional EEs associated with introduced retrofits. The abbreviation is SB: System Boundary, EEs: Embodied Emissions, OEs: Operational Emissions, TLEs: Total Life cycle Emissions, Cradle: raw-material extraction, Use: Operation, Grave: Disposal, Enve: Building Envelope, HVAC: Heating /Ventilation / Air-Condition, VTC: Vacuum Tube Collector, DHW: Domestic Hot Water, PV: photovoltaic (solar-cell) panels. The negative sign represents the reduction in TLEs relative to the baseline case.

Table 8 Limitations of design strategies used to cut the EEs

Embodied Strategies	Description
The Use of Timber	There are three sources of EEs associated with timber. The first is transportation. The second is timber's production process. The third is the carbon associated within the material itself, as it could be regarded as negative-, neutral-, or low- carbon materials. However, [35] reports that the emissions associated with the timber can vary depending on assumptions on biogenic carbon (the carbon stored with the timbers [32]) and on forest management; for example, under a condition where the biogenic carbon is assumed to be large and forest is assumed to be unsustainably managed, using timber will contribute a large number of GHG emissions.
The use of composite and innovative materials	There are three sources of EEs associated with the alternative materials. The first is transportation [61]. The second is the materials' production. The third is the recycle processes [69].
SCMs usage	There are two sources of EEs associated with SCMs. The first is transportation [50-52]. The second is allowable portion of cement used in concrete mix, as [15] states that fly ash, natural pozzolans, ground granulated blast-furnace slag, and silica fume are prohibited to be used over 35%, 20%, 70%, and 15% respectively.
The improvement of materials	There are still GHG emissions from materials' production processes, despite its reduction of material usage as shown in Table 5.
Design-for-Disassembly	There are three sources of EEs associated with these structures. The first is transportation. The second is materials' production process [61]. The third is materials' recycle processes [69].
Steel and Timber's Recycle	There are still GHG emissions present during the recycling process of steel and timber [69]. This is because steel and timber's recycling processes still involve the use of fossil fuels, despite the removal of demands for virgin materials. Furthermore, the recycle rates of steel and timber in Thailand are 55% and less than 50% respectively [16]. These portions are considered as relatively low [16].

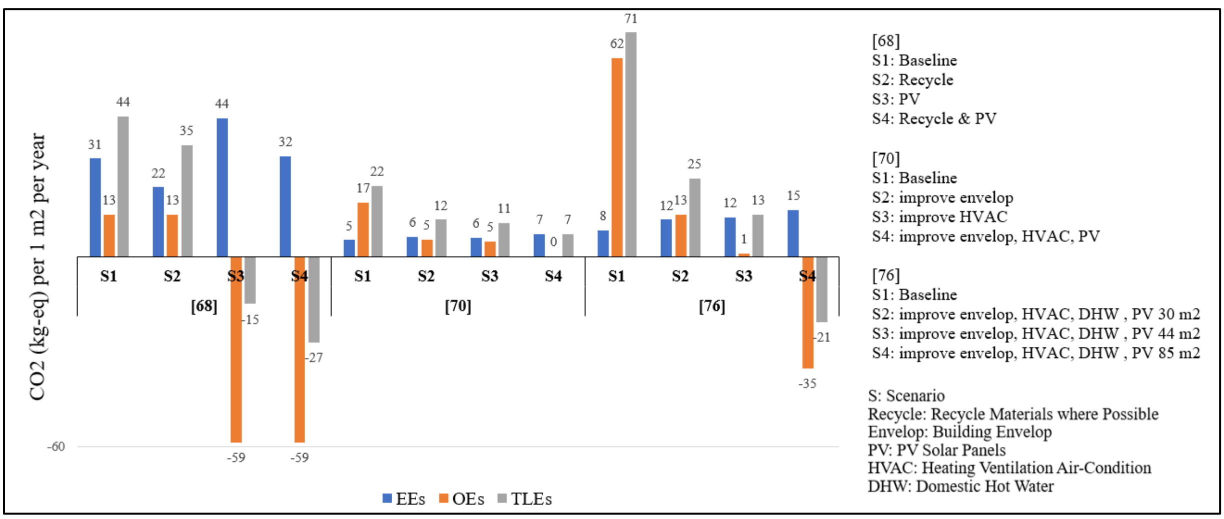

Figure 2 Life cycle emissions of buildings with and without PV solar-cell panels

The first is to develop a novel method for designing buildings with lightweight structural elements such as hollow concrete beams and columns, beams with web opening, etc. Doing so will reduce the demands for raw materials while providing the same structural services whilst reducing the EEs. The second is to develop a novel method for designing buildings with the sole use of SCMs. This suggestion is not only drawn based on its improvable structural property, but also based on its environmental performances which contribute to lower GHG emissions compared to ordinary cement [48-50]. The third is to study the structural properties of various industrial wastes and bio-based materials, or their by-products (such as used glasses, used plastics, construction wastes, agricultural by-products, etc.) and develop them as (or as part of) structural load-bearing elements. Doing so will reduce the demand for carbon-intensive materials, transform the building from being linear to circular, and lessen the EEs of buildings subsequentially. The fourth is to study the thermal properties of various industrial wastes and bio-based materials, or their by-products, to develop them as (or as part of) building envelops such as insulations, wall&roof materials, etc. Doing so will lessen the demand for chemical-based insulations whilst maximizing the occupants' thermal comfort. Thus, the building is subjected to unnoticeable EEs and is able to reduce the OEs in the long-run. The fifth is to develop combination of design strategies that can provide the maximum EEs and OEs mitigation. For example, the efficiency of PV solar-cell panels could be maximized by placing them where the solar radian is at maximum [74], using them together with building insulation [76], and with other commercial gadgets (such as thin film, batteries), and recycling them when possible. Doing so will keep the total emissions of buildings at its minimum and provide a greater chance for the building to achieve net-zero GHG emissions. Besides the research improvements, designers can apply management strategy during the design stage [80]. This strategy consists of four main steps: (1) set environmental targets for the buildings, (2) design the building applying the presented and suggested design strategies, (3) assess the environmental performance of the buildings via LCA and other tools preferably Circularity Indicator (a decision-making tool for designers that assess the circularity of a product) [62], and (4) adjust the building till it satisfies the targets.

Conclusions

The embodied and operational phases have equal chances of being the hotspot for buildings as the emissions in each phase depends on the choice of material, the choice of energy-saving retrofits, and the electricity grid profile. In this study, five design strategies were reviewed: to substitute low-carbon materials for carbon-intensive materials, to improve structural performance of carbon-intensive materials, to increase the circularity of buildings; as well as to use passive and active measures. It was found that, in theory, the design strategies demonstrate great potential on leading Thailand's building sector to net-zero GHG emissions goal given an ideal condition that all buildings use renewable energy-based on-site electricity generator such as PV solar-cell panels on a large scale. Nonetheless, there are various limitations preventing this ideal situation to arise. Thus, this study highlights five possible research improvements and a hands-on management strategy to push forward Thailand's building sector toward the net-zero emissions goal ultimately.

References

[1] Energy Policy and Planning Office. 2021. Energy Statistic of Thailand 2021. Thailand's Ministry of Energy.

[2] Iqbal, M. I., Himmler, R., & Gheewala, S. H. 2017. Potential life cycle energy savings through a transition from typical to energy plus households: A case study from Thailand. Energy and Buildings, 134: 295-305.

[3] EPPO, Thailand's Energy Policy and Planning Office. 2015. Energy Efficiency Plan; EEP 2015. Thailand's Ministry of Energy.

[4] DEDE, Department of Alternative Energy Development and Efficiency. 2018. Energy Efficiency Plan 2018 - 2037. Thailand's Ministry of Energy.

[5] Ministry of Natural Resources and Environment. 2020. Thailand Third Biennial Update Report. United Nation Climate Change.

[6] UNGCNT, United Nation Global Compact Network Thailand. 2021. Thailand's Long-term Greenhouse Gas Emission Development Strategy, presented at COP26, Thailand Pavilion.

[7] EN 15978:2011. 2011. Sustainability of Construction Works. Assessment of Environmental Performance of Buildings-Calculation method.

[8] ISO 21931-1:2010. 2010. Sustainability in Building Construction—Framework for Methods of Assessment of the Environmental Performance of Construction Works - Part 1: Buildings, International Organization for Standardization, Geneva.

[9] Thailand's Office of Natural Resources and Environmental Policy and Planning. 2019. Master Key Plan for Climate Change between 2015 and 2050.

[10] Ministry of Higher Education, Science, Research and Innovation. 2020.

Strategies to drive forward Thailand by Bio-Circular-Green Economic Model (BCG) 2021 - 2027.

[11] U.S. Green Building Council. 2021. LEED v4.1 Building Design and Construction. [Accessed March, 2022]. Available from: https://www.usgbc.org/leed/v41#bdc

[12] European Commission. 2020. Circular economy principle for building design. [Accessed March, 2022]. Available from: https://ec.europa.eu/growth/content/designing-buildings-context-circular-economy_en

[13] Thai Green Building Institute. 2017. TREES for new construction and major renovation. [Accessed March, 2022]. Available from: https://www.tgbi.or.th/uploads/trees/2017_03_TREES-NC-Eng.pdf

[14] DEDE, Department of Alternative Energy Development and Efficiency. 2017. Building Energy Code by Department of Alternative Energy Development and Efficiency.

[15] American Concrete Institute. 2002. Standard Practice for Selecting Proportions for Normal, Heavyweight, and Mass Concrete (ACI 211.1-91). [Accessed March, 2022]. Available from: https://kashanu.ac.ir/Files/aci%20211_1_91.pdf

[16] Piyapanphong, S. 2018. Country Report (Kingdom of Thailand). Eighth Regional 3R Forum in Asia and the Pacific "Achieving Clean Water, Clean Land and Clean Air through 3R and Resource Efficiency- A 21st Century Vision for Asia-pacific Communities," India. [Accessed March, 2022]. Available from: uncrd.or.jp/content/documents/5857Thailand_Country%20Report.pdf

[17] EPPO, Thailand's Energy Policy and Planning Office. 2018. Power Development Plan (PDP).

[18] Rajbhandari, S., & Limmeechokchai, B. 2020. Assessment of greenhouse gas mitigation pathways for Thailand towards achievement of the 2°C and 1.5°C Paris Agreement targets. Climate Policy, 21(4): 492-513.

[19] Hasik, V., Ororbia, M., Warn, G. P., & Bilec, M. M. 2019. Whole building life cycle environmental impacts and costs: A sensitivity study of design and service decisions. Building and Environment, 163: 106316.

[20] Ghose, A., McLaren, S. J., Dowdell, D., & Phipps, R. 2017. Environmental assessment of deep energy refurbishment for energy efficiency-case study of an office building in New Zealand. Building and Environment, 117: 274-287.

[21] Norouzi, M., Colclough, S., Jiménez, L., Gavaldà, J., & Boer, D. 2022. Low-energy buildings in combination with grid decarbonization, life cycle assessment of passive house buildings in Northern Ireland. Energy and Buildings, 261: 111936.

[22] Liu, S., Schulz, U. W., Sapar, M. H., & Qian, S. 2016. Evaluation of the environmental performance of the chilled ceiling system using life cycle assessment (LCA): A case study in Singapore. Building and Environment, 102: 207-216.

[23] González-Prieto, D., Fernández-Nava, Y., Marañón, E., & Prieto, M. M. 2021. Environmental life cycle assessment based on the retrofitting of a twentieth-century heritage building in Spain, with electricity decarbonization scenarios. Building Research & Information, 49(8): 859-877.

[24] Raugei, M., Keena, N., Novelli, N., Aly Etman, M., & Dyson, A. 2021. Life cycle assessment of an ecological living module equipped with conventional rooftop or integrated concentrating photovoltaics. Journal of Industrial Ecology, 25(5): 1207-1221.

[25] Burek, J., & Nutter, D. 2018. Life cycle assessment of grocery, perishable, and general merchandise multi-facility distribution center networks. Energy and Buildings, 174: 388-401.

[26] Nematchoua, M. K., Asadi, S., Obonyo, E., & Reiter, S. 2021. Environmental analysis of health damages coming from a residential neighborhood built in 150 countries. Journal of Housing and the Built Environment.

[27] Chastas, P., Theodosiou, T., Kontoleon, K. J., & Bikas, D. 2018. Normalising and assessing carbon emissions in the building sector: A review on the embodied CO2 emissions of residential buildings. Building and Environment, 130: 212-226.

[28] Kiss, B., & Szalay, Z. 2022. Sensitivity of buildings' carbon footprint to electricity decarbonization: a life cycle–based multi-objective optimization approach. The International Journal of Life Cycle Assessment.

[29] de Oliveira Fernandes, M. A., Keijzer, E., van Leeuwen, S., Kuindersma, P., Melo, L., Hinkema, M., & Gonçalves Gutierrez, K. 2021. Material-versus energy-related impacts: Analysing environmental trade-offs in building retrofit scenarios in the Netherlands. Energy and Buildings, 231: 110650.

[30] Lausselet, C., Ellingsen, L. A., Strømman, A. H., & Brattebø, H. 2019. A life-cycle assessment model for zero emission neighborhoods. Journal of Industrial Ecology, 24(3): 500-516.

[31] Ramírez-Villegas, R., Eriksson, O., & Olofsson, T. 2019. Environmental Payback of Renovation Strategies in a Northern Climate—the Impact of Nuclear Power and Fossil Fuels in the Electricity Supply. Energies, 13(1): 80.

[32] Zeitz, A., Griffin, C., & Dusicka, P. 2019. Comparing the embodied carbon and energy of a mass timber structure system to typical steel and concrete alternatives for parking garages. Energy and Buildings, 199: 126-133.

[33] Moncaster, A., Pomponi, F., Symons, K., & Guthrie, P. 2018. Why method matters: Temporal, spatial and physical variations in LCA and their impact on choice of structural system. Energy and Buildings, 173: 389-398.

[34] Lu, H. R., el Hanandeh, A., & Gilbert, B. P. 2017. A comparative life cycle study of alternative materials for Australian multi-storey apartment building frame constructions: Environmental and economic perspective. Journal of Cleaner Production, 166: 458-473.

[35] Himes, A., & Busby, G. 2020. Wood buildings as a climate solution. Developments in the Built Environment, 4: 100030.

[36] Hart, J., D'Amico, B., & Pomponi, F. 2021. Whole-life embodied carbon in multistory buildings: Steel, concrete and timber structures. Journal of Industrial Ecology, 25(2): 403-418.

[37] Tavares, V., Lacerda, N., & Freire, F. 2019. Embodied energy and greenhouse gas emissions analysis of a prefabricated modular house: The "Moby" case study. Journal of Cleaner Production, 212: 1044-1053.

[38] Pierobon, F., Huang, M., Simonen, K., & Ganguly, I. 2019. Environmental benefits of using hybrid CLT structure in midrise non-residential construction: An LCA based comparative case study in the U.S. Pacific Northwest. Journal of Building Engineering, 26: 100862.

[39] Escamilla, E. Z., Habert, G., Daza, J. C., Archilla, H., Fernández, J. C., & Trujillo, D. 2018. Industrial or Traditional Bamboo Construction? Comparative Life Cycle Assessment (LCA) of Bamboo-Based Buildings. Sustainability, 10(9): 3096.

[40] Yang, X., Zhang, S., & Wang, K. 2021. Quantitative study of life cycle carbon emissions from 7 timber buildings in China. The International Journal of Life Cycle Assessment, 26(9): 1721-1734.

[41] Bukoski, J. J., Chaiwiwatworakul, P., & Gheewala, S. H. 2016. The Life Cycle Assessment of an Energy-Positive Peri-Urban Residence in a Tropical Regime. Journal of Industrial Ecology, 21(5): 1115-1127.

[42] Hahnel, G., Whyte, A., & Biswas, W. K. 2021. A comparative life cycle assessment of structural flooring systems in Western Australia. Journal of Building Engineering, 35: 102109.

[43] Zhang, X., Xu, J., Zhang, X., & Li, Y. 2021. Life cycle carbon emission reduction potential of a new steel-bamboo composite frame structure for residential houses. Journal of Building Engineering, 39: 102295.

[44] Balasbaneh, A. T., & bin Marsono, A. K. 2017. Strategies for reducing greenhouse gas emissions from residential sector by proposing new building structures in hot and humid climatic conditions. Building and Environment, 124: 357-368.

[45] Zhang, X., & Wang, F. 2015. Life-cycle assessment and control measures for carbon emissions of typical buildings in China. Building and Environment, 86: 89-97.

[46] Samani, P., Mendes, A., Leal, V., Guedes, J. M., & Correia, N. 2015. A sustainability assessment of advanced materials for novel housing solutions. Building and Environment, 92: 182-191.

[47] Dong, Y., Ng, S. T., & Liu, P. 2021. A comprehensive analysis towards benchmarking of life cycle assessment of buildings based on systematic review. Building and Environment, 204: 108162.

[48] Zhao, J., Tong, L., Li, B., Chen, T., Wang, C., Yang, G., & Zheng, Y. 2021. Eco-friendly geopolymer materials: A review of performance improvement, potential application and sustainability assessment. Journal of Cleaner Production, 307: 127085.

[49] Xiao, R., Ma, Y., Jiang, X., Zhang, M., Zhang, Y., Wang, Y., et. al. 2020. Strength, microstructure, efflorescence behavior and environmental impacts of waste glass geopolymers cured at ambient temperature. Journal of Cleaner Production, 252; 119610.

[50] Dollente, I. J. R., Tan, R. R., Promentilla, M. A. B. 2021. Life Cycle Assessment of Precast Geopolymer Products. Chemical Engineering Transactions, 88: 799-804.

[51] Lovecchio, N., Shaikh, F., Rosano, M., Ceravolo, R., & Biswas, W. 2020. Environmental assessment of supplementary cementitious materials and engineered nanomaterials concrete. AIMS Environmental Science, 7(1): 13-30.

[52] Nath, P., Sarker, P. K., & Biswas, W. K. 2018. Effect of fly ash on the service life, carbon footprint and embodied energy of high strength concrete in the marine environment. Energy and Buildings, 158: 1694-1702.

[53] Valencia-Barba, Y. E., Gómez-Soberón, J. M., Gómez-Soberón, M. C., & López-Gayarre, F. 2020. An Epitome of Building Floor Systems by Means of LCA Criteria. Sustainability, 12(13): 5442.

[54] Paik, I., & Na, S. 2019. Evaluation of Carbon Dioxide Emissions amongst Alternative Slab Systems during the Construction Phase in a Building Project. Applied Sciences, 9(20): 4333.

[55] Na, & Paik. 2019. Reducing Greenhouse Gas Emissions and Costs with the Alternative Structural System for Slab: A Comparative Analysis of South Korea Cases. Sustainability, 11(19): 5238.

[56] Garcez, M. R., Rohden, A. B., & Graupner De Godoy, L. G. 2018. The role of concrete compressive strength on the service life and life cycle of a RC structure: Case study. Journal of Cleaner Production, 172: 27-38.

[57] Stoiber, N., Hammerl, M., & Kromoser, B. 2021. Cradle-to-gate life cycle assessment of CFRP reinforcement for concrete structures: Calculation basis and exemplary application. Journal of Cleaner Production, 280: 124300.

[58] Teng, Y., & Pan, W. 2019. Systematic embodied carbon assessment and reduction of prefabricated high-rise public residential buildings in Hong Kong. Journal of Cleaner Production, 238: 117791.

[59] Mavrokapnidis, D., Mitropoulou, C. C., & Lagaros, N. D. 2019. Environmental assessment of cost optimized structural systems in tall buildings. Journal of Building Engineering, 24: 100730.

[60] Eleftheriadis, S., Duffour, P., & Mumovic, D. 2018. BIM-embedded life cycle carbon assessment of RC buildings using optimised structural design alternatives. Energy and Buildings, 173: 587-600.

[61] Dong, Y. H., & Ng, S. T. 2015. A life cycle assessment model for evaluating the environmental impacts of building construction in Hong Kong. Building and Environment, 89: 183-191.

[62] Ellen MacArthur Foundation. 2015. Circularity Indicators An approach to measuring circularity. [Accessed March, 2022]. Available from: https://emf.thirdlight.com/link/3jtevhlkbukz-9of4s4/@/preview/1?o

[63] Rasmussen, F. N., Birkved, M., & Birgisdóttir, H. 2020. Low- carbon design strategies for new residential buildings – lessons from architectural practice. Architectural Engineering and Design Management, 16(5): 374-390.

[64] Eberhardt, L. C. M., Birgisdóttir, H., & Birkved, M. 2018. Life cycle assessment of a Danish office building designed

for disassembly. Building Research & Information, 47(6): 666-680.

[65] Eckelman, M. J., Brown, C., Troup, L. N., Wang, L., Webster, M. D., & Hajjar, J. F. 2018. Life cycle energy and environmental benefits of novel design-for-deconstruction structural systems in steel buildings. Building and Environment, 143: 421-430.

[66] Arrigoni, A., Zucchinelli, M., Collatina, D., & Dotelli, G. 2018. Life cycle environmental benefits of a forward-thinking design phase for buildings: the case study of a temporary pavilion built for an international exhibition. Journal of Cleaner Production, 187: 974-983.

[67] Vitale, P., Spagnuolo, A., Lubritto, C., & Arena, U. 2018. Environmental performances of residential buildings with a structure in cold formed steel or reinforced concrete. Journal of Cleaner Production, 189: 839-852.

[68] Tulevech, S. M., Hage, D. J., Jorgensen, S. K., Guensler, C. L., Himmler, R., & Gheewala, S. H. 2018. Life cycle assessment: a multi-scenario case study of a low-energy industrial building in Thailand. Energy and Buildings, 168: 191-200.

[69] U.S. Environmental Protection Agency. 2020. Documentation for Greenhouse Gas Emission and Energy Factors Used in the Waste Reduction Model (WARM).

[70] Rabani, M., Madessa, H. B., Ljungström, M., Aamodt, L., Løvvold, S., & Nord, N. 2021. Life cycle analysis of GHG emissions from the building retrofitting: The case of a Norwegian office building. Building and Environment, 204: 108159.

[71] Vavanou, A., Schwartz, Y., & Mumovic, D. 2021. The life cycle impact of refurbishment packages on residential buildings with different initial thermal conditions. Journal of Housing and the Built Environment.

[72] Hu, M. 2019. Life-cycle environmental assessment of energy-retrofit strategies on a campus scale. Building Research & Information, 48(6): 659-680.

[73] Mateus, R., Silva, S. M., & de Almeida, M. G. 2019. Environmental and cost life cycle analysis of the impact of using solar systems in energy renovation of Southern European single-family buildings. Renewable Energy, 137: 82-92.

[74] Ramírez-Villegas, R., Eriksson, O., & Olofsson, T. 2019. Life Cycle Assessment of Building Renovation Measures–Trade-off between Building Materials and Energy. Energies, 12(3): 344.

[75] Mangan, S. D., & Oral, G. K. 2016. Assessment of residential building performances for the different climate zones of Turkey in terms of life cycle energy and cost efficiency. Energy and Buildings, 110: 362-376.

[76] Iqbal, M. I., Himmler, R., & Gheewala, S. H. 2018. Environmental impacts reduction potential through a PV based transition from typical to energy plus houses in Thailand: A life cycle perspective. Sustainable Cities and Society, 37: 307-322.

[77] Cubi, E., Zibin, N. F., Thompson, S. J., & Bergerson, J. 2015. Sustainability of Rooftop Technologies in Cold Climates: Comparative Life Cycle Assessment of White Roofs, Green Roofs, and Photovoltaic Panels. Journal of Industrial Ecology, 20(2): 249-262.

[78] Lawania, K. K., & Biswas, W. K. 2016. Cost-effective GHG mitigation strategies for Western Australia's housing sector: a life cycle management approach. Clean Technologies and Environmental Policy, 18(8): 2419-2428.

[79] Pombo, O., Allacker, K., Rivela, B., & Neila, J. 2016. Sustainability assessment of energy saving measures: A multi-criteria approach for residential buildings retrofitting—A case study of the Spanish housing stock. Energy and Buildings, 116: 384-394.

[80] Saadé, M., Erradhouani, B., Pawlak, S., Appendino, F., Peuportier, B., & Roux, C. 2022. Combining circular and LCA indicators for the early design of urban projects. The International Journal of Life Cycle Assessment, 27(1): 1-19.

Thai Environmental Engineering Journal Vol. 36 No. 2 (2022) : 25-34
www.eeat.or.th

River Runoff under Climate Change Using Dynamic Basin Parameters in Lam Dom Yai River Basin, Thailand

Udomsook Suracharttumrongrat* and Krit Sriworamas

Department of Civil Engineering, Faculty of Engineering, Ubon ratchathani University,
Ubon Ratchathani 34190, Thailand
*E-mail : Udomsooksu@gmail.com

Abstract

This study aims to study effects of climate change (CC) and land use change (LUC) on future river flows of Lam Dom Yai (LDY) basin covering 5,000 km^2 located in the northeast of Thailand. The study developed a climate hydrologic model (SWAT model) utilizing basin's key spatiotemporal parameters as dynamic parameters comparable to utilizing constant or static parameters. The GIS-based ARC –SWAT model was developed and applied using 78 years of future climatic data from MRI-GCM which are statistically downscaled with observed data. Additionally CA-Markov technique was adopted to simulate temporal and spatial pattern of land use in periodically as the model input taken into account LUC. Results of the study indicated model reliability of both dynamic and static parameters. Dynamic parameters computed better model performance for daily, monthly and annual flow simulation basis than those of applying static parameters, the model with dynamic parameters is consequently recommended. For the case study of LDY basin in the future with the selected CC scenario RCP 4.5, the mean annual flows of LDY for the case of using dynamic and static parameters would be increased respectively 6.1 and 4.9 percent more than the past mean annual flow. Additionally, the future mean monthly flows and extreme daily flows would be significantly increased in September and October, and decreased in February and March respectively. Furthermore, high flows would be deferred from September to October.

Keywords : Dynamic basin parameters; Climate change; Land use change; Climate hydrologic model; Land use change model

Introduction

Global warming and climate change becomes the world's critical phenomenon that challenge all nations' co-operation in greenhouse gas (GHG) reduction to decelerate global warming and essential adaptive measures preparation to alleviate CC impacts respectively. According to the, IPCC, 2021 during 1950-2020 higher global temperature was increased up to 1.09°C on average. Increasing of GHG significantly causes global warming and CC consequently affects hydrologic system comprising surface runoff, groundwater, and evapotranspiration.

Numerous international studies have researched quantitative hydrologic response due to long term future CC by applying different global climate models (GCM) [1, 2] with downscale techniques and various hydrologic models. Results indicated that effects from CC would be uncertain in either increasing or decreasing trends of river flows. Increasing trend of river flows and floods were determined for example in Mekong River [3], Canada [4], Myanmar [5], Brazil [6], Ping River in Thailand [7], and Korea [8]. On the other hand, decreasing trend of runoff was examined in Vietnam [9].

Additionally, some researches [10, 11] considering CC and LUC affecting hydrologic response has been employed. A study of deforestation in Brazil [12] and rapid urbanization only or both of urbanization and CC in Canada would affect increasing mean annual flow and flood flows [4]. On the other hand, LUC due to reforestation in China [13], Kenya [14], and Thailand [15] would result in contrarily decreasing mean annual flow and extreme flood volume.

Most of researches using Soil Water Assessment Tool Model (SWAT) [16] adopted fixed or static basin parameters in the model calibration period and applied for forecasting hydrologic response in future period. Nevertheless, little research on consideration of spatiotemporal parameters under CC and LUC situation has been conducted, therefore a research on comparison of river runoff from the SWAT model between using dynamic basin parameters and using static basin parameters in a particular basin in Thailand should be determined.

Results would be beneficial in selection of dynamic or static parameters approach that suitable for required temporal scale basis and accuracy, as well as time and budget constraints. Additionally, the LDY model could be applied as an essential tool to forecast future hydrologic situation under CC for concerned agencies to prepare CC adaptive measures i.e. land use management by reforestation or perennial planting, redesign or enhance capacity of hydraulic structures, and review of water management operating rule curves of water resources.

Material and Methods

Study area

Lam Dom Yai river basin is one of four main sub basins of the Lower Mun River Basin located in the northeast of Thailand. The basin is located in Ubon Ratchathani province covering 5,000 sq.km or one-third of the catchment area of the lower Mun river basin. At present most of the area is rainfed agriculture approximately 54% of the catchment area is rainfed paddy, 13% of field crops, and 13% of perennial, whereas only 15% of the area is forest. According to past land use maps, changing of forest area was vast decreasing from 34% in year 1985 to 25% in year 2000 and down to 16% in the year 2019, together with global CC effects, consequently more severe droughts and floods have been frequently occurred causing severe losses on environments, social and mainly on economic of agriculture sector in Ubon Ratchathani province, the fifth largest province of Thailand producing the third highest GPP of the northeast region. It is therefore essential to develop a tool to forecast future change of hydrologic response due to CC and LUC and applied for considering appropriate adaptive measures against the adverse effects.

Objectives

The objectives of the study aim to firstly developing a reliable hydrologic rainfall-runoff model of Lam Dom Yai River Basin, considering dynamic basin parameters comparing to static basin parameters, and secondly studying how CC affecting river runoff i.e. average annual flows, monthly flows, and extreme daily flows in near future period (2022-2047), mid future period (2048-2073), and far future period (2074-2099).

Methodology

A mathematical hydrologic (Rainfall – Runoff) model named Arc SWAT (version 2012.10) was developed for the study basin on the principle of soil water balance equation as follow;

$$SW_t = SW_0 + \sum_{i=0}^{n} \left(P_{day} - Q_{surf} - E_a - W_{seep} - Q_{qw}\right)$$

where SW_t is the soil moisture (mm) at the time i, P_{day} is the precipitation (mm), Q_{surf} is the streamflow (mm), E_a is evapotranspiration (mm), W_{seep} is the water flow to the unsaturated zone (mm), and Q_{qw} is the ground water flow (mm).

Study Approach is depicted in Figure 2 comprising two main procedures i.e. (1) SWAT Model development consisting of input data, calibration and verification by static and dynamic parameters (2) Simulation of future river runoff.

1. Model Development

1.1 Model Input Data

Three key physical data are basically required by the Arc SWAT model, i.e. 1) topographic map or digital elevation model (DEM) of 1:50,000 scale, 2) soil series map of 1:250,000 scale, and 3) land use maps of 1:50,000 scale of four different years, i.e., year 2000, year 2008, year 2017, and year 2019 as shown in Figures 1, 3 and 4, respectively.

The other type of data is meteo-hydrologic data comprising (1) daily maximum and minimum temperatures of the meteorologic station at Amphoe Muang Ubon Ratchathani and data set of six rain gauge stations were selected basing on well - spreaded locations and valid observed data availability (2) daily streamflow data set of six selected discharge stations were used for model calibration namely M152, M153 and M154 in the upstream reach, M170 in the middle reach, and TS7 and LDY at Lam Dom Yai Regulator in the downstream reach, respectively, (Figure 1).

1.2 Model Calibration

Calibration of the SWAT model's groups of parameters mainly comprising surface runoff, groundwater, river channel, soil type, land cover, were accomplished by upstream, middle, and downstream reaches with the past recorded data of climate, hydrology and land use maps during the period of 2001-2017. Four consecutive periods of 4-5 years were calibrated to obtain dynamic parameters of each period whereas the static parameters were calibrated by only one best set of parameters through 17 years of calibration period.

To obtain more accurate results, three more land use maps of the year 2005, 2012 and 2015 which were simulated by CA Markov's model using following equation of transition probabilities matrix were added.

$$S(t+1) = P_{ij} \times S(t) \qquad (1)$$

Where $S(t), S(t+1)$are the system status at the time of t or $t+1$; P_{ij} is the transition probability matrix in a state which is calculated as follows;

$$P_{ij} = \begin{bmatrix} P_{11} & P_{12} & \cdots & P_{1n} \\ P_{21} & P_{22} & \cdots & P_{2n} \\ \cdots & \cdots & \cdots & \cdots \\ P_{n1} & P_{n2} & \cdots & P_{nn} \end{bmatrix} \qquad (2)$$

$$\left(0 \le P_{ij} < 1 \; and \; \sum_{j=1}^{N} P_{ij} = 1 \, . \, (i.j = 1,2,\ldots,n)\right)$$

1.3 Model Verification

According to no available observed data in the upper basin since 2010, verification with the observed stations at middle reach (M170) and downstream reach (TS7 and LDY) during 2018 to 2021 were applied.

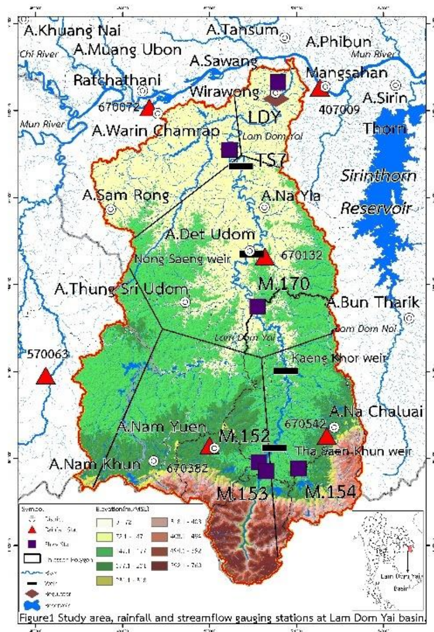

Figure 1 Study area, rainfall and streamflow gauging stations at Lam Dom Yai basin

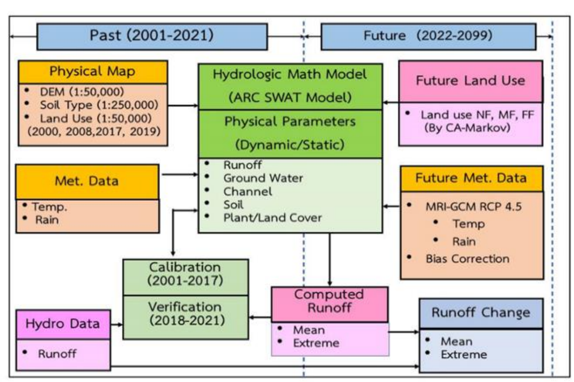

Figure 2 Conceptual approach of the study

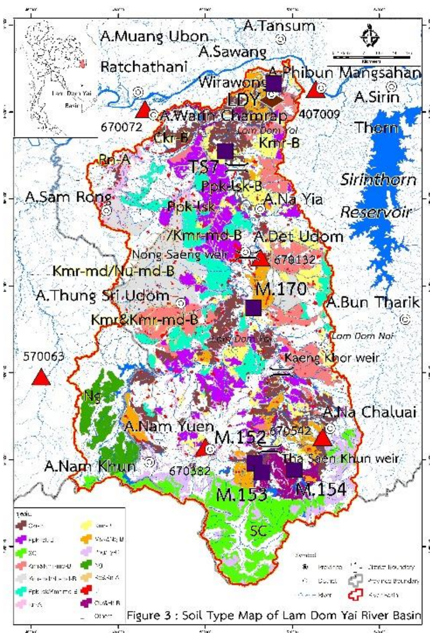

Figure 3 Soil type map of Lam Dom Yai river basin

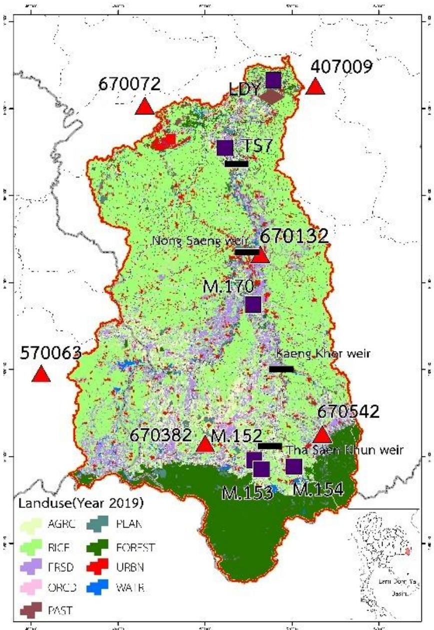

Figure 4 Land use map of year 2019

1.4 Comparison of Model's Parameters

Reliability of the model applying dynamic parameters and static parameters were compared by utilizing three indicators at good performance rating i.e. 1) Correlation coefficient (R^2) ranging 0.75-0.85, 2) Nash–Sutcliffe Coefficient of Effective (NSCOE) ranging 0.7-0.8, and 3) Bias factor (BIAS) ranging ±5-10% [17].

2. Simulation of Future River Runoff.

The calibrated model was then adopted as the tool for simulation of the river runoff under future CC condition from 2022 to 2099. Three future time periods were defined as near future (NF) for years 2022-2047, mid future (MF) for years 2048-2073, and far future (FF) for years 2074-2099, respectively. Following data were prepared,

2.1 Future Climate Data

Future daily climate data set of temperature and rainfall during 2001-2099 were obtained from the GCM model. The Hydro – Informatics Institute (HII) of Thailand has manipulated various GCM data for Thailand by statistical downscaling technique. Rainfall data of MRI –GCM model were selected since the MRI-GCM model utilized finer grid resolution and the resulted R^2 and S.D. of the downscale data compared to observed data were more preferable both temporal and space to those of other six GCM models [18].

The downscaled MRI-GCM rainfall data of RCP 4.5 were manipulated bias correction using the Standard Deviation Ratio (SDR) method [19]. The SDR method presented good results of R^2 and SD in term of temporal and space in wet season and especially in dry period comparable to the other methods, [18].

2.2 Future Land Use Map

Future land use maps were periodically generated for three future periods interval from 2022 to 2099 by CA-Markov method [20, 15] based on past land use changing rate during 2010 – 2019.

2.3 Future Parameters

Model parameters were applied using both the resulted static and dynamic parameters changing rate obtained from the calibration.

Results

Calibration and Verification Results

Figures 5 to 7 show results of daily simulated flows compared to observed flows and correlation coefficients of upper to downstream reaches. The calibrated results using static parameters showed significant reliability ranges of R^2 (0.75-0.94), NSCOE (0.75-0.93), and BIAS (4.84-13.13). The verified results showed good compatibility with observed data both in hydrograph pattern and magnitude. The resulted indicators of R^2, NSCOE, and BIAS were in the ranges of 0.65-0.95, 0.60-0.93, and 3.6-16.65%, respectively.

The calibrated results using dynamic parameters showed better significant reliability ranges of R^2 (0.80-0.96), NSCOE (0.75-0.96), and BIAS (4.8-12.0%). The verified results indicated good compatibility with observed data. The resulted ranges of R^2, NSCOE, and BIAS were 0.76-0.98, 0.70-0.94, and 1.37-7.7%, respectively. The daily, monthly, and annual flows resulted from using static parameters showed small less significance test of R^2, NSCOE, and BIAS than those using dynamic parameters.

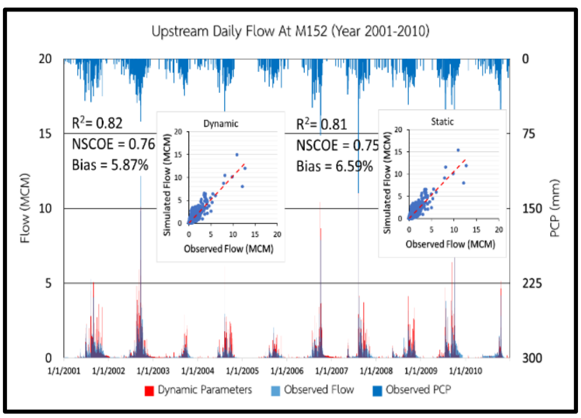

Figure 5 Calibrated results of daily flows at M152 (upstream reach) by dynamic and static parameters

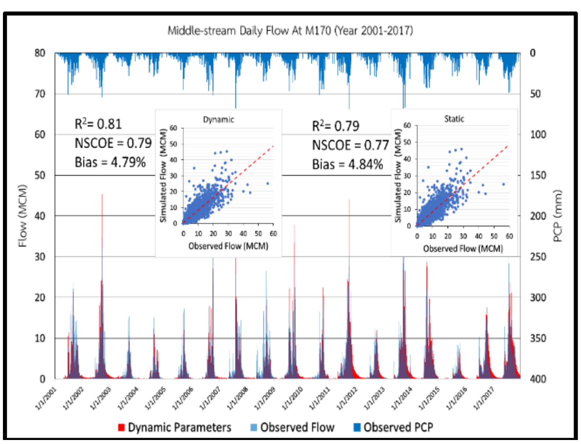

Figure 6 Calibrated results of daily flows at M170 (Middle reach) by dynamic and static parameters

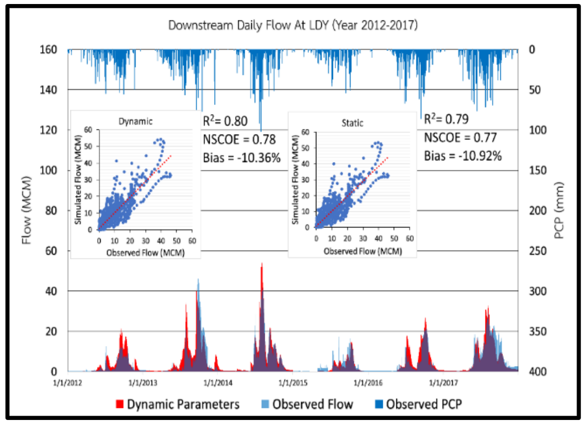

Figure 7 Calibrated results of daily flows at LDY (downstream reach) by dynamic and static parameters

Results of Model Parameters

Key parameters concerned were adopted referring to previous studies on main parameters significantly affecting runoff calculation [21, 22].

1. Static Parameters

In case of static parameters, the calibrated parameters were assumed constant upon calibration period of which parameters summarized in Figure 8.

2. Dynamic Parameters

Following results of 8 selected key parameters values and their changing trends for future are presented in Figure 8,

1) Groundwater : Decreasing of AIPHA-BF(Baseflow alpha factor) and GWQMN (Threshold depth of water in the shallow aquifer required for return flow). Increasing of GW_DELAY (Groundwater delay) and REVAPMN (Threshold depth of water in shallow aquifer for revaporation).

2) Surface–runoff : Increasing of CN2.Mgt (Initial SCS CNII Value). Decreasing of OV_N (Overland N Value).

3) Channel : Increasing of CH-K2 (Effective hydraulic conductivity). Decreasing of CH-N2 (Manning N value for main channel).

4) Land cover : Decreasing of EPCO (Plant uptake compensation factor).

5) Soil : Increasing of ESCO (Soil evaporation compensation factor), SOL_AWC (Available water capacity of the soil layer), and SOL_K (Saturated hydraulic conductivity).

3. Future Conditions

3.1 Future Climates

Future rainfall data from the MRI–GCM scenario RCP 4.5 at six stations were bias corrected with observed rainfall data during past period as summarized in Table 1. All stations' data indicated increasing of future rainfall approximately 5-10% or equivalent to 6.7% in term of basin rainfall more than those of past period, whereas the average maximum and minimum daily temperature would be increased by approximately 1.0°C and 2.0 °C respectively in the far future period.

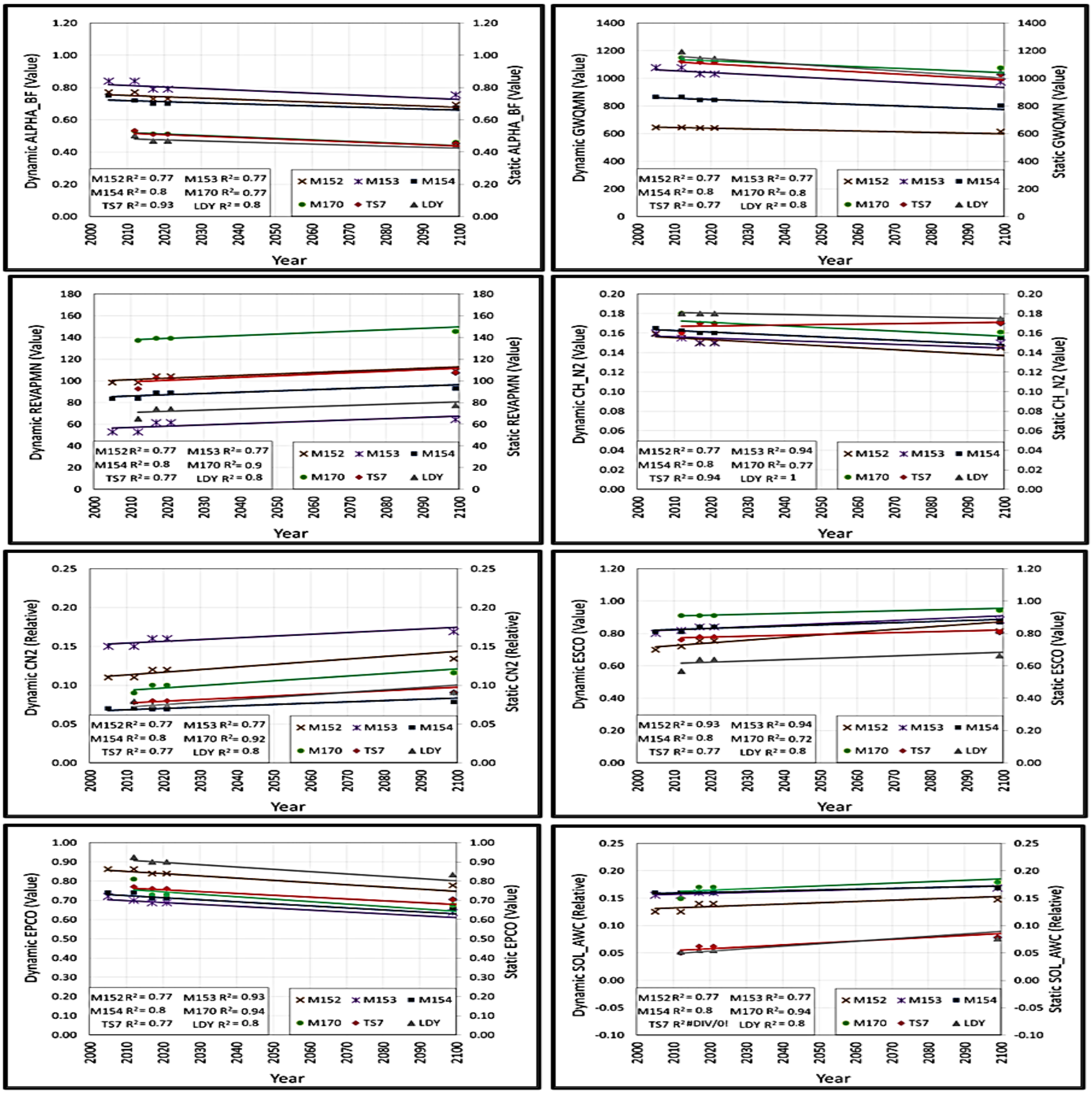

Figure 8 Adapted future SWAT's key dynamic and static parameters of Lam Dom Yai sub – basins

Table 1 MRI-GCM future rainfall and temperature, under CC scenario RCP 4.5

Stations	Average RCM Annual Rainfall (After Bias Correction), mm							
	2001-2021	2022-2047	Diff (%)	2048-2073	Diff (%)	2074-2099	Diff (%)	2022-2099	Diff (%)
Rainfall	PAST	RCM NF	fr. Past	RCM MF	fr. Past	RCM FF	fr. Past	Av. NF-FF	fr. Past
1.1) A. Na Chaluai STA. 670542	1431	1562	9.20	1569	9.63	1573	9.93	1568	9.58
1.2) A. Nam Yuen STA. 670382	1151	1202	4.49	1221	6.10	1252	8.81	1225	6.47
1.3) A. Det Udom STA. 670132	1371	1431	4.37	1465	6.91	1480	7.99	1459	6.42
1.4) A. Phibun Mangsahan STA. 670022	1432	1481	3.42	1594	11.34	1591	11.11	1555	8.62
1.5) A. Warin Chamrap STA. 670072	1292	1296	0.34	1409	9.10	1390	7.62	1365	5.68
1.6) A. Kantharalak STA. 570063	1333	1357	1.80	1490	11.76	1488	11.62	1445	8.39
Climate	Average Max and Min Daily Temperature, °C								
2.1) A. Meung Ubon	33	34	1.11	34	1.53	35	3.20	34	1.94
Ratchathani	23	24	7.71	25	12.39	26	14.58	25	11.56

3.2 Future River Runoff (RCP 4.5)

Figure 9 shows the results of the simulated daily runoff of future 78-years (2022-2099). The mean annual flows, using dynamic parameters would be higher than observed data in the past period at 22.8% for upstream reach (M152), 16.7% for middle reach (M170), and 6.1% for downstream reach (LDY), respectively as summarized in Table 2. Whereas mean annual flows using static parameters would also be higher than observed data in the past period at 9.8% for upstream reach (M152), 23% for middle reach (M170), and 4.9% for downstream reach (LDY), respectively. In summary, mean annual flows from the dynamic parameters would be greater than those from the static parameters for 1.2-13%.

In term of monthly basis, the model (dynamic parameters) indicated that future wet season flows would be greater than the past especially in October approximately 33% for M152, 24% for M170, and 6% for LDY. Whereas mean daily peak flows would be greater than those of the past at 18%, 31%, and 10%, respectively (Figure 10). In addition, the future higher flow hydrographs would be shifted later from September to October.

Future dry season flows would overall be greater than the past due to more rainfall but some months be drier than the past especially in the upstream and downstream river reaches during February and March in the range of 2-50%. Mean daily minimum discharges would be decreased at 0.7% for M152, increased at 33% for M170, and increased at 8% for LDY, respectively.

This implies future CC would affect LDY runoff on more volume, greater extreme flood flows, drier minimum flows in the upper reach, and deferred high flow occurrence period.

Table 2 Summary of future average annual flows by dynamic and static parameters. unit : (MCM/yr)

Stations	PAST (2001-2021)			NF (2022-2047)						MF (2048-2073)						FF (2074-2099)						Total (2022-2099)					
	Bs.PCP	$\bar{Q}$ (MCM/yr)		Bs.PCP		$\bar{Q}$ (MCM/yr)		$\bar{Q}$Diff (%)		Bs.PCP		$\bar{Q}$ (MCM/yr)		$\bar{Q}$Diff (%)		Bs.PCP		$\bar{Q}$ (MCM/yr)		$\bar{Q}$Diff (%)		Bs.PCP		$\bar{Q}$ (MCM/yr)		$\bar{Q}$Diff (%)	
	mm/yr	Dynamic	Static	mm/yr	Diif %	Dynamic	Static	Dynamic	Static	mm/yr	Diif %	Dynamic	Static	Dynamic	Static	mm/yr	Diif %	Dynamic	Static	Dynamic	Static	mm/yr	Diif %	Dynamic	Static	Dynamic	Static
M152 Upstream Reach	1151	101	98	1202	4.5%	124	100	23.4%	20.4%	1221	6.1%	133	108	31.7%	28.4%	1252	8.8%	137	115	36.2%	32.8%	1225	6.5%	124	108	22.8%	9.8%
M170 Midstream Reach	1368	962	944	1468	7.4%	1114	1088	15.9%	13.1%	1483	8.5%	1205	1196	25.3%	24.4%	1495	9.3%	1207	1198	25.5%	24.6%	1482	8.4%	1122	1161	16.7%	23%
Lamdomyai Downstream Reach	1309	1824	1787	1368	4.5%	1908	1818	4.6%	0.3%	1415	8.1%	1934	1879	6%	3.1%	1427	9%	1964	1928	7.7%	5.7%	1403	7.2%	1935	1875	6.1%	4.9%

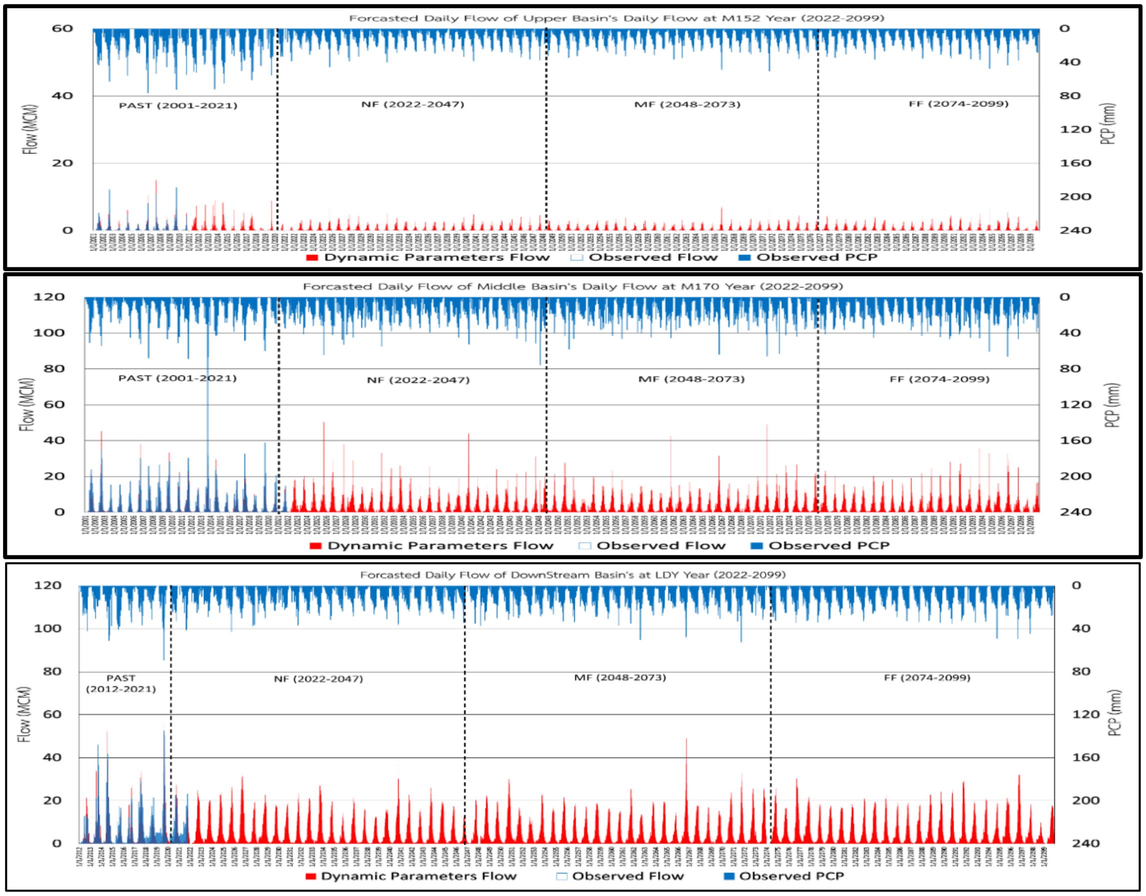

Figure 9 Forecasted future daily flows at M152, M170, and LDY (Year 2022-2099)

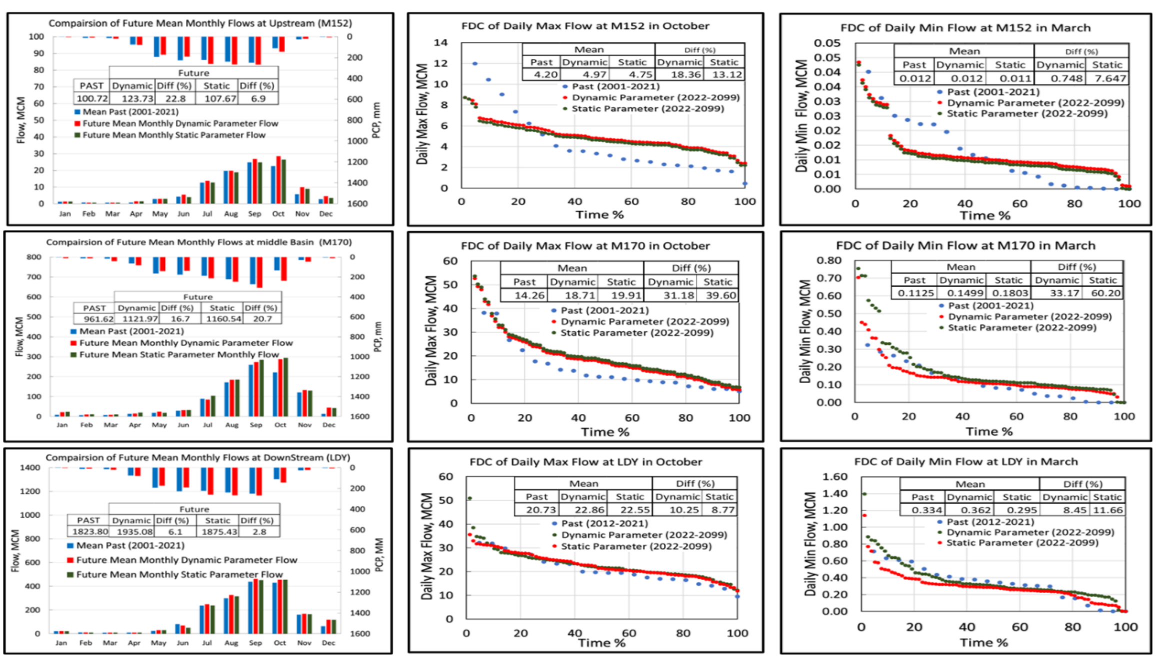

Figure 10 Future mean monthly flows, Flow Duration Curves (FDC) of daily maximum flow in October, and FDC of daily minimum flow in March

Conclusion and Recommendation

Conclusions

The developed SWAT model shows good correlation between computed flows and the observed flows in daily, monthly and annual basis. The results indicated that dynamic parameters give better correlation to the observed data. Consequently, forecasting future hydrologic response using dynamic basin parameters is recommended.

The future mean annual flows of the basin over 78 years using dynamic parameters would be increasing trend at 22.8%, 16.7%, and 6.1%, for upstream, middle, and downstream reaches, respectively which were more than those of applying static parameters by 13.0%, 6% and 1.2%, respectively.

Recommendations

1. The study has not taken into account irrigation water usage along the river and tributaries. The existing irrigation areas of 30,000 rai utilized water from the river approximately average flow volume of 40-50 mcm per year. Consequently, the calibrated flows especially in dry reason would be calculated more volume than observed flows. Further studies on the irrigation water demand and other main demands should be considered.

2. LDY' s overbank flood flows could not be actually field measured, instead, responsible agencies calculated the floods by applied rating curve extrapolation technique of which results might be deviated from the actual flows. A hydrodynamic model calibrated with floodplain flow velocity should be additionally developed in parallel to rectify overbank flows for further study.

3. Monitoring and review of model's parameters of LDY should be manipulated in the future to improve the changing trend and rates of the parameters. Other adjacent river basin models are suggested to be developed and comparison study of applying dynamic parameters and static parameters should be prepared. Sufficient results of model parameters could be analyzed and summarized as regional basin parameters that could be applied for modeling other ungauged river basins.

4. Further researches on quantitative effects of LUC on the river flow regime comparable to effects of CC should be examined.

5. Further applications on feasible land use management measures (e.g. reforestation, crop planning), design revision of existing and future hydraulic structures' capacities, and review of operating rule curves of water resources, should be carried out to alleviate CC problems.

Acknowledgement

Sincerely thanks to RID, MD, HII, and DLD, who kindly supported all valuable data, especially RID Region 7's officers who supported updated essential data, information, and hospitality accompanying during site investigation.

References

[1] David, Neeli. J. 2011. Climate Change and Climate Modeling, Library of Congress Cataloging in Publication data. WWW.cambridge.org/9780521841573.

[2] Jones R. G., et al. 2004. Generating High Resolution Climate Change Scenarios Using PRECIS. Report, Met Office Hadley Centre.

[3] Long, P. H., Hannu. L., Matti, K., Jorma, K., Michelle, T. H. v. V., Iwan, S., Rik, L., Pavel, K., & Fulco, L. 2016. Mekong River flow and hydrological extremes under climate change. *Hydrology and Earth System Sciences 20* (7), 3027-3041. https://doi.org/10.5194/hess-20-3027-2016

[4] Babak, F., Anil, G., Saman, R., Monireh, F. and Danielle, J. M. 2017. An integrated modelling system to predict hydrological processes under climate and land-use/cover change scenarios. *Water* 2017, 9, 767.
From https://doi.org/10.3390/w9100767

[5] Shrestha, M., Shrestha, S., Datta. and Avishek. 2017. Assessment of climate change impact on water diversion from the Bago River to the Moeyingyi Wetland, Myanmar. *Current Science, 12*(2), 377-384.

[6] Farinosi, F., Arias, E. M., Lee, E., Longo, M., Pereira, F.F., Livino, A., Moorcroft, R. P. and Briscoe, J. 2019. Future Climate and Land Use Change Impacts on River Flows in the Tapajos Basin in the Brazilian Amazon. *Earth's Future*, Vol.7, Issue 8.

[7] Wuthiwongyothin, S., Su, H. J., Ishidakei, K. and Levent, K. M. 2017. The effect of climate change on hydrology based dynamically downscaling and physically downscaling and physically-based hydrology model at Upper Ping river basin, Thailand. *Internet Journal of Society for Social Management Systems*, *11*(1).

[8] Seonhui, N., Mikyoung, C., Kwansue, J. and Jinhyeog, P. 2019. Prospect of discharge at Daecheong and Yongdam Dam Watershed under future greenhouse gas scenarios using SWAT Model. *Engineering Journal*, *23*(6). From https://doi.org/10.4186/ej.2019.23.6.469

[9] Nguyen, T. H., Le, H. T., Vo, N. Q. T., Duong, N. M., Nguyen, D. L., & Nguyen, K. L. 2017. Assessing the impacts of climate change on water resources in the Srepok watershed, Central Highland of Vietnam. *Journal of Water and Climate Change, 8*(3), 524-534. https://doi.org/10.2166/wcc.2017.135

[10] Chem, H., Fleskens, L., Baartman, J., Wang, F., Moolenaar, S. and Ritsema, C. 2020. Impacts of land use change and climate effects on streamflow in the Chinese Loess Plateau : A meta-analysis. *Science of The Environment* Vol.703, 134989.

[11] Yang, L., Feng, Q., Yin, Z., Deo, C. R., Wen, X., Si, J. and Li, C. 2017. Separation of the Climate and Land Cover Impacts on the Flow Regime Changes in Two Watersheds of Northeastern Tibatan Plateau. *Hindawi Journals*, Vol.2017. from https://doi.org/ 10.1155/2017/6310401.

[12] Rodrigues, L. E.,Elmiro, A.T., M., Braga, A.F., Jacobi, M. C. and Rossi, D.R. 2015. Impact of change in land use in the flow of the Para' River Basin, MG. Scielo Vol.19.no.1.

[13] Zhengxiang, Y., Xiuling, M., Liangliang, D. and Tijiu, C. 2020. Assessments of impacts of climate and forest change on water resources using SWAT model in a Subboreal watershed in northern Da Hinggan Mountains. *Water 2020, 12*(6), 1565. https://doi.org/10.3390/w12061

[14] Kiplagat, K. D., Kollongei, K., & Kiptum, K. 2018. Modelling the Impacts of land Use Change on Stream Flow in the Kimwarer Catchment Using Swat. *American Journal of water Science and Engineering*, 2018; Vol.4(4): 107-116 ISSN: 2575-1875.

[15] Sriworamas, K., Prasanchum, H. and Supakosol, J. 2019. The effect of forest rehabilitation on runoff and hydrological factors in the upstream area of the Ubonratana Reservoir in Thailand. *Journal of Water and Climate Change*, 2019039. from https://doi.org/10.2166/wcc.2019.039

[16] Tan L. M., Gaaman W. P., Srinivasan R., Arnold G. J. and Yang Y. X. 2019. A Review of SWAT Studies in Southeast Asia: Applications, Challenges and Future Directions. Water 11(5): 914. from https://DOI:10.3390/w11050914

[17] Moriasi, D. N., Gitau, M. W., Pa, N., Dagupati, P. 2015. Hydrologic and water quality models: Performance measures and evaluation criteria, American Society of Agricultural and Biological Engineers, Vol. 58(6): 1763-1785.

[18] Chaowiwat, W. 2013. Adoptation of Reservoir Operation to Climate Change Conditions: Sirikit Dam, Thailand. From http://cuir.car.chula.ac.th/handle/123456 789/42551

[19] Cheng, C. S. and Li, Q. 2008. Auld H. Statistical downscaling of hourly and daily climate scenarios for various meteorological variables in South-central Canada. *Theor. Appl. Climatol*. 2008; 91: 129-147.

[20] Lingling, S., Chao, Z., Jianyu, Y., et.al., 2011. Simulation of Land Use Spatial Pattern of Towns and Villages Base on CA-Markov Model. Mathematical and Computer Modelling 54 (2011), 938-943.

[21] kushwaha, A., Jain, K. M. 2013. Hydrological Simulation in a Forest Dominated Watershed in Himalayan Region using SWAT Model. Water Recour Manage (2013) 27: 3005-3023. https://doi/ 10.1007/s11269-013-0329-9

[22] Kubah, S., Jain, M. 2017. Rainfall-Runoff Modeling of a River Basin using SWAT Model. International Journal of Engineering Research & Technology (IJERT), Vol. 6 Issue 12, December – 2017.

Thai Environmental Engineering Journal Vol. 36 No. 2 (2022) : 35-43
www.eeat.or.th

COD Removal Efficiency of Pararubber Wastewater by Ozonation using the Central Composite Design Model

Siramanee Chinlee[1] and Wipada Dachapanya[2*]

[1]Master Program in Environmental Engineering, Faculty of Engineering,
Ubon Ratchathani University, Ubonratchathani 34190, Thailand
[2]Faculty of Engineering, Ubon Ratchathani University, Ubonratchathani 34190, Thailand
[*]E-mail : wipada.d@ubu.ac.th, siramanee.chi@gmail.com

Abstract

Pararubber is one of the major plants contributing to both Thai and Asian's economy. Pararubber wastewater having a high strength can cause several environmental problems to community nearby the industry. The research aimed to study the characteristics of pararubber wastewater and investigate the optimal conditions for treatment of pararubber wastewater using the ozonation process. The results revealed that the pararubber wastewater has a black color with a pungent odor like sludge from a septic tank. Wastewater characteristics obtained from the preliminary analysis are as follows; pH of 4.99, Chemical Oxygen Demand (COD) of 55,448.52 mg/L, Total Dissolved Solid (TDS) of 10,240 mg/L, and SS of 1,516.67 mg/L. Factors affecting the ozonation process studied are dosage rate of ozone and contact time. The Central Composite Design (CCD) model or box-wilson design, which is an experimental design at 3 levels (popularly represented by symbols -1, 0, +1) and useful in response surface methodology (RSM) for generating a second order (quadratic) model for the response variables, was applied to investigate the optimal condition for the treatment process. From the results, it was found that both of factors significantly affected the COD removal efficiency and can be expressed in the form of equations or a mathematical model for predicting COD removal efficiency, in which %COD R.E. = 13.3408 + 0.0613A + 0.5587B + 0.000619A*B - 0.000063A^2 - 0.004270B^2. The coefficient of determination was 92.14%. The mathematic model was applied to develop the graph displaying the relationship between these two factors and COD removal efficiency using the Responsive Surface Methodology. It was found that the removal efficiency of COD was increased with increasing contact time and dosage rate of ozone, which has a maximum value of 89.67% at ozone dosage rate of 900 mg/hr and contact time of 120 minutes.

Keywords : Wastewater treatment; Pararubber wastewater; Ozonation; Response surface methodology; Central Composite design model

Introduction

The pararubber processing industry is one of the industries that is important to Thai economy in terms of both income and employment. Thailand is one of the leaders in pararubber producer with the product of 4.5 Mton/yr accounting for 35.7% of the world's production [1]. The pararubber processing industry, however, produces high strength of wastewater from the production process. Pararubber wastewater have a very high concentration of organic matter and acid odor which leads to pollution problems affecting community nearby. There are several methods for treating pararubber wastewater such as anaerobic filter, UASB, and biological method incorporated with sulphate reduction system, which are the conventional systems [2, 3]. In addition, there are advanced or alternative processes including electro chemical method, solar distillation systems, flocculation and flotation method, Fenton process, and so on [4-7]. Previous studies revealed that the advanced oxidation process is one of the treatment processes that have been found to be effective in reducing pollutants in wastewater or change them into more easily degradable compounds using hydroxyl radical which is a strong oxidizing agent that can oxidize various toxic organic matter [8]. This research uses ozonation process for treatment of pararubber wastewater. Ozone is a strong oxidant and can react with many substances by both direct and indirect reaction especially the indirect oxidation mechanism has a better ability to oxidize when ozone reacts with wastewater to break down into hydroxyl radical ($OH^{\bullet}$), which are highly susceptible to oxidizing organic compounds as well. Ozone degrades chemical bonds of complex organic compounds into simple structures [7]. In addition, ozone is readily converted to oxygen, which is beneficial for water. Thus this technology does not create further problems such as odor, taste, and chemical residual in water. Therefore, ozone can be applied to treat wastewater including wastewater from the pararubber processing industry [7].

The response surface methodology (RSM) is a method of experimental design and statistical analysis. RSM is widely used to analyze the relationship of variables where the responds of interest depends on several variables [9]. The purpose of the RSM is to determine the best value of the response or of the experiment. The analyzed experimental results will come out in the form of a set of correlation equations. Currently, there are complete programs such as Design-Expert that have been developed to help in the complexity of processing data quickly and accurately including displaying the data and presenting the conclusions of the experimental results in both variables and graphs. Treatment efficiency of ozonation process can be affected by several factors including dosage rate of ozone and contact time. The objective of this research was to study the characteristics of pararubber wastewater and investigate the suitable conditions for treatment of pararubber wastewater using ozonation process. The Central Composite Design (CCD) model is the most commonly used fractional factorial design in the response surface model. In this model, the center points are augmented with a group of axial points called star points. With this design, quickly first-order and second-order terms can be generated for the response variables without requirement of using a complete three-level factorial experiment [10]. Thus, the CCD with Design-Expert (Trial Version 13), which is a widely used tool for experimental design and statistical analysis [11], was exploited to obtain the optimal conditions and statistical analysis.

Methodology

Analysis of pararubber wastewater characteristics

Pararubber wastewater from a pararubber factory in Ubonratchathani province was sampled and analyzed prior to the ozonation treatment. The characteristics of water sample is shown in Table 1 [12].

Table 1 Analysis of Wastewater parameters and methods

Parameters	Method	characteristics of pararubber wastewater
1. pH	pH Meter	4.99 ±0.01
2. COD (mg/L)	Close Reflux, Colorimetric Method	55,448.52 ±192.39
3. Suspended solid; SS (mg/L)	Gravimetric Method	1,516.67 ±16.07
4. Total dissolved sold; TDS (mg/L)	Gravimetric Method	10,240 ±9.54

Ozone dosage rate measurement

Ozone dosage rate obtained from the ozone generator' were performed followed the standard method [12]. The first step is passing the ozone gas through two serial KI trap (Traps A and B) for about 10 min. For best results, gas flow rate should be kept below approximately 1 L/min. Each trap is a gas washing bottle containing a known volume (at least 200 mL) of 2% KI. Contents of each trap was quantitatively transferred into a beaker. Next, 10 mL of 2N H_2SO_4 was added and titrated with standardizer (0.005N $Na_2S_2O_3$) until the yellow iodine color almost disappeared. Then, adding 1 to 2 mL starch indicator solution and continue titrating until the blue color disappeared. A known volume (at least 200 mL) of sample was added into a separate gas washing bottle (label gas washing bottles to avoid contaminating the reaction vessel with iodide). Finally, ozone gas was directed through this reaction vessel [12]. The equation for calculating dosage rate of ozone is shown in Equation 1 [12].

$$\text{Dosage rate of ozone (mg/min)} = \frac{(A+B)\times N\times 24}{T} \quad (1)$$

In which
A = mL titrant for trap A
B = mL titrant for trap B
N = Normality of $Na_2S_2O_3$
T = Ozonation time, min

Experimental design

Treatment of pararubber wastewater using ozonation were conducted to study the impact of ozone dosage rate and contact time on COD removal efficiency. These two factors were varied as shown in Table 2. The CCD model was applied for experimental design. Totally, there were 13 sets of experiments as shown in Table 3, triplet of each set were repeated. Wastewater from a pararubber processing industry was collected and diluted with the ratio of 1:10 so that the COD value of water sample would be in the range of 5,000-6,000 mg/L, which is about 5 times of the COD value from our previous work [7]. Ozone was blown into 2 L of diluted wastewater in a 5 L Erlenmeyer flask closed system as displayed in Fig. 1.

Mathematical model derivation, statistical analysis, and model validation

The mathematical model derivation and statistical analysis were carried out by the Design-Expert (Trial Version 13). The first part involved the model derivation and the second part included the analysis of variable variance (ANOVA). In this step, the mathematical model or empirical regression model and graphical data (ANOVA, variance analysis) were obtained from analysis of the optimal response of the operation factors via the RSM model. Analysis of variance examines the sources of variance for a model based on the P-values of the terms in the tables of the analyzed variance compared to the given statistical significance. Equation 2, a second-degree polynomial regression model, was obtained from the experimental data of 13 runs that were analyzed through the CCD matrix [13].

$$y=\beta_0+\sum_{i=1}^{k}\beta_i X_i+\sum_{i=1}^{k}\beta_{ii}X_i^2+\sum\sum_{i<j}\beta_{ij}X_iX_J+\varepsilon \quad (2)$$

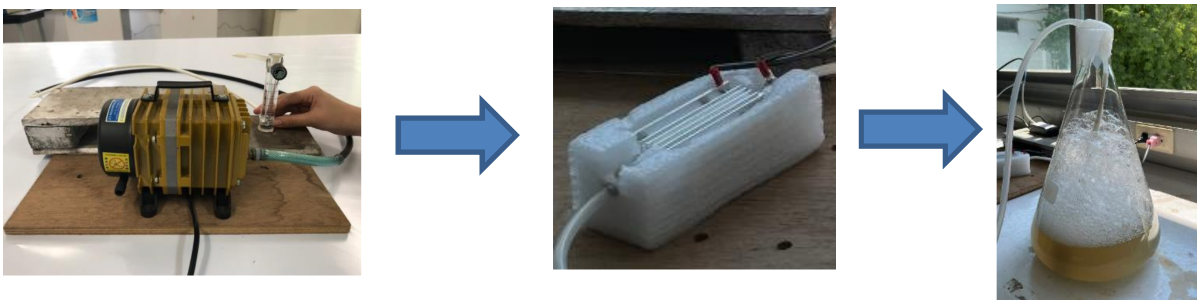

Figure 1 Experimental set up of wastewater treatment by ozonation process

Table 2 Degree of factors

Factors	level		
	low	middle	high
1. Dosage rate of ozone (mg/hr)	500	700	900
2. Contact time (min)	60	90	120

Table 3 Sets of experiment received from the CCD model

Experiments	Dosage rate of ozone (mg/hr)	Contact time (min)
1	500	60
2	900	60
3	500	120
4	900	120
5	500	90
6	900	90
7	700	60
8	700	120
9	700	90
10	700	90
11	700	90
12	700	90
13	700	90

in which y is the predicted response, X_i, X_j are experimental factors, k is number of factor, β_0 is a constant, $\beta_i, \beta_{ii}, \beta_{ij}$ are regression coefficients, $\sum_{i=1}^{k} \beta_i X_i$ is a linear effect term, $\sum_{i=1}^{k} \beta_{ii} X_i^2$ is a quadratic effect term, and $\sum\sum_{i<j} \beta_{ij} X_i X_J + \varepsilon$ is a cross-product effect term.

The quadratic model received from the RSM was validated by conducting a set of experiment under the following conditions; the ozone dosage of 600 mg/hr and contact time of 100 min. COD removal efficiencies obtained from the experiment and model prediction were compared to ensure the model validation.

Investigation of the optimal conditions

Determination of the optimal factor for optimal treatment efficacy was performed by using the response optimizer function in a statistical program. The response optimizer function was exploited to explore the level of the optimal conditions with the measured Composite Desirability: D, which has a value between 0-1. If D value is equal to 1, the response is completely satisfied [14].

Results and Discussions

Analysis of pararubber wastewater

From the characteristics analysis of pararubber wastewater using the methods in Table 1, it was found that the values of COD, TDS, SS, and pH were 55,448.52±192.39 mg/L, 10,240±9.54 mg/L, 1,516.67±16.07 mg/L, and 4.99±0.01, respectively. Pararubber wastewater also has strong acid odor and dark brown color.

Treatment of pararubber wastewater using ozonation

1. COD removal efficiency

COD removal efficiencies obtained in this study were in the range of 60-90%, which are comparable with the results from previous study [7]. The effluent properties pass the standards [15] and can be released into natural water sources. COD removal efficiencies received from the experiments and model prediction are listed in Table 4. As seen from the table, the predicted values are in a good agreement with the experimental values. Thus, it can be concluded that this mathematical model is accurate. Then the data of COD removal efficiency were input into the Design Expert model to check for the data accuracy.

2. Statistical analysis

2.1 Mathematical model and variance analysis

In this part, mathematical model for predicting COD removal efficiency of pararubber wastewater treatment by ozonation process was derived from the RSM model. The final empirical model suggested by the RSM model was the quadratic model as written in Equation 3. The P-value of the quadratic equation (Equation 3) is 0.0275 indicating that the quadratic model is significant. The P-value of Lack-of-Fit is higher than 0.05 and the R^2 of 0.9235 is in reasonable agreement with the adjusted R^2 of 0.8689 (the difference is less than 0.2) as shown in Table 5. Thus it could be concluded that the accuracy of the quadratic model is satisfied [16-17].

$$\text{COD R.E.} = 13.3408 + 0.0613A + 0.5587B + 0.000619A*B - 0.000063A^2 - 0.004270B^2 \quad (3)$$

In which COD R.E. = COD removal efficiency (%)
A = dosage rate of ozone (mg/hr)
B = contact time (min)

The results show that most of the terms in Equation 3 except for the second last and the last term have significant effect on COD removal using ozonation. Table 6 demonstrates the variance analysis for response surface quadratic model. The statistical significance for the regression coefficient of the model terms were confirmed by the p-value (less than 0.0500). The model F-value of 16.90 implies the model is significant. From the results, it is could be concluded that the quadratic model can be successfully applied to predict the optimum conditions for the response of the maximum COD removal efficiency via ozonation.

Figure 2 demonstrates the normal percent probability versus externally studentized plot of the residuals. As seen from the figure, it is confirmed that any apparent problems with the normal probability plot could not be observed. A good relationship between input and output variables could be derived from the quadratic model that was established by forming a normal probability plot of the residuals. The normality assumptions were assured as the residual plot approximated along a straight line indicating that the quadratic model is accurate for decision.

Table 4 Comparison of COD removal efficiencies from experiments and model prediction

Experiments	Dosage rate of ozone (mg/hr)	Contact time (min)	COD removal efficiency (%)	
			Experimental values	Predicted values
1	500	60	63.24±0.52	65.02
2	900	60	68.86±0.45	69.22
3	500	120	69.18±0.48	71.00
4	900	120	89.16±0.48	90.06
5	500	90	75.45±0.92	71.85
6	900	90	84.25±1.52	83.49
7	700	60	71.78±0.49	69.64
8	700	120	85.26±0.05	83.04
9	700	90	81.64±0.48	80.18
10	700	90	76.25±0.49	80.18
11	700	90	79.16±0.52	80.18
12	700	90	80.87±0.75	80.18
13	700	90	78.63±0.48	80.18

Table 5 Model summary statistics for COD removal

Source	R^2	Sequential p-value	Lack of Fit p-value	Adjusted R^2	Predicted R^2	
Linear	0.7043	0.0023	0.0423	0.6451	0.2834	
2FI	0.7865	0.0954	0.0588	0.7154	-0.2002	
Quadratic	**0.9235**	**0.0275**	**0.1956**	**0.8689**	**0.5898**	**Suggested**
Cubic	0.9325	0.7319	0.0670	0.8380	-3.8161	**Aliased**

Table 6 Variance analysis (ANOVA) for response surface quadratic model

Source	Sum of Squares	df	Mean Square	F-value	p-value	
Model	619.73	5	123.95	16.90	0.0009	**Significant**
A	203.00	1	203.00	27.69	0.0012	
B	269.61	1	269.61	36.77	0.0005	
A*B	55.20	1	55.20	7.53	0.0288	
A^2	17.45	1	17.45	2.38	0.1668	
B^2	40.80	1	40.80	5.56	0.0504	
Residual	51.33	7	7.33			
Lack of Fit	33.61	3	11.20	2.53	0.1956	**not significant**
Pure Error	17.71	4	4.43			
Cor Total	671.06	12				

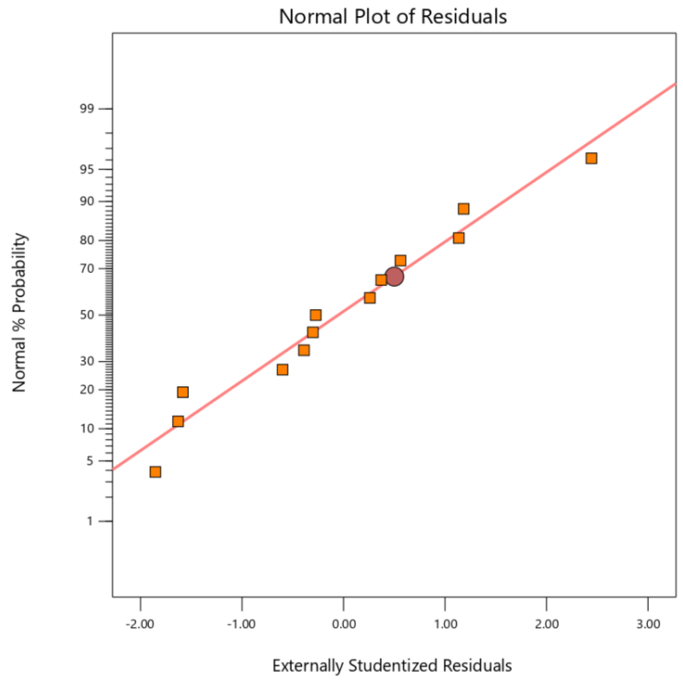

Figure 2 Normal percent probability of residuals versus externally studentized residuals plots for COD removal using ozonation

2.2 Model validation

The quadratic model or correlation equation between the response, which is the COD removal efficiency, and the affecting factors (ozone dosage rate and contact time) as obtained in Equation 2 was validated for the model accuracy for prediction. A set of experiment was conducted under the following conditions; the ozone dosage rate of 600 mg/hr and contact time of 100 min, to evaluate the model validation. The COD removal efficiencies obtained from the experiment and the model prediction were 75.94±0.58 and 77.67, respectively. The values are in good agreement confirming that the quadratic model received from the RSM can be successfully used to predict COD removal efficiency via ozonation.

2.3 Optimal conditions

Investigation of the optimum conditions for the removal efficiency of pararubber wastewater treatment by ozonation process was accomplished using the response optimizer function in a statistical package. A function is used to find the optimal value of a factor and measure the composite desirability (D), which has a value between 0-1. If D is equal to 1, then the result is completely satisfied. From the response optimizer results, five conditions were derived from the model, however, the optimal conditions suggested by the model were at the ozone dosage rate of 900 mg/L and the contact time of 120 min. Since these conditions yield the highest COD removal efficiency of 90.0605 and the D value of 1.000 as shown in Figure 3.

Upon receiving the optimal conditions from the model, a set of experiment (triplet runs) was conducted to confirm the optimal conditions. The average value of COD removal efficiency obtained from the experiment was 89.66±0.48, which agrees well with that from the model. This result confirms great appropriateness of the quadratic model for optimization of COD removal via ozonation.

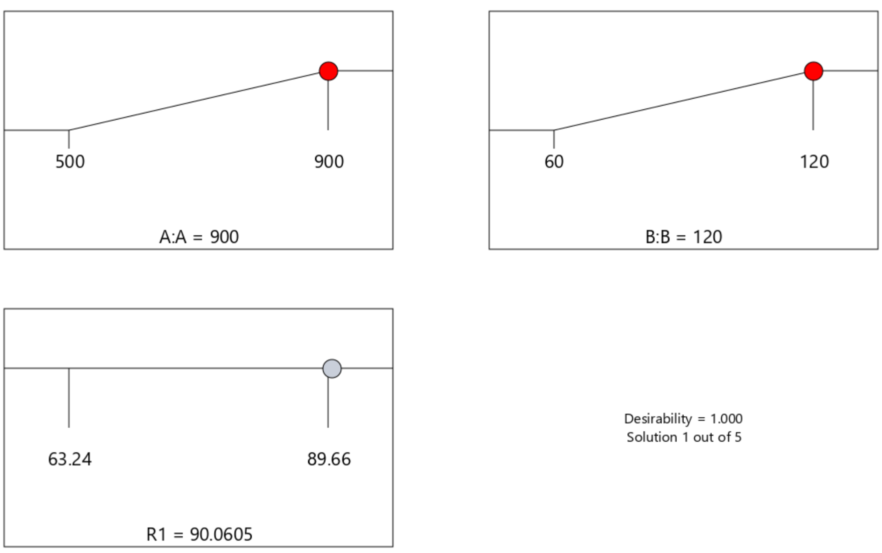

Figure 3 Desirability ramps for COD removal via ozonation at the optimal conditions

Conclusion

COD removal efficiency obtained in this study were in the range of 60-90%. The effluent properties pass the standards [15] and can be released into natural water sources. The most suitable mathematical model for prediction of COD removal efficiency was found to be a quadratic model. The optimal conditions suggested by the RSM model were at the ozone dosage rate of 900 mg/hr and the contact time of 120 min. The results from this study could be applied for the treatment of wastewater from pararubbing industry. However, the effect of pH on the COD removal efficiency should be further investigated.

References

[1] Dechapanya, W., Taweewut, K., Mungkornkaew, P. and Lakawipat, T. 2019. Treatment of Pararubber Wastewater Using Fenton Processes. UBU Engineering Journal. 12(2): 63-76.

[2] Anotai, J., Tontisirin, P. and Churod, P. 2007. Integrated Treatment Scheme for Rubber Thread Wastewater: Sulphide Precipitation and Biological Processes. Hazard Material. 14: 1-7.

[3] Mohammadi, M., Man, H.C., Hassan, M.A. and Phang Lai Yee, P.L. 2010. Treatment of Wastewater from Rubber Industry in Malaysia. African Journal of Biotechnology. 9(38): 6233-6243.

[4] Vijayaraghavan, K., Yazid, A.Y.A. and Ahmad, D. 2008. Electrolytic Treatment of Latex Wastewater. Desalination. 219(1-3): 214-221

[5] Srisuwan, N. 1996. Rubber Gloves Plant Wastewater Treatment by Floatation. Master of Science Thesis in Environmental Management. Prince of Songkla University.

[6] Tuprakay, S.R. and Tuprakay, S. 2015. Wastewater Treatment from Rubber Processing by Using Solar Distillation System. SDU Research Journal. 8(2): 35-52.

[7] Wongkamchao, Y. and Dechapanya, W. 2020. Optimization of Pararubber Wastewater Treatment using Fenton Process by Central Composite Design. Collection of articles in National Academic Conferences Ubon Ratchathani University. 226-235.

[8] Dechapanya, W., Nontula, S., Phudthabun, S., Sanongraj, S. and Mattaraj, S. 2022. Treatment of Gaseous Formaldehyde in a Gross Anatomy Laboratory Using Ozonation. Ladkrabang Engineering Journal. 39(1): 11-22.

[9] Maneesai, O. and Srisattayakul, P. 2014. A study the Optimization of Molybdenum Carbide Coating by Sputtering. Rajamangala University of Technology Krungthep.

[10] Bhattacharya, S. A. 2021. Central Composite Design for Response Surface Methodology and Its Application in Pharmacy. In book: Response Surface Methodology in Engineering Science. IntechOpen. 1-19. DOI: 10.5772/intechopen.95835.

[11] Tansomros, P. and Wichitpanya, S. 2021. Optimal Condition for the Removal of Copper (II) using Dowex-m4195 Chelating Resin. Senior Project in Environmental Engineering Program. Mahasarakham University.

[12] Rice, E.W. Bridgewater, L., American Public Health Association, American Water Works Association, and Water Environment Federation. 2012. Standard Method for the Examination of Water and Wastewater. Ed.22. Washington D.C.: American Public Health Association. 50-51.

[13] Chanpirak, A., Dumnin, P. and Hongpuay, A. 2018. Optimization of Oil Extraction from Spent Coffee Grounds (Coffea canephora var. robusta/Coffea Arabica) by Hexane Using Response Surface Methodology. The Journal of KMUTNB. 28(4): 799-811.

[14] Limratchapong, T. and Huayluek, N. 2019. Design of Experiment for Evaluating the Optimal Condition in Coffee Beans Roasting. Senior Project in Management and Logistics Engineering, College of Innovative Technology and Engineering, Dhurakij Pundit University.

[15] Announcement of the Ministry of Science Technology and the Environment. 1996. Determination of Standards for Controlling Wastewater Discharge from Sources of Industrial Factories and Industrial Estates.

[16] Montogomery, D.C. 2001. Design and analysis of experiments. New York: John Wiley & Sons Inc. 427-510.

[17] Suwannahong, K., Wongcharee, S., Kreanuarte, J. and Kreetachat, T. 2021. Pre-treatment of Acetic Acid from Food Processing Wastewater Using Response Surface Methodology via Fenton Oxidation Process for Sustainable Water Reuse. Journal of Sustainable Development of Energy, Water and Environment Systems. 9(4). DOI: https://doi.org/10.13044/j.sdewes.d8.0363.

Thai Environmental Engineering Journal Vol. 36 No. 2 (2022) : 45-53
www.eeat.or.th

Appropriate Forecasting Techniques Analysis for Number of Important Tourists Visiting Bangkok Forecasting Error Reduction After the COVID-19 Pandemic

Chatpon Mongkalig[*] and Nisakorn Nakornkao

Institute of Metropolitan Development, Navamindradhiraj University
Dusit District, Bangkok 10300, Thailand
[*]E-mail : chatpon@yahoo.com

Abstract

The objectives of this research are to analyze and conduct demand forecasting by using forecasting techniques in the Bangkok area. The study included conducting the experiments and determining the appropriate forecasting techniques for the number of tourists forecast in each of the top ten countries, which were the Thai tourists and tourists from the People's Republic of China, Japan, South Korea, India, UK, USA, Singapore, Malaysia, and Australia who come to travel and stay in Bangkok. The conducted demand forecasting included accommodation forecasting. In addition, medical and wellness tourism were additional study findings. Supply plan for tourist accommodation was proposed. Time series analysis methods including moving average, single exponential smoothing, double exponential smoothing, and Winters' method were used in the experiments for forecasting the number of tourists traveling and staying in Bangkok. According to the ANOVA, the forecasting method had a significant effect on MAPE and MAD. From the experimental results, it was found that the most suitable forecasting method was the Winters' method, with a seasonal length of 12 months. The focus group was conducted for the number of tourists forecasting verification and validation. For supply plan analysis, tourist accommodation optimistic demand (demand under normal situation) was higher than the tourist accommodation capacity by 47.86%. Additionally, tourist accommodation pessimistic demand (demand under new normal situation) was higher than the tourist accommodation capacity during the high season of December and January by 10.12%. For medical and wellness tourism, Thai government should formulate policies to drive the successful healthcare tourism. The promotion projects of medical and wellness tourism by increasing the supply of medical and wellness tourism, supporting the needs of various groups of tourists, and developing innovative medical research and new technologies should be conducted. These projects could increase the potential of Thailand medical and wellness tourism. Thailand's medical and wellness tourism yields high revenue at 1,200,000 million baht per year and is growing among the fastest in the world with an average growth of 13% per year. Moreover, the COVID-19 vaccination is an important strategy for the countries' main target group of tourists to minimize deaths, severe disease, curtail the health system impact, and fully resume socio-economic and tourism activity.

Keywords : Forecasting Techniques; Analysis of Variance; Forecasting Error Reduction; Time Series Analysis

Introduction

The 3R (Reduce-Reuse-Recycle) Concept is a sequence of steps on how to manage waste properly and prevent waste effects on environment. The top priority is Reduce, which is to reduce waste generation, then Reuse, and then Recycle. Demand forecasting and supply plan in excess will cause an increase in accommodation and food preparing for tourists, resulting in an increase in waste generation. Therefore, accurate forecasting the number of tourists in Bangkok is an important decision that affects waste reduction of tourism and decreases Thai tourism costs. According to the Thailand tourism statistics report of the Ministry of Tourism and Sports [1], the tourism business plays an important role in the Thai economic system. The income from tourism contributes to the economic value of the country. Tourism affects money circulation and income distribution for Bangkok. According to the report [1], it was found that income from tourism accounted for about 20% of the Gross Domestic Product, or GDP (the monetary value of the final goods or services produced within the country) [1]. The pandemic of coronavirus disease (COVID-19) resulted in a significant decrease in international tourists visiting Thailand during the year 2020 - 2021 when compared to the same period in 2019. Pareto chart of the target countries which had the highest ranking in terms of the number of tourists who visited and stayed in Bangkok was shown in Figure 1. Before the outbreak of COVID-19, the top ten countries which had the highest ranking in terms of the number of tourists who visited and stayed in Bangkok were Thailand, the People's Republic of China, Japan, South Korea, India, UK, USA, Singapore, Malaysia, and Australia, covering more than 80 percent of all tourists to Bangkok.

The objectives of this research are to analyze and conduct demand forecasting by using forecasting techniques in the Bangkok area; conduct the experiments; and determine the appropriate forecasting techniques for the forecasting of the number of tourists who visited Bangkok and came from the top ten countries, which were the Thai tourists and tourists from China, Japan, South Korea, India, UK, USA, Singapore, Malaysia, and Australia who come to travel and stay in Bangkok. The conducted demand forecasting included accommodation forecasting. In addition, medical and wellness tourism were additional study findings.

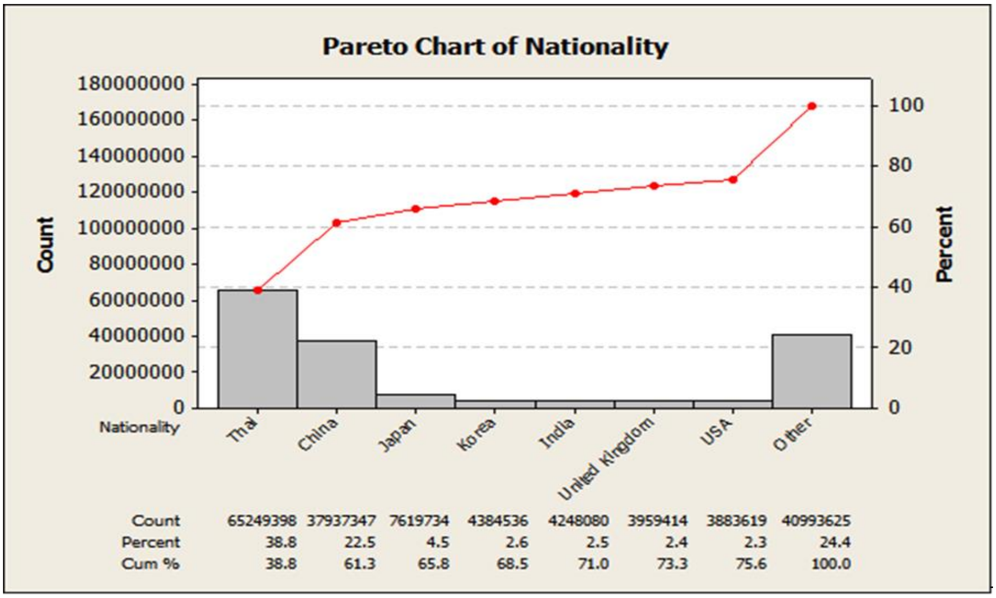

Figure 1 Pareto diagram of the number of tourists from the important countries

Methodology

Data from Thailand's tourism statistics report of the Ministry of Tourism and Sports [1] was collected prior due to the COVID-19 pandemic during the years 2015 - 2019. The data from the table named "Guest arrivals at accommodation establishments (monthly data)" [1] were used to forecast the number of target group tourists visited and stayed in Bangkok. The tool is to analyze and find the appropriate method for forecasting the number of target group tourists using the Time Series was the Analysis of Variance (ANOVA). The design of Experiment (DOE) [2] was used to analyze and find the most appropriate method that reduced the forecasting error between the fitted values and the actual numbers of the target group of tourists, which were the domestic tourists (Thai tourists), tourists from China, Japan, South Korea, India, UK, USA, Singapore, Malaysia, and Australia who travelled and stayed in Bangkok. The forecasting techniques include moving average, single exponential smoothing, double exponential smoothing, and Winters' method were applied [3]. The forecasting methods were analyzed as the factor for the demand forecasting error reduction [4]. Guidelines in planning to cope with the tourist demands (Supply Plan) [5], which were acquired from the suitable and effective forecasting method, are provided for tourism, hotels, and accommodation in Bangkok. The country is a blocking factor. The Randomized Complete Block Design (RCBD) was experimented. The response variables were the Mean Absolute Percentage Error (MAPE) and the Mean Absolute Deviation (MAD). The Analysis of Variance (ANOVA) was applied to determine the most appropriate forecasting method [6]. Prior to the Analysis of Variance (ANOVA), the ANOVA assumptions were checked in the Model Adequacy Checking [7] as follows:

The Mean Absolute Percentage Error (MAPE) was used in the Model Adequacy Checking.

According to the model adequacy checking, it was found that residuals were normally distributed in Figure 2. The independence assumption was checked in Figure 3. The variance of residuals was constant in Figure 4. Therefore, the ANOVA was suitable for the analysis of the forecasting method which had a significant effect on the Mean Absolute Percentage Error (MAPE) [8].

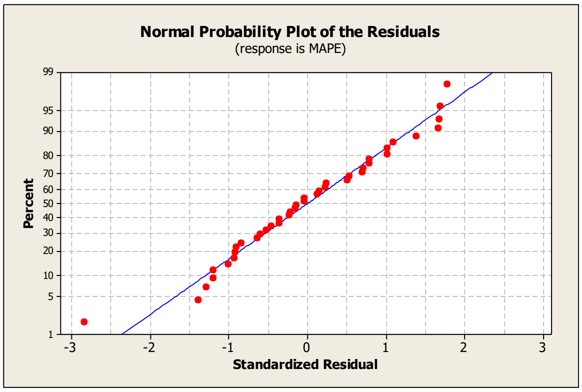

Figure 2 Normal probability plot of the residuals

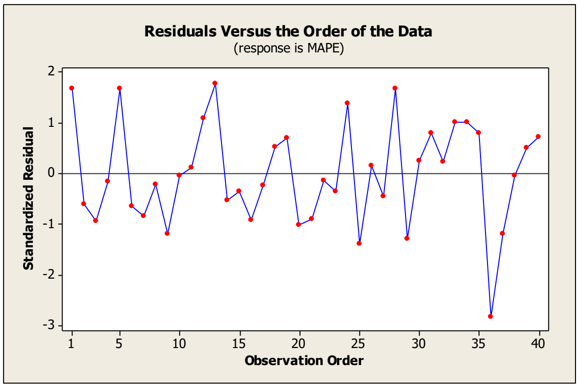

Figure 3 Independence assumption checking

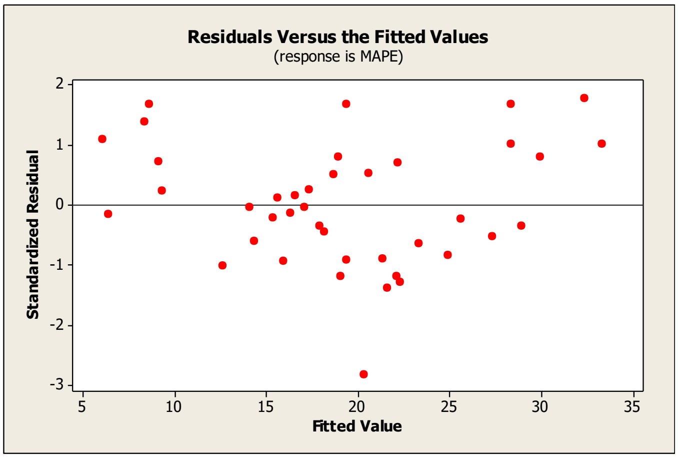

Figure 4 Constant variance assumption checking

Results and Discussion

Table 1 The ANOVA table for the experiment which MAPE was the response variable

General Linear Model: MAPE versus Forecasting Method, Country

Factor	Type	Levels	Values
Forecasting Method	fixed	4	Double Exponential Smoothing, Moving Average, Single Exponential Smoothing, Winters' Method
Country	fixed	10	Australia, China, India, Japan, Malaysia, Singapore, South Korea, Thailand, UK, USA

Analysis of Variance for MAPE, using Adjusted SS for Tests

Source	DF	Seq SS	Adj SS	Adj MS	F	P
Forecasting Method	3	1304.63	1304.63	434.88	33.69	0.000
Country	9	954.78	954.78	106.09	8.22	0.000
Error	27	348.54	348.54	12.91		
Total	39	2607.96				

S = 3.59292 R-Sq = 86.64% R-Sq (adj) = 80.70%

Table 2 The ANOVA table for the experiment which MAD was the response variable

General Linear Model: MAD versus Forecasting Method, Country

Factor	Type	Levels	Values
Forecasting Method	fixed	4	Double Exponential Smoothing, Moving Average, Single Exponential Smoothing, Winters' Method
Country	fixed	10	Australia, China, India, Japan, Malaysia, Singapore, South Korea, Thailand, UK, USA

Analysis of Variance for MAD, using Adjusted SS for Tests

Source	DF	Seq SS	Adj SS	Adj MS	F	P
Forecasting Method	3	5514109488	5514109488	1838036496	3.00	0.048
Country	9	1.05781E+11	1.05781E+11	11753497277	19.19	0.000
Error	27	16533643437	16533643437	612357164		
Total	39	1.27829E+11				

S = 24745.9 R-Sq = 87.07% R-Sq (adj) = 81.32%

From the analysis of variance (ANOVA) with Mean Absolute Percentage Error (MAPE) as a response variable in Table 1, it was found that forecasting method had a significant effect on the MAPE since the P-Value was less than the significance level of 0.05. Additionally, from the analysis of variance (ANOVA) with Mean Absolute Deviation (MAD) as a response variable in Table 2, the forecasting method had a significant effect on the MAD since the P-Value was less than the significance level of 0.05. According to the Randomized Complete Block Design (RCBD), the tourist nationality factor, which was classified by the nationality of tourists who visited and stayed in Bangkok, was a blocking factor [9]. It was not a factor to be analyzed in this research.

As shown in Figures 7 and Figure 8, the Main Effects Plots [10] for MAPE and MAD were used to analyze and determine the most appropriate forecasting technique to forecast the number of tourists for each target group, which were domestic tourists (Thai tourists), tourists from the People's Republic of China, Japan, South Korea, India, UK, USA, Singapore, Malaysia, and Australia who travelled and stayed in Bangkok.

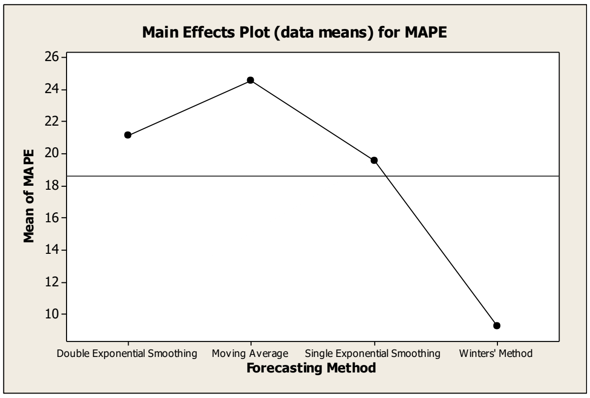

Figure 5 Main Effects Plot for MAPE

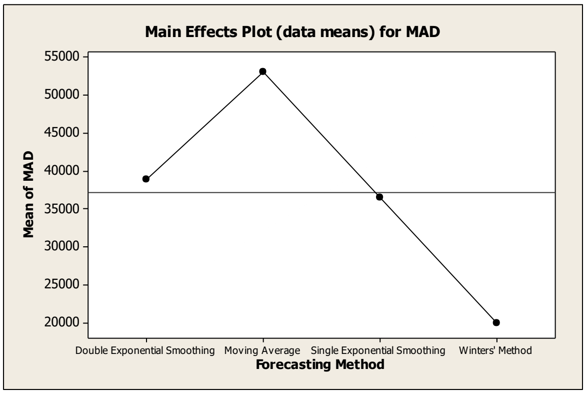

Figure 6 Main Effects Plot for MAD

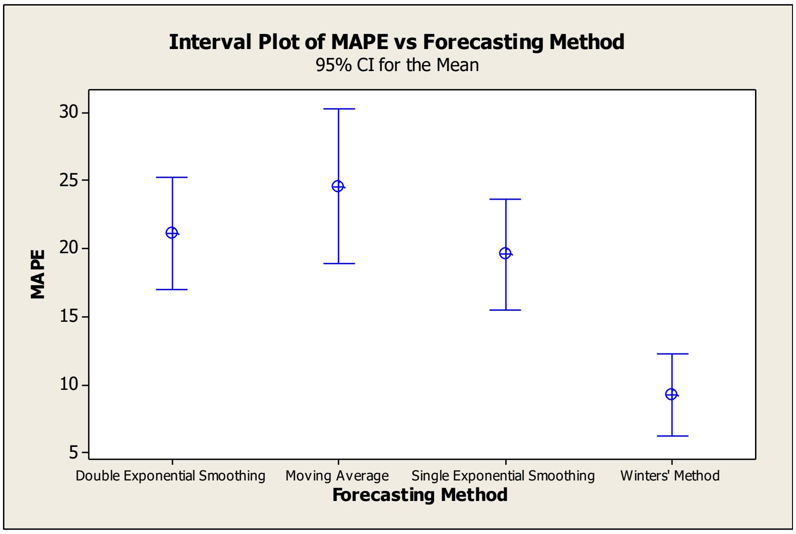

Figure 7 Interval Plot of MAPE for the most appropriate forecasting method analysis

From the Interval Plot graph to analyze the most suitable forecasting method in Figure 7, it was found that the 95% confidence interval of the Mean Absolute Percentage Error (MAPE) using the Winters' Method with a seasonal length of 12 months was the smallest value. In addition, the 95% confidence interval of the Mean Absolute Percentage Error (MAPE) using the Winters' Method and the 95% confidence interval of the Mean Absolute Percentage Error (MAPE) using other forecasting techniques were not overlapped. Therefore, the MAPE obtained from the Winters' Method forecasting with a seasonal length of 12 months was significantly lower than the MAPE obtained from other forecasting techniques. Due to the number of tourists in each target group, such as domestic tourists (Thai tourists), tourists from China, Japan, South Korea, India, UK, USA, Singapore, Malaysia, and Australia who visit and stay in Bangkok are cyclical or seasonal. Therefore, it can be concluded that the Winters' Method forecasting with a seasonal length of 12 months is the most appropriate forecasting method.

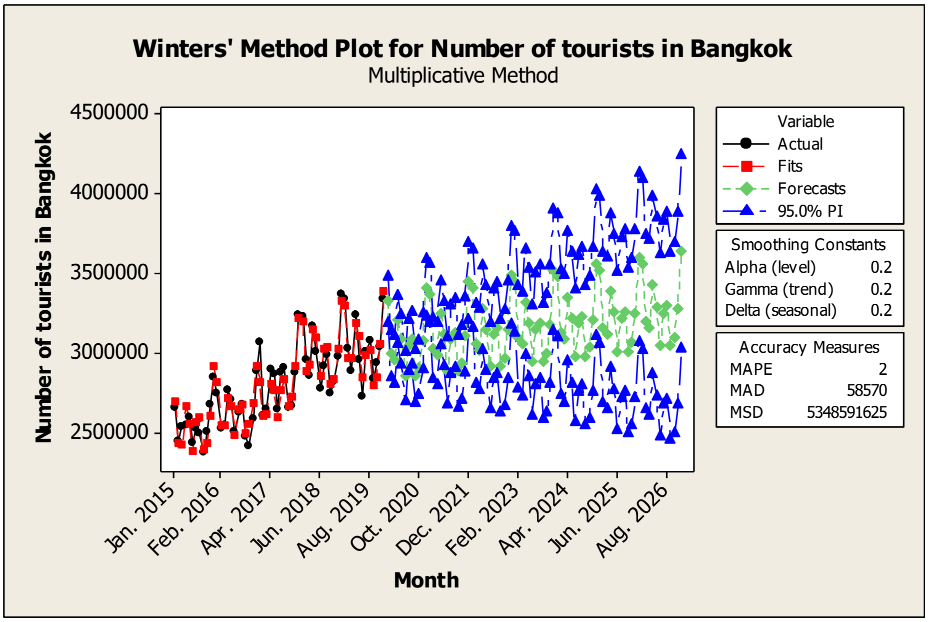

Figure 8 Winters' method plot for the number of tourists in Bangkok forecasting

According to Winters' method plot for the number of tourists in Bangkok forecast in Figure 8, in the forecasting of the number of Thai and foreign tourists visiting and staying in Bangkok in the next five years, 2022 – 2026 is highly accurate since the MAPE is 2% and the forecasting accuracy is 98%. The forecast of the number of Thai and foreign tourists in Bangkok in high season tourism in December 2026 was more than 3,600,000 travelers. The focus group was conducted for the number of tourists forecasting verification and validation. The comparative analysis of plan for providing accommodation (Supply Plan) was conducted by comparing the five-year forecasting values of accommodation supply to the accommodation demand of Thai and international tourists who visited and stayed in Bangkok. Data from the National Statistical Office's Accommodation Survey [11] were used prior to the COVID-19 pandemic during the years 2015 - 2019. The data included tourist demand for accommodation in Bangkok; length of stay; number of tourists per room; and accommodation supply. The forecasting values of pessimistic accommodation demand were attained by analyzing the length of stay during the COVID-19 outbreak as displayed in Figure 9. From Figure 9, the average accommodation demand of Thai and international tourists visiting and staying in Bangkok in situation where there is high demand (optimistic demand or demand under normal situation) is 8,222,720 man-days, while the supply capacity of all types of accommodation in Bangkok is 4,272,764 man-days. The optimistic demand is higher than the accommodation supply capacity at 3,949,956 man-days or 47.86%.

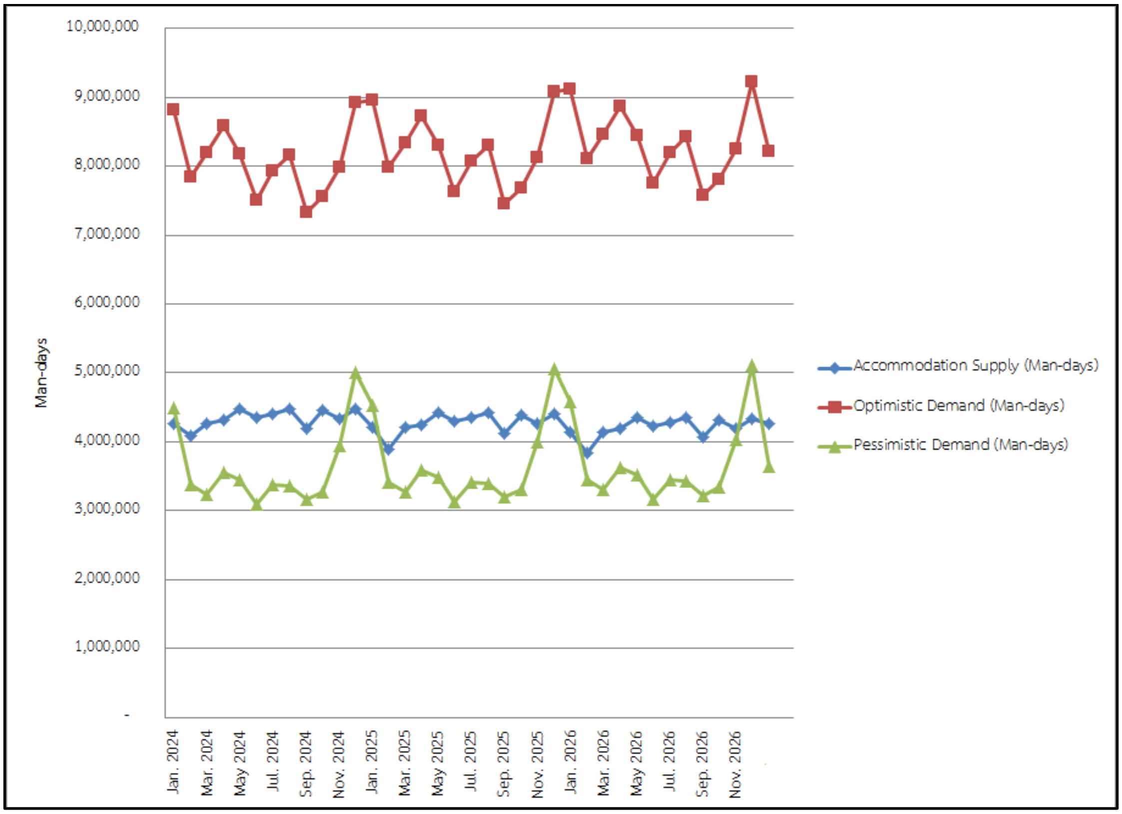

Figure 9 Comparative analysis of accommodation demand and supply forecasting (2024 – 2026) of Thai and International tourists in Bangkok

According to Figure 9, it can be found that the average accommodation demand of Thai and international tourists visiting and staying in Bangkok in situation where there is low demand (pessimistic demand or demand under COVID-19 situation which the DMHTT new normal action plan is necessary) is 3,649,048 man-days, while the supply capacity of all types of accommodation is 4,272,764 man-days. According to the announcement from Thailand Center for COVID-19 Situation Administration (CCSA) [12], DMHTT stands for D : Distancing, M : Mask Wearing, H : Hand Washing, T : Testing, and T : Thai Cha Na COVID-19 application. The pessimistic demand is higher than the accommodation supply capacity during the high season of the months of December and January at 10.12%. From the Figure 9, comparing between the optimistic demand/ the demand under the normal situation and the pessimistic demand/ the demand under COVID-19 situation (the new normal action plan is still implemented), the demand under the normal situation is higher than the demand under the COVID-19 situation with new normal action plan by 225%.

In between or after the COVID-19 situation, tourism is considered an important sector of Thai economy, with a total income of foreign tourists in 2019. In addition, tourists in Thailand spend more than 3,010 billion baht, so if Thai tourism can be promoted to improve the competitiveness, medical and wellness tourism will be a part of the wellness economy. The Thai tourism industry relies on it to attract high-paying tourists or high-end groups. The medical and wellness tourism that focuses on overall healthcare promotion as well as taking care of and preventing diseases will be an important opportunity to cope with the changes that will occur, and turn tourism back to being an important sector of the sustainable Thai economy again. This is in line with the country's policy to elevate Thailand towards quality tourism. It is of high value and attracts potential tourists, both Thais and foreigners.

The reasons why medical and wellness tourism is an important opportunity for Thailand are: (1) the overview of global medical and wellness tourism is of high quality and growing fast, with the medical and wellness tourism growth rate of 43% [13]. (2) Medical and wellness tourism can be a complementary activity to other types of tourism. Medical and wellness tourism accounts for 14% of the global tourism industry's value. (3) Medical and wellness tourism costs 61% more than general tourism. This group of tourists is a group with purchasing power and is willing to pay for new experiences. It also takes longer to travel for the medical and wellness tourism. (4) It is an extension of the potential of Thailand because Thailand has natural resources and a favorable culture, as well as strengths in service and tourism. In addition, Thailand's medical and wellness tourism is growing among the fastest in the world with an average growth of 13% per year.

Conclusions

In forecasting the number of tourists in each target group, which are domestic tourists (Thai tourists), tourists from China, Japan, South Korea, India, UK, USA, Singapore, Malaysia, and Australia who visited and stayed in Bangkok, it was found that the forecasting method had a statistically significant effect on the Mean Absolute Percentage Error (MAPE) and the Mean Absolute Deviation (MAD). The most appropriate forecasting technique with the smallest value of the MAPE and the MAD was the Winters' Method with a 12-month seasonal length. The comparative analysis of the accommodation supply plan was conducted by comparing the 2024 - 2026 forecasting values of accommodation supply to the accommodation demand of Thai and international tourists who visited and stayed in Bangkok. In a situation where there is high demand (optimistic demand or the demand under normal situation), the average accommodation demand of Thai and international tourists visiting and staying in Bangkok is higher than the supply capacity (optimistic demand over supply) at 3,949,956 man-days or 47.86%. In a situation where there is low demand (pessimistic demand or the demand under the COVID-19 new normal situation), the pessimistic demand is higher than the accommodation supply capacity (pessimistic demand over supply) during the high season of the months of December and January at 10.12%. Application of Thailand tourism and tourist accommodation promotion projects will increase the number of accommodation entrepreneurs and the number of rooms for tourists, and thus the accommodation demand and supply will be balanced efficiently. Therefore, the tourist hotel and guest house entrepreneurs should be promoted by tourist tax incentive projects, tourism promotion projects, Thailand tourism advertisement promotion, tax reduction, and soft loans for entrepreneurs to increase tourist accommodation capacity. In addition to medical and wellness tourism, Thai government should formulate policies to drive the successful healthcare tourism. Medical and wellness tourism is estimated to be around 10 million per year. The promotion projects of medical and wellness tourism by increasing the supply of medical and wellness tourism, supporting the needs of various groups of tourists and developing innovative medical research and new technologies should be conducted. These projects could increase the potential of Thailand medical and wellness tourism. Moreover, the COVID-19 vaccination is an important strategy for countries of main target group of tourists to minimize deaths, severe disease, curtail the health system impact, and fully resume socio-economic and tourism activity.

Acknowledgement

This research project was financially supported by Navamindradhiraj University Research Fund.

References

[1] Office of the Permanent Secretary, Ministry of Tourism and Sports. 2019. Thailand tourism statistics report for the year 2019. Ministry of Tourism and Sports, Bangkok.

[2] Montgomery, D.C. 2019. Design and Analysis of Experiments. John Wiley & Sons Inc., New York.

[3] Box, G.E.P., Jenkins, G.M., Reinsel, G.C. and Ljung, G.M. 2015. Time Series Analysis: Forecasting and Control.

[4] Makridakis, S.G., Wheelwright, S.C. and Hyndman, R.J. 1998. Forecasting: Methods and Applications. John Wiley & Sons Inc., New York.

[5] Pellerin, R. and Perrier, N. 2019. A review of methods, techniques and tools for project planning and control. International Journal of Production Research. 57: 2160–2178.

[6] Yu, P., Low, M.Y. and Zhou, W. 2018. Design of experiments and regression modelling in food flavour and sensory analysis: A review. Trends in Food Science & Technology. 71: 202-215.

[7] Dean, A., Voss, D. and Draguljic, D. 2017. Design and Analysis of Experiments. Springer, New York.

[8] Asilahijani, H., Steiner, S.H. and MacKay, R.J. 2010. Reducing variation in an existing process with robust parameter design. Quality Engineering. 22: 30–45.

[9] Montgomery, D.C. 2019. Introduction to Statistical Quality Control. John Wiley & Sons Inc., New York.

[10] Montgomery, D.C. and Runger, G.C. 2014. Applied Statistics and Probability for Engineers. John Wiley & Sons Inc., New York.

[11] National Statistical Office Thailand. 2020. The 2020 Accommodation Survey. National Statistical Office (NSO), Ministry of Digital Economy and Society, Bangkok.

[12] Center for COVID-19 Situation Administration (CCSA). 2020. Announcement from Center for COVID-19 Situation Administration (CCSA). Department of Disease Control, Ministry of Public Health, Bangkok.

[13] Global Wellness Institute. 2022. Global Wellness Trends Report: The Future of Wellness 2022. New York.

Thai Environmental Engineering Journal Vol. 36 No. 2 (2022) : 55-59
www.eeat.or.th

A Study of the Treatment Efficiency for the Ozonation Effluent Recycling Process in Cassava Starch Factory

Chitchanok Surawit[1], Sompop Sanongraj[2*], Wipada Dechapanya[2], Supatpong Mattaraj[2], Tiammanee Rattanaweerapan[2] and Karnika Ratanapongleka[2]

[1]Environmental Engineering Student, Department of Chemical Engineering, Faculty of Engineering, Ubon Ratchathani University, Ubon Ratchathani 34190, Thailand
[2]Faculty of Engineering, Ubon Ratchathani University, Ubon Ratchathani 34190, Thailand
[*]E-mail : sompop.s@ubu.ac.th

Abstract

The research was to determine the treatment efficiency for the ozonation effluent recycling process in cassava starch factory. Also, the flow rate entering the process was measured continuously during operating the process. In the process, there were mainly four major components: Section 1, effluent storage pond, Section 2, algae filtration system, Section 3 ozone tank and decomposing pond, Section 4 sedimentation tank and sand filter pond. From study results, it was found that the average flow rate entering the process was 197.86±5.23 m^3/hr. Effluent characteristics (before and after) of the ozonation effluent recycling process found that the average pH, total dissolved solid (TDS), chemical oxygen demand (COD) and the suspended solids (SS) were 9.19±0.03 and 8.13±0.03, 2,344±15.00 and 2,445±13.00 mg/l, 213±2.21. and 83±6.31 mg/l, and 112±5.87 and 15±4.39 mg/l, respectively. For COD and SS removal efficiency, the averaged percentages were equal to 61% and 87%, respectively. Overall, all parameters of the treated effluent passed the industrial effluent standard. However, the treated effluent was only used for washing raw cassava due to a quite high TDS. Therefore, a further study on a quality-improvement of the treated effluent, especially TDS, needs to be considered.

Keywords : recycling effluent; cassava; ozonation; starch factory; algae

Introduction

Water is an important resource that is necessary in the industrial sector. Therefore, it should be used for a maximum benefit. A tapioca starch factory is a type of a factory that produces a lot of wastewater (10-20 m^3/ton of starch production) [1]. A tapioca starch factory with the production capacity of 650 tons per day in Nakhon Ratchasima province has foreseen the importance of wastewater that occured. Within factory activities, various experiments have been conducted on reducing unnecessary wastewater as well as reusing the collected effluent. Typically, the factory has a wastewater treatment system using natural ponds (area of 1000 rai or 160 hectares) with no effluent drainage from the system. The factory intends to recycle the effluent collected from natural ponds back to use in the factory. In the natural wastewater treatment system, the effulent collected was from the last pond called C 6. There was a lot of algae (also algae smell) as shown in Figure 1. For laboratory-scale experiments, the factory tried to treat the effluent with a chemical oxidation method, in which the used of oxidizing agents such as chlorine compounds, ozone, and hydrogen peroxide. From the experimental results, it was found that the addition of ozone could treat the effluent satisfactorily and it did not produce any harmful residues according to other research papers [2-5]. Most of algae (represented in term of SS) in the effluent was significantly removed after ozonation and sedimentation (as well as its smell). Therefore, the factory conducted the ozonation effluent recycling process to treat the effluent from the final pond (C6) as shown in the overall flow diagram in Figure 2. The treated effluent characteristics were continuously analyzed and monitored.

Figure 1 Effluent Characteristic in C 6 Pond

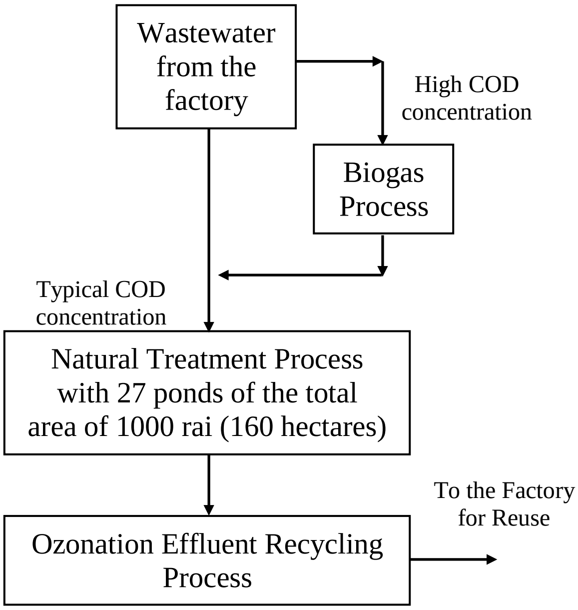

Figure 2 Overall Wastewater Flow Diagram of the Factory

Methodology

In the Ozonation effluent recycling process, there were mainly four major components: Section 1, effluent storage pond, Section 2, algae filtration system, Section 3 ozone tank and decomposing pond, Section 4 sedimentation tank and sand filter pond as shown in Figure 3.

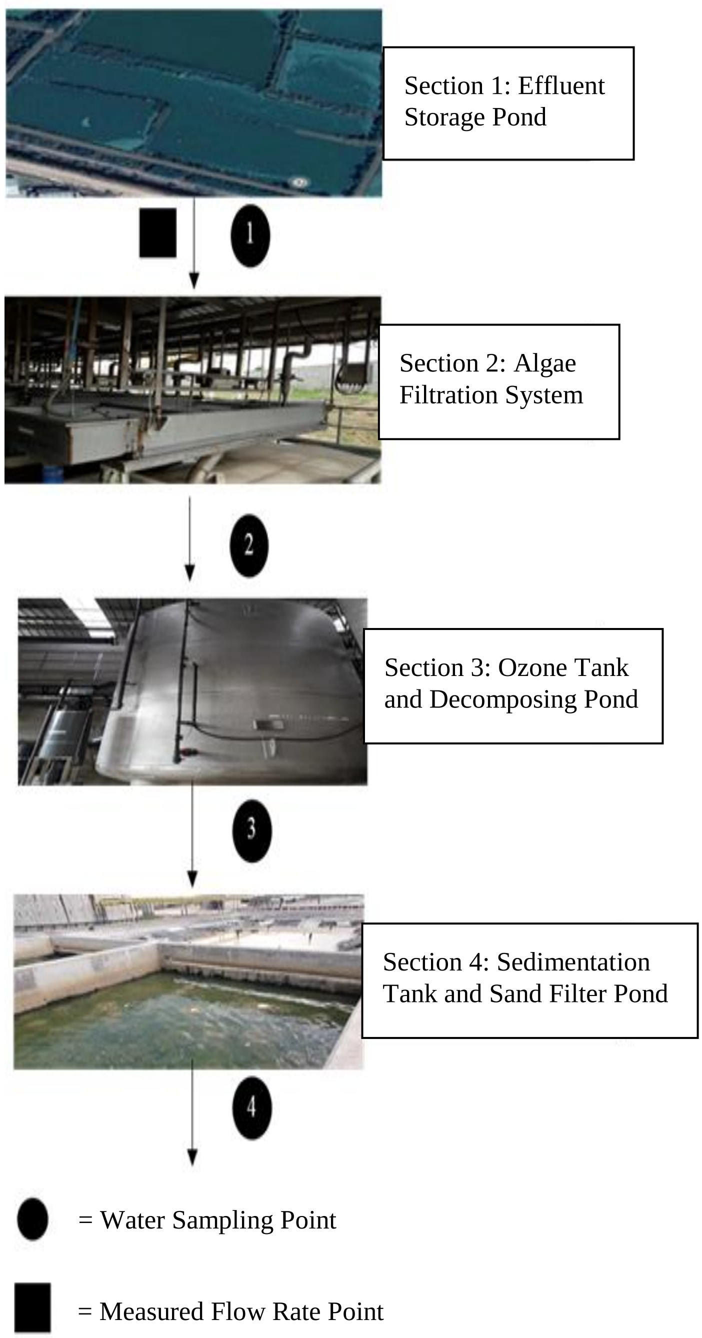

Figure 3 Effluent Recycling Process Components and Sampling Points

From Figure 3, Section 1: effluent storage pond (C6) has a volume capacity around 100,000 m^3 with < 2 m of depth. Typically, sunlight can shine through the bottom of the pond. There is a lot of algae in the pond as mentioned in Figure 1. Section 2: in order to get rid of algae initially, there are 20 units of algae filters using 60-80 µm nylon filter cloths (local material). Each filter unit has a dimension (width x length x height) of 1.20×3.40×0.45 m with controlled filtering velocity < 8 m/hr. Section 3: the ozone tank and decomposing pond (as shown in Figure 4) have volumes of 42 m^3 (contact time > 10 min.) and 192 m^3 (contact time > 30 min.), respectively. There are 2 units of ozone generators (Prominent, Germany) with a capacity of 630 gO_3/hr for each unit. Ozone dosage was automatically control using ORP controller (> 200 mV with pH of 6.5). Section 4: the sedimentation tank (as shown in Figure 5) has a volume of 4,000 m^3 (controlled overflow rate < 2 m/hr) and the sand filter with 100 m^2 of filtration (controlled filtering velocity < 8 m/hr).

For the ozonation effluent recycling process, flow rate entering the process and water characteristics of each section were determined every day for 7 weeks as shown in Figure 3. Analysis of water characteristics were performed followed the mothods as shown in Table 1 [6]. Due to focusing on algae removal, the parameters used to calculate the efficiency were focused on COD and SS only.

Results and Discussions

For the ozonation effluent recycling process, the average effluent flow rate (Qavg) were measured equalt to 197±5.23 m^3/hr (4,728 ± 125.52 m^3/day) as summarized in Table 2.

Figure 4 Decomposing Pond

Figure 5 Sedimentation Tank

Table 1 Analysis of Wastewater Characteristic Parameters and Methods

Parameters	Method
1. pH	pH Meter
2. COD (mg/l)	Close Reflux, Colorimetric Method
3. Suspended solid; SS (mg/l)	Gravimetric Method
4.Total dissolved sold; TDS (mg/l)	Gravimetric Method

Table 2 Flow Rate Entering to the Ozonation Effluent Recycling Process

Qavg, m^3/hr	Qmax, m^3/hr	Qmin, m^3/hr
197.86±5.23	254.25±9.84	71.37±3.78

Form Table 2, the effluent flow rate varies within a range of 71.37±3.78 m^3/hr (1,712 ± 90.72 m^3/day) to 254.25±9.84 m^3/hr (6,102 ± 236.16 m^3/day) during 7 weeks of operation. For each water sampling point (as shown in Figure 3), analytical parameter results were summarized as shown Table 3

Table 3 Analytical Parameter Results

Parameters	Water sampling point				Standards [3]
	1*	**2***	**3***	**4***	
pH	9.19±0.03	7.79±0.20	7.84±0.09	8.13±0.03	5.0-9.2
TDS, mg/l	2344±15.00	2407±27.59	2412±12	2445±13.00	<5,000
COD, mg/l	213±2.21	164±19.75	133±7.7	83±6.31	< 120
SS, mg/l	112±5.87	71±11.72	68±17.00	15±4.39	<30

From Table 3, it was found that the pH, TDS, COD and SS of treated effluent after the ozonation effluent recycling process were about 8.13, 2,445 mg/l, 82.83 mg/l, and 14.83 mg/l, respectively. All these parameters passed the industrial effluent standard [3]. There was no significant difference between TDSs (before and after) of effluent recycling process due to no TDS-removal units in the process. Therefore, there were no efficiency calculations for TDS. Removal efficiencies of COD and SS were calculated to be around 61% and 87%, respectively. This indicated that there was slightly amont of algae (also algae smell) in the treated effluent as expected. The treated effluent was fairly clear and had very little smell. However, it had a bit high concention of TDS due to a high concentration of the effluent at the beginning. Therefore, this treated effluent was only used for a general purpose such as washing raw cassava (this treated effluent can replace 100% of the original tap water used). On the basis of electricity cost, the operating cost of the treated effluent produced is approximately 5 baht per cubic meter. Although this operation cost is higher than the cost of production of the factory's own water supply. However, this ozonation recycling process can be used as an alternative to prevent flooding of stored effluent.

Conclusion

After the ozonation effluent recycling process, the treated effluent can be used back to the raw cassava washing step in the factory due to a bit high concentration of TDS and no direct disinfection unit. However, a further improvement of the treated effluent quality, especially for TDS and disinfection technology, needs to be conducted for factory’s activities that use higher water quality.

Acknowledgement

This research was partially supported by General Starch Company Limited corresponding to a co-op study with the Faculty of Engineering, Ubon Ratchathani University. We thank our colleagues who provided insight and expertise that greatly assisted the research,

References

[1] Kunlaya Rojpanit, et.al. 2017. Tapioca Flour Plant Wastewater Treatment with Isolated Effective Indigenous Bacteria from Wastewater. Thai Journal of Science and Technology, 6(2): 140-151.

[2] Gerrity et al. 2014. Applicability of Ozone and Biological Activated Carbon for Potable Reuse, Ozone: Science& Engineering, 36(2): 123-137.

[3] Gerrity et al. 2013. Potable reuse treatment trains throughout the world. Journal of Water Supply: Research and Technology AQUA, 62, 6.

[4] Margot et al. 2013. Treatment of micropollutants in municipal wastewater: Ozone or powdered activated carbon. Science of the Total Environment, 461-462C: 480-498.

[5] Lee et al. 2013. Prediction of Micropollutant Elimination during Ozonation of Municipal Wastewater Effluents: Use of Kinetic and Water Specific Information. Environmental Science and Technology. 47(11).

[6] American Public Health Association, American Water Works Association, and Water Environment Federation (2012) Standard method for the examination of water and wastewater. Ed.22, Washington, DC, USA.

[7] Ministry of Industry. 2017. Industrial Effluent Standards. Notification of Ministry of Industry. Thailand.

Thai Environmental Engineering Journal Vol. 36 No. 2 (2022) : 61-68
www.eeat.or.th

Health Risk Assessment of Toxic Metals in Different Types of Lettuce Leafy Vegetables Consumption in Bangkok

Zin Htoo Hlyan[1] and Penradee Chanpiwat[2*]

[1]International Program on Hazardous Substance and Environmental Management (IP-HSM), Graduate School, Chulalongkorn University, Bangkok 10330, Thailand
[2]Environmental Research Institute (ERIC), Chulalongkorn University, Bangkok 10330, Thailand
[*]E-mail : penradee.c@chula.ac.th

Abstract

The objectives of this study were to: 1) determine the levels of toxic metals, such as arsenic (As), cadmium (Cd), and lead (Pb) in lettuce leafy vegetables sold in Bangkok; and 2) determine any potential health risks associated with exposure to As, Cd, and Pb through consumption of lettuce leafy vegetables. A total of 120 lettuce samples named "red coral (RC)", "green oak (GO)" and "coral lettuce (CL)", which are grown in soil and hydroponic systems, were randomly collected from local fresh supermarkets in Bangkok. Inductively coupled plasma mass spectroscopy (ICP-MS) was used to determine the overall amounts of hazardous metals. The lettuce vegetables which were grown in soil, the total As, Cd, and Pb concentrations in CL, RC, and GO ranged from 0.02 to 0.26 mg/kg, 0.03 to 2.49 mg/kg, and 0.02 to 0.53 mg/kg, respectively. Total As, Cd, and Pb concentrations in CL, RC, and GO for the hydroponically grown lettuce vegetables ranged from 0.01 to 0.09 mg/kg, 0.02 to 0.42 mg/kg, and 0.01 to 0.31 mg/kg, respectively. According to the analysis results, the HI values in adults were significantly higher than ($p<0.05$) those of adolescents and children. Moreover, the HI values of metals through consumption of lettuce vegetables were predominantly dominated by Cd exposure. The HI values of metals were in the following order in the adult population: 3.92 for RC, 2.63 for CL, and 2.04 for GO grown in soil. In contrast, the HI values of hydroponically grown vegetables were in the following order in the adult population: 1.37 for RC, 1.27 for GO, and 0.17 for CL. The present result showed that the HI of metals were higher than 1 (HI>1), indicating an unacceptable level of adverse non-carcinogenic health effects for the population.

Keywords : Leafy lettuce vegetables; Arsenic, Cadmium and Lead; Health risk assessment

Introduction

Carbohydrates, vegetables and fruits, proteins, fats, and dairy are the five basic dietary groups for human well-being and should be consumed on a daily basis since each food offers particular nutritional benefits [1]. Vegetables and fruits are required in greater quantities than other foods such as meat, fish, and beans, as well as milk. In general, vegetables and fruits are beneficial to one's overall health [2]. Among various types of vegetables, leafy vegetables are important dietary components of essential and nutrient-dense foods for human health. Antioxidants, bioactive chemicals (A, C, E), and fibers are abundant in leafy vegetables to reduce the risk of dying prematurely and have a 70% lower risk of heart disease [3]. Consumption of raw and cooked vegetables on a regular basis is good for human growth and development [4] and the prevention of infectious diseases as well as the risk reduction of chronic diseases such as cancer, diabetes, and cardiac disease [5]. Vegetables, on the other hand, can absorb various chemicals and pollutants by root or foliar uptake and accumulate them in different parts of their crops [5]. Moreover, long-term exposure to Hg, As, Pb, and Cd, even at low levels, is widely established to have negative health impacts [6].

Metals in vegetables are being evaluated for potential health concerns in industrialized countries, despite the fact that just a few studies have been conducted in developing countries [7]. Therefore, there is growing interest in the research of toxic metal accumulations and their potential health hazards in humans through the ingestion exposure of leafy vegetable consumption. Particularly, Thailand is one of the developing countries that there have been limited studies on the determinations of toxic metals and the evaluations of their health hazards in foods, especially the leafy vegetables. This study was conducted to 1) determine the levels of toxic metals, such as (As Cd, and Pb) in salad lettuce leafy vegetables sold in Bangkok and 2) determine the potential human health risks of As, Cd, and Pb exposure via salad leafy vegetables consumption. This research is expected to ensure the safety of lettuce vegetable consumption in the Thai population which can be consequently beneficial to prevent public health from the exposure of toxicants through food ingestion.

Methodology

Samples collection

Regarding consumer preferences for leafy vegetable consumption, three different types of lettuce, "red coral (RC)", "green oak (GO)", and "coral lettuce (CL)" which were grown in the soil or hydroponic solution were collected during June-September 2021. RC (n = 40), GO (n = 40), and CL (n = 40) were randomly collected from local markets located in the representative areas of Bangkok. A total of 15 representative districts and 6 fresh supermarkets were chosen for sample collection based on number of registered population and market availability. Approximately 300 g of each vegetable was randomly collected and stored at 4 ^{o}C until sample preparation.

Samples preparation

All samples were washed to remove all soil particles and other residuals using deionized (DI) water at least three times. After that, the inedible parts were discarded. The remaining edible parts were air-dried at room temperature before being dried in a hot air oven at 60 ^{o}C for 48 hours. The moisture content was obtained after weighing the wet weight and dry weight of each sample. Then, each dried sample was ground into a fine powder with a commercial aluminum blender and passed through a 40-mesh (0.420 mm) sieve. Finally, the sample was stored in a desiccator until further analyses.

Samples digestion

Vegetable samples were digested following the US. EPA method. In brief, about 0.50 g of each dried sample was weighed into a 15-mL polyethylene tube. Then, 5 mL of 69% superpure nitric acid (HNO_3) and 5 mL of hydrogen peroxide (H_2O_2) were added into the tube. After that, the tube was capped and left in the hood at room temperature for 48 hours. To obtain a consistent solution, the sample solution was heated in a heating block at 80-90 °C for 15 minutes without boiling before being elevated to 95 °C and boiling for at least 4 hours. The additions of 2.5 mL of HNO_3 and 1.5 mL of H_2O_2 were added into the sample solution when the sample still had brown fume and bubbles. The digestion process was continued until a clear solution was obtained. After the digestion process, the sample was filtered through the Whatman No 40-filter paper. Afterward, 9 mL of deionized water (18.2 MΩ.cm, ELGA PURELAB Maxima) was added into a tube containing the acid digested solution for total metal analyses. This solution was stored at 4 °C until further analysis. The standard reference materials (SRM) of tomato leaf flour (NIST SRM 1573a) as well as blank samples were treated in the same manner as sample digestion to verify the accuracy of the digestion method. The acceptable recovery ranges of As and Cd were obtained (101%).

Instrumental analyses

The total concentrations of As, Cd, and Pb were analyzed by an inductively coupled plasma–mass spectrometry (ICP-MS) (Agilent 7500c, Tokyo, Japan). The SRM of trace elements in water (NIST SRM 1643e) was used to ensure the accuracy of the instrumental analyses. The acceptable recovery ranges of As and Cd were also obtained (97%).

Assessment of human health risk

The potential health risks to humans associated with long-term exposure to these three metals through ingestion of leafy vegetables were calculated using Eqs. 1 to 5.

ADD = (CV x IR x EF x ED) / (BW x AT) (Eq. 1)

Where, ADD is average daily dose (mg/kg·day), CV is concentration of metal in vegetable (mg/kg), IR is ingestion rate (kg·day), EF is exposure frequency (days/year), ED is exposure duration (years), BW is body weight (kg), and AT is average time (days). The input values for the constant variables which were used in this step are summarized in Table 1.

Table 1 Input parameters to characterize exposure values

Variable	Unit	Children (3 to 12.9 years)	Adolescents (13 to 17.9 years)	Adults (18 to 64.9 years)
ED	years	10	5	47
EF	days/year	365	365	365
AT (ED*365)	days	3650	1825	17155
BW [8]	kg	32.29	52.78	70
IR [9]	kg·day	0.00041	0.00086	0.00138

Next, the hazard quotient was estimated to assess the non-carcinogenic risk using Eq. 2.

Hazard quotient (HQ) = ADD / RfD (Eq. 2)

Where, RfD is oral reference dose and ADD is average daily dose (mg/kg. day)

Moreover, a hazard index (HI) following Eq. 3 was used to determine the potential risk to human health when more than one metal was ingested. An exposed population was at an unacceptable risk when HI was greater than or equal to 1.

$HI = HQ_{As} + HQ_{Cd} + HQ_{Pb}$ (Eq. 3)

For the cancer risk assessment, Eqs. 4 to Eq. 5 were used to evaluate the risk of cancer that may develop in human as a result of the ingestion exposure of carcinogen.

LADD = (CV x IR x EF x ED) / (BW x AT) (Eq. 4)

Where, LADD is lifetime average daily dose for cancer risk.

Cancer risk (CR) = SF× LADD (Eq. 5)

Where, SF is a slope factor of particular carcinogen. The values for potential human health risk assessment used in this study are summarized in Table 2.

Statistical analyses

ANOVA was used to determine the significant differences in the concentrations of As, Cd, and Pb accumulated in the different types of vegetables as well as within the same type of vegetable with different cultivation methods. In addition, the significant differences in the potential health risks were determined when more than one metal was ingested in the different groups of the population. A significant level of 0.05 was used in this study.

Results and Discussions

Total concentrations of As, Cd and Pb in different types of lettuce vegetables

Table 3 summarized the total concentrations of As, Cd and Pb contained in the lettuce leafy vegetables.

Table 2 Values of the oral reference dose (RfD) and slope factor (SF) of As, Cd and Pb [10]

Reference values for health effect endpoints	As	Cd	Pb
RfD (mg/kg·day)	3×10^{-4}	1×10^{-3}	3.5×10^{-3}
SF ((mg/kg·day))$^{-1}$	1.5	-	-

Table 3 Concentrations of As, Cd and Pb in lettuce leafy vegetables

Vegetable	Element	Soil cultivation					Hydroponic cultivation				
Red coral		Mini	Max	Mean	Median	SE	Mini	Max	Mean	Median	SE
(n=40)	As	0.01	0.19	0.06	0.04	0.01	0.01	0.10	0.04	0.04	0.00
	Cd	0.03	2.49	0.26	0.25	0.07	0.02	0.42	0.12	0.11	0.01
	Pb	0.02	0.47	0.19	0.13	0.02	0.02	0.29	0.09	0.08	0.01
Green oak (n=40)	As	0.01	0.08	0.04	0.04	0.00	0.01	0.06	0.03	0.03	0.00
	Cd	0.04	0.97	0.23	0.14	0.04	0.05	0.39	0.16	0.15	0.01
	Pb	0.02	0.53	0.15	0.13	0.02	0.01	0.31	0.14	0.15	0.01
Coral lettuce (n=40)	As	0.02	0.26	0.06	0.05	0.01	0.02	0.09	0.04	0.03	0.00
	Cd	0.02	0.98	0.18	0.12	0.03	0.06	0.20	0.11	0.11	0.00
	Pb	0.04	0.37	0.13	0.14	0.01	0.05	0.24	0.12	0.11	0.01
MOPH standard	As	2 mg/kg		Cd	0.2 mg/kg		Pb	0.1 mg/kg			
WHO standard	As	0.1 mg/kg		Cd	0.2 mg/kg		Pb	0.3 mg/kg			

Remark: SE is standard error, MOPH is Ministry of Public Health, WHO is World Health Organization

The total concentrations of As, Cd and Pb in three different types of lettuce leafy vegetables named RC, GO and CL are summarized in Table 3. It was found that As concentrations in RC, GO and CL leafy vegetables cultivated by both methods were lower than the Ministry of Public Health Thailand standard (2 mg/kg) [11]. There were no significant differences (p>0.05) in As concentrations in different types of vegetables from the different cultivation methods. In comparison to the World Health Organization's standard of 0.1 mg/kg [12], levels of As in RC and CL were higher than the standard, except GO, which was grown by soil cultivation. When compared to the regulated limits from MOPH and the WHO standard (0.2 mg/kg), it was found that total Cd concentrations in RC, GO, and CL leafy vegetables cultivated in soil were higher than both standards. The statistical analyses indicated significantly higher total Cd concentrations in the RC which was cultivated in the soil than those of other vegetables (p<0.05). In addition, Cd levels in RC grown in soil were about 1.5 times greater than GO and CL. All vegetables cultivated in a hydroponic system had higher Cd levels than the standard, except for CL. The total Pb concentrations in leafy vegetables cultivated by both methods were higher than the MOPH standard of 0.1 mg/kg [11]. In addition, when compared to the World Health Organization standard of 0.3 mg/kg [12], levels of Pb in RC, GO, and CL, which were grown by soil cultivation, were higher than the standard. With the exception of CL, the total Pb levels in vegetables that were hydroponically grown were within the WHO limit. Although the Pb contents in vegetables cultivated under two systems were higher than the MOPH standard, there were no significant differences (p>0.05) in Pb concentrations in different types of vegetables.

The findings of this study were also compared to those of salad leafy vegetables cultivated in soil reported in previous studies from different countries. Malan et al. [13] reported As concentrations of 1.50 to 4.14 mg/kg in lettuce grown at Philippi horticultural area, which were approximately four times higher than the results of this study. Chunhabundit [14] discovered that leafy vegetables which were obtained from Bangkok's major supermarkets and grocery stores, lettuce, had higher Cd levels than spinach. Farooq et al. [15] discovered that

Pb concentrations in lettuce and spinach grown in Pakistan's industrial districts ranged from 2.25 to 2.41 mg/kg, which was around 1.7 times higher than the Pb concentrations in the current study. Based on the results of total concentrations of all metals of interest found in lettuce vegetables in this present study, the concentration of each metal varied depending on the varieties of leafy vegetables. To begin with, for instance, the maximum As concentration was observed in CL, the maximum Cd concentration was found in RC, whereas the maximum Pb concentration was determined in GO.

This study showed that soil-cultivated vegetables typically contained higher total concentrations of all metals of interest than those of hydroponically grown vegetables. This can be explained by the fact that soil generally contains both essential and non-essential metals, including As, Cd, and Pb. There are several studies reported about metal contamination in agricultural soils. For example, soil samples from the Ayutthaya Province contained contamination levels of As, Cd, and Pb ranging from 0.26 to 1.4, 0.01 to 0.05, and 0.46 to 8.19 mg/kg, respectively, but all the amounts were below the Thai soil quality standard [16]. In addition, it might be the geological properties of soils and parent rocks, as well as anthropogenic activity, such as the application of chemical fertilizer, that can elevate the metal concentrations in soil to higher than natural levels. It was found that the lower pH in soil after nitrogen and phosphate fertilizer applications can cause metal desorption from the soil matrix and result in higher concentrations of As, Cd, and Pb in vegetables [17]. Moreover, agricultural soil pollution by metals is one of the most pressing challenges in China, according to Zhao et al. [3], but it also occurs in Pakistan [18], South Korea [19], India [20] and Serbia [21]). The research described above show that agro-ecosystem contamination is a worldwide problem that has an impact on healthy vegetable production.

Non-carcinogenic health risks from different lettuce leafy vegetables consumptions

1. Overall hazard index (HI) of leafy vegetables consumption

A hazard index (HI) was used to determine the overall potential non-carcinogenic risks to human health when all these three metals (As, Cd, and Pb) were ingested via the leafy vegetable's consumption. The summary of HI values is shown in Table 4. According to the analysis results, the HI values in adults were significantly higher than ($p<0.05$) those of adolescents and children. The present result showed that the HI of the metals was higher than 1 (HI>1), indicating an unacceptable level of adverse non-carcinogenic health effects for the population. The contribution of Cd to the overall HI values was approximately 70%. The HI values were in the following order in the adult population: 3.92 for RC, 2.63 for CL, and 2.04 for GO grown in soil cultivation. In contrast, the HI values of hydroponically grown vegetables were in the following order in the adult population: 1.37 for RC, 1.27 for GO, and 0.17 for CL. The present result showed that the HI of the metals was higher than 1 (HI>1), indicating an unacceptable level of adverse non-carcinogenic health effects for the population.

As a result of HI values greater than acceptable, several health impacts can be developed after long-term consumption of leafy vegetables. For example, the first signs of acute arsenic poisoning symptoms include vomiting, diarrhea, and stomach pain, and long-term exposure can lead to serious health problems like skin cancer [22]. Cadmium has a biological half-life of 10-35 years in humans, with the kidneys being the primary site of accumulation. Diabetes, renal disease, and heart attacks have all been linked to chronic cadmium exposure [23]. High Pb exposure has also been related to impacts on adult reproduction, including decreased sperm count in males and spontaneous abortion in women [24].

2. Carcinogenic health risks from different lettuce leafy vegetables consumption

The cancer risk values in all population groups via consumption of different leafy vegetables grown in different cultivation methods are summarized in Table 5. Since As is the only element which is classified as a Class A cancer according to EPA's Integrated Risk Information System (IRIS) [25], the results of the cancer risk assessment in the study were then evaluated only for the As exposure from the leafy vegetables consumption. The results showed that cancer risk (CR) of As exposure through the soil grown RC vegetable consumption in children, adolescents and adults ranged from 1.67×10^{-7}, 1.07×10^{-7} and 1.21×10^{-6}. In addition, the cancer risk of As exposure in the adult population through lettuce leafy vegetables consumption in this study was within acceptable (cancer risk $\leq 10^{-6}$). Therefore, it can be concluded all groups of the population are safe from cancer risk, though the vegetables are consumed on a daily basis.

Table 4 The values of hazard index (HI) through consumption of different lettuce leafy vegetables

Population	Element	Red coral		Green oak		Coral lettuce	
		Soil	Hydro	Soil	Hydro	Soil	Hydro
Children	As	0.13	0.08	0.07	0.06	0.17	0.08
	Cd	0.38	0.09	0.18	0.10	0.17	0.06
	Pb	0.03	0.02	0.03	0.02	0.03	0.02
	$HI=HQ_{As}+HQ_{Cd}+HQ_{Pb}$	0.54	0.19	0.28	0.18	0.36	0.16
Adolescents	As	0.08	0.05	0.05	0.04	0.11	0.08
	Cd	0.24	0.06	0.12	0.06	0.11	0.04
	Pb	0.02	0.01	0.02	0.01	0.02	0.01
	$HI=HQ_{As}+HQ_{Cd}+HQ_{Pb}$	0.34	0.12	0.19	0.11	0.23	0.13
Adults	As	0.94	0.61	0.51	0.40	1.22	0.58
	Cd	2.76	0.63	1.31	0.71	1.23	0.45
	Pb	0.22	0.13	0.22	0.16	0.18	0.14
	$HI=HQ_{As}+HQ_{Cd}+HQ_{Pb}$	3.92	1.37	2.04	1.27	2.63	0.17

Table 5 Cancer risk of As exposure though the different lettuce leafy vegetables consumption

Element	Population	Red coral		Green oak		Coral lettuce	
		Soil	Hydro	Soil	Hydro	Soil	Hydro
As	Children	1.67×10^{-7}	1.13×10^{-7}	1.03×10^{-7}	8.00×10^{-8}	1.65×10^{-7}	1.14×10^{-7}
	Adolescents	1.07×10^{-7}	7.25×10^{-8}	6.62×10^{-8}	5.13×10^{-8}	1.06×10^{-7}	7.31×10^{-8}
	Adults	1.21×10^{-6}	8.20×10^{-7}	7.49×10^{-7}	5.81×10^{-7}	1.20×10^{-6}	8.28×10^{-7}

Conclusion

This study observed the concentrations of As, Cd, and Pb in different types of lettuce vegetables that were sold in Bangkok's fresh markets at the representative areas. The total concentration of each metal was determined, and the health risk assessment was calculated to point out the potential health risk to the population through lettuce vegetable consumption. The concentrations of all metals in soil-grown leafy vegetables were consistently greater than those in hydroponically grown leafy vegetables. For instance, the maximum As concentration was found in soil-grown coral lettuce. Interestingly, red coral had the highest Cd concentration among the different types of vegetables for both cultivations. About 25% of all vegetable samples contained Cd and lettuce consumption was not safe for Cd exposure. The maximum Pb contents were found in green oak, which is grown in soil.

The hazard index (HI) values of metals through consumption of lettuce vegetables were predominantly dominated by Cd exposure. Adults are the group of people who may encounter non-carcinogenic health impacts more often than adolescents and children. According to the non-carcinogenic health risk calculation on the current study results, it is assumed the GO and CL are safe to eat every day rather than RC. For carcinogenic health risk, the cancer risk of As exposure in the population through lettuce consumption in this study was acceptable (cancer risk$\leq 10^{-6}$). Therefore, all groups of the population are safe from cancer risk even though they consume vegetables daily. According to the findings of this study, public awareness of the public health implications of metal contamination should be increased in order to ensure the safety of RC lettuce consumption. Moreover, practical and general recommendations should be introduced to reduce the metal's exposure via lettuce consumption.

Acknowledgement

This study was financially supported by International Program on Hazardous Substance Management (IP-HSM) and the Environmental Research Institute (ERIC) at Chulalongkorn University, Thailand. In particular, the authors would like to express their gratitude to the ERIC for providing laboratory facilities.

References

[1] Gupta, N., Yadav, K. K., Kumar, V., Krishnan, S., Kumar, S., Nejad, Z. D., Khan, M. M., & Alam, J. 2021. Evaluating heavy metals contamination in soil and vegetables in the region of North India: Levels, transfer and potential human health risk analysis. Environmental toxicology and pharmacology, 82, 103563.

[2] Aysha, M., Zakir, H., Haque, R., Quadir, Q., Choudhury, T. R., Quraishi, S., & Mollah, M. 2017. Health risk assessment for population via consumption of vegetables grown in soils artificially contaminated with arsenic. Archives of Current Research International, 10(3): 1-12.

[3] Zhou, H., Yang, W.T., Zhou, X., Liu, L., Gu, J.F., Wang, W.L., Zou, J.L., Tian, T., Peng, P.Q., & Liao, B.H. 2016. Accumulation of heavy metals in vegetable species planted in contaminated soils and the health risk assessment. International Journal of Environmental Research and Public Health, 13(3): 289.

[4] Ikem, A., & Egiebor, N. O. 2005. Assessment of trace elements in canned fishes (mackerel, tuna, salmon, sardines and herrings) marketed in Georgia and Alabama (United States of America). Journal of Food Composition and Analysis, 18(8): 771-787.

[5] Babandi, A., Ya'u, M., Muhammad Yakasai, H., Shehu, D., Babagana, K., Ibrahim, A., Anosike, C., & Ezeanyika, L. 2020. Non-carcinogenic and carcinogenic risk potentials of metals exposure from vegetables grown in Sharada industrial area Kano, Nigeria. Journal of Chemical Health Risks, 10(1): 1-15.

[6] Llobet, J., Falco, G., Casas, C., Teixido, A., & Domingo, J. 2003. Concentrations of arsenic, cadmium, mercury, and lead in common foods and estimated daily intake by children, adolescents, adults, and seniors of Catalonia, Spain. Journal of Agricultural and Food Chemistry, 51(3): 838-842.

[7] Baghaie, A. H., & Fereydoni, M. 2019. The potential risk of heavy metals on human health due to the daily consumption of vegetables. Environmental Health Engineering and Management Journal, 6(1): 11-16.

[8] FAO. 2012. National survey on thai people Food and Agricultural Organization.

[9] MOAC. 2009. National Bureau of Agricultural Commodity and Food Standards. Ministry of Agriculture and Cooperatives.

[10] EPA. 2011. Integrated risk information system. Environmental Protection Agency.

[11] MOPH. 2020. Standards for Contaminants in Food. Ministry of Public Health (No 414) B.E. 2563.

[12] WHO. 2020. Standards for Contaminants in Foods. World Health Organization (WHO).

[13] Malan, M., Müller, F., Cyster, L., Raitt, L., & Aalbers, J. 2015. Heavy metals in the irrigation water, soils and vegetables in the Philippi horticultural area in the Western Cape Province of South Africa. Environmental Monitoring and Assessment, 187(1): 1-8.

[14] Chunhabundit, R. 2016. Cadmium exposure and potential health risk from foods in contaminated area, Thailand. Toxicological Research, 32(1): 65-72.

[15] Farooq, M., Anwar, F., & Rashid, U. 2008. Appraisal of heavy metal contents in different vegetables grown in the vicinity of an industrial area. Pakistan Journal of Botany, 40(5): 2099-2106.

[16] Kladsomboon, S., Jaiyen, C., Choprathumma, C., Tusai, T., & Apilux, A. 2020. Heavy metals contamination in soil, surface water, crops, and resident blood in Uthai District, Phra Nakhon Si Ayutthaya, Thailand. Environmental Geochemistry and Health, 42(2): 545-561.

[17] Wångstrand, H., Eriksson, J., & Öborn, I. 2007. Cadmium concentration in winter wheat as affected by nitrogen fertilization. European Journal of Agronomy, 26(3): 209-214.

[18] Jadoon, W. A., & Malik, R. N. 2019. Geochemical approach for heavy metals in suburban agricultural soils of Sialkot, Pakistan. SN Applied Sciences, 1(2): 1-11.

[19] Kang, M.-J., Kwon, Y. K., Yu, S., Lee, P.-K., Park, H.S., & Song, N. 2019. Assessment of Zn pollution sources and apportionment in agricultural soils impacted by a Zn smelter in South Korea. Journal of Hazardous Materials, 364, 475-487.

[20] Kaur, I., Gupta, A., Singh, B. P., Sharma, S., & Kumar, A. 2019. Assessment of radon and potentially toxic metals in agricultural soils of Punjab, India. Microchemical Journal, 146, 444-454.

[21] Spahić, M. P., Manojlović, D., Tančić, P., Cvetković, Ž., Nikić, Z., Kovačević, R., & Sakan, S. 2019. Environmental impact of industrial and agricultural activities to the trace element content in soil of Srem (Serbia). Environmental Monitoring and Assessment, 191(3): 1-22.

[22] Argos, M., Kalra, T., Rathouz, P. J., Chen, Y., Pierce, B., Parvez, F., Islam, T., Ahmed, A., Rakibuz-Zaman, M., & Hasan, R. 2010. Arsenic exposure from drinking water, and all-cause and chronic-disease mortalities in Bangladesh (HEALS): a prospective cohort study. The Lancet, 376(9737), 252-258.

[23] WHO. (2010). Exposure to cadmium: a major public health concern. World Health Organization (WHO).

[24] Zheng, N., Wang, Q., & Zheng, D. 2007. Health risk of Hg, Pb, Cd, Zn, and Cu to the inhabitants around Huludao Zinc Plant in China via consumption of vegetables. Science of the Total Environment, 383(1-3): 81-89.

[25] EPA, U. S. 2011. Carcinogenic health risks, Integrated Risk Information System. United State Environmental Protection Agency (EPA).

Thai Environmental Engineering Journal Vol. 36 No. 2 (2022) : 69-77
www.eeat.or.th

DBPs Formation by Chlorination and Chloramination of Water and Treated Water at Short and Long Reaction Times

Krittaporn Sitham[1], Suthatip Sinyoung[1] and Charongpun Musikavong[2,3*]

[1]Department of Civil and Environmental Engineering, Faculty of Engineering,
Prince of Songkla University, Songkhla 90112, Thailand
[2]Environmental Assessment and Technology for Hazardous Waste Management Research Center,
Department of Civil and Environmental Engineering, Faculty of Engineering,
Prince of Songkla University, Songkhla 90112, Thailand
[3]Center of Excellence on Hazardous Substance Management (HSM), Bangkok 10330, Thailand
[*]E-mail : mcharongpun@eng.psu.ac.th, charongpun@gmail.com

Abstract

This work investigated disinfection by-products formation potential (DBPFP) by chlorination and chloramination. Raw water was collected from the U-Tapao canal, Songkhla, Thailand. This work used poly aluminum chloride (PACl) of 15 mg/L and aluminum chlorohydrate (ACH) of 1 percent w/v in coagulation experiments. DBPFPs were conducted on raw water and PACl-treated water and ACH-treated water at 1-day and 7-day reaction times. The raw water had a turbidity of 31.3 NTU and a DOC of 2.52 mg/L. The turbidity was reduced by PACl and ACH to levels below the water supply standard. DOC was reduced by 27 and 32 percent by PACl and ACH, respectively. The most prominent DBPFP found in chlorinated and chloraminated samples was trihalomethane formation potential (THMFP). THMFP levels of 171 and 425 µg/L were detected in the chlorinated raw water after 1-day and 7-day reaction times, respectively. In the chloraminated raw water, THMFP of 4.7 and 8.5 µg/L were detected, respectively. At 1-day reaction time, iodo-trihalomethane formation potential (I-THMFP), haloacetronitrile formation potential (HANFP), and trichloronitromethane formation potential (TCNMFP) of the chlorinated raw water were higher than that of the chloraminated raw water. At 7-day reaction time, I-THMFP of the chlorinated raw water was higher than that of the chloraminated raw water. HANFP and TCNMFP of the chlorinated raw water were lower than that of the chloraminated raw water. PACl and ACH are capable of lowering DBPFP, particularly THMFP and I-THMFP, in chlorinated water and HANFP in chloraminaed water. For treated water at 1-day and 7-day reaction times, chlorination had a greater impact on THMFP and I-THMFP than chloramination. The HANFP of chlorinated samples was higher than that of chloraminated samples after 1-day reaction time, whereas the HANFP of chloraminated samples was higher than that of chlorinated samples after 7-day reaction time.

Keywords : Aluminum chlorohydrate; Dissolved organic carbon; Haloacetronitriles; Halonitromethanes; Polyaluminium Chloride; Trihalomethanes

Introduction

Disinfection is an essential process at a drinking water treatment plant (WTP) that ensures the stability of microorganisms in the water supply as it passes though the water distribution system to the water consumer. Disinfectants such as chlorine and chloramine are commonly used in WTPs. The interaction between free chlorine residual and dissolved organic matter (DOM) in raw water and treated water is the most important factor for disinfection by-products (DBPs) formation during disinfection [1]. The components of DOM have a direct impact on the types of DBPs formation. Dissolved organic carbon (DOC) can form carbonaceous DBPs like trihalomethanes (THMs) when it reacts with disinfectants [2, 3]. In addition, the reaction of dissolved organic nitrogen (DON) with disinfectants can result in nitrogenous DBPs like haloacetonitriles (HANs) and halonitromethanes (HNMs) [2, 4, 5]. Chlorine is widely used for disinfection in Thailand and other countries.

The types of disinfectants can affect the formation of DBPs.The United States is now turning to chloramine as a tap water disinfectant instead of chlorine because it has a lesser risk of creating disinfection by-products (DBPs) than chlorine [6]. However, the formation of DBPs linked to chloramine, such as dihalo-acetonitriles, *N*-nitrosodimethylanine (NDMA), THMs, and dihaloacetic acid, can occur when chloramine reacts with DOM [7]. In the chloramination process, however, the inorganic chloramines monochloramine (NH_2Cl), di-chloramine ($NHCl_2$), and trichloramine (NCl_3) usually are detected. THMs, haloacetic acids (HAAs), haloaldehydes, haloacetamides, haloacetronitriles (HANs), and halonitromethanes can be formed when chloramines react with dry deposition particulate matter (HNMs) [8].

Coagulation is a common method for reducing turbidity in raw water. Coagulation has the potential to reduce DOC and color. A low dose of polyaluminium chloride (PACl) of 5-6 mg/L and aluminum chlorohydrate (ACH) of 1 percent w/v can reduce turbidity and color while also slightly lowering the potential for disinfection by-product formation (DBPFP) [9]. The type of coagulant used can affect pollutant removal performance. In this study, PACl and ACH were used as coagulants.

The U-Tapao canal in Songkhla, Thailand is used as the raw water source for three WTPs in Songkhla. The canal receives water from the Sadao reservoir and wastewater and treated wastewater from the community, agricultural, and industrial activities along the canal [3, 10]. The water qualities of the U-Tapao canal have presented with high turbidity and high color. This is caused by DOM, inorganic matter, plankton, and other microscopic organisms. The three WTPs use coagulation, sedimentation, filtration, and disinfection to remove suspended solids, colloids, color, and pathogenic microorganisms. The coagulant is PACl, and chlorine is used in the disinfection process. The remaining DOM in treated water can react with disinfectants to form DBPs. In addition, the most important considerations in the formation of DBPs are disinfection types and reaction times. The goal of this study is to compare the formation potential (FP) of THMs, iodo-trihalomethanes (I-THMs), HANs, and HNMs in raw water from the U-Tapao canal and treated water by PACl and ACH at 1-day and 7-day chlorination and chloramination.

Material and Methods

Sampling Sites and Sample Collection

Raw water from WTP was collected from the U-Tapao Canal, Songkhla, Thailand in January 2021 to determine its characteristics. The coagulation and disinfection experiments were then carried out using the raw water. All samples were stored at or below 4 ºC until analysis and experiments.

Experimental Procedure

The experimental procedure consisted of three parts. The first step was to determine the properties of the raw water, which included pH, alkalinity, turbidity, color, ultraviolet adsorption at 254 nm (UV-254), and DOC. The second part was the coagulation experiments. This work used PACl and ACH in the coagulation experiments using a jar-test apparatus. We used the optimal dosage of

PACl and ACH for turbidity reduction by coagulation from previous work. The optimal dosages of PACl [11] and ACH [9] were 15 mg/L and 1 percent w/v, respectively. The optimal dosage of turbidity was selected because the WTP operation mostly emphasizes turbidity reduction due to the perception of water consumers. As a results, the amount of coagulant used at WTPs must reduce turbidity to lower than the water supply standard. We set the jar-test apparatus for rapid mixing at 100 rpm for 1 minute and then on slow mixing at 60 rpm for 8 minutes, 40 rpm for 8 minutes, and 25 rpm for 5 minutes, respectively. pH was controlled at 6.8-7.2 by sodium hydroxide and sulfuric acid addition. After a 30-min rest period, the supernatant was measured for its turbidity and color. The treated water was measured for its pH, alkalinity, turbidity, color, UV-254, and DOC. The raw water and treated water were filtered by GF/F filter prior to the analyses of DOC and UV-254.

In the third experiment, the filtered raw water and treated water were used in the test. We used chlorine and chloramine as disinfectants. This work conducted the experiments in triplicate and used sodium hypochlorite solution for chlorination. We freshly prepared the chloramine (NH_2Cl) solution by adding NaOCl at the Cl_2:N mass ratio of 5:1 at pH 7-8.5 for 30 min and this was used in chloramination [12].

The experiments were conducted with the reaction times of one day and seven days. During the reaction times, the pH was kept constant at 7±0.2. At the end of the reaction times, free chlorine residuals of 3-5 mg/L for chlorinated samples [13] and monochloramine residuals of 1-3 mg/L for chloraminated samples [14] were measured.

We extracted the DBPs with methyl tert-butyl ether (MTBE); purity was 99.9% with 4-bromofluorobenzene as an internal standard [15]. The extraction conditions were modified from a previously reported procedure [16]. We mixed 17.5 μL of internal standard into 35 mL of water sample. After thoroughly shaking the sample, 7 mg sodium sulphate anhydrous, 1 mg copper (II), and 1 mg sulfate 5-hydrate were added. Then we added 2 mL of MTBE and shook for 1 minute. We collected MTBE in vials at a top layer of 2 mL and stored it below 4 °C before GC analysis. The GC conditions are described in more detail elsewhere [2]. This work analyzed four THMs species consisting of trichloromethane or chloroform (TCM), bromodichloromethane (BDCM), dibromochloromethane (DBCM), and tri-bromomethane (TBM), five I-THMs species consisting of dichloroiodomethane (DCIM), bromochloroiodomethane (BCIM), bromodi-iodomethane (BDIM), chlorodiiodomethane (CDIM), and triiodomethane (TIM), four HANs species consisting of trichloroacetonitrile (TCAN), dichloroacetonitrile (DCAN), bromo-chloroacetonitrile (BCAN), and dibromo-acetonitrile (DBAN), and one HNMs (trichloronitromethane, TCNM) of the disinfected samples at one day and seven days reaction times.

Analytical Methods

The pH was directly measured using a HACH pH meter. Alkalinity was determined following the standard method 2320 B (Titration method). Turbidity and color were measured by a turbidity meter and UV/VIS spectrophotometer. We carried out DBPFP for chlorinated and chloraminated samples, including THMs, I-THMs, HANs, and HNMs, which were determined according to the standard method 5710B [13], except for the level of monochloramine residuals for chloraminated samples, we followed the recommendation from the previous work [14].

Results and Discussion

Characteristics of Raw Water and Treated Water

Raw water characteristics are important in selecting the best approach to improve water quality. The pH and alkalinity of the raw water were 6.4 and 20 mg/L, respectively indicating that coagulation could be used for treating the raw water. Water consumers are commonly concerned about turbidity and color. The WTP must reduce turbidity and color to lower than the drinking water standard. The turbidity and color of the raw water were 31.3 NTU and 30.6 Pt-Co (Table 1), respectively. The turbidity value was higher than the standard of

4 NTU [17]. DOC and UV-254 in raw water were detected at 2.52 mg/L and 0.144 cm^{-1}, respectively. Raw water from the U-Tapao Canal had DOC and UV-254 values of 3.7-5.6 mg/L and 0.100-0.284 cm^{-1}, respectively [9, 18]. In this study, the DOC of raw water was lower than in previous studies. UV-254 was within the UV-254 range reported in previous work.

Using a 15 mg/L PACl and a 1 percent w/v ACH, the turbidity was reduced to below the Provincial Waterworks Authority standard of 4 NTU. Color was reduced from 30.6 Pt-Co to 3.67 Pt-Co (88 percent reduction) and 2.45 Pt-Co (92 percent reduction) using PACl and ACH coagulation, respectively. In terms of turbidity and color reduction, the PACl and ACH coagulations performed similarly. When it came to surrogates for DOM reduction, the ACH coagulation had a 32 percent reduction in DOC and a 67 percent reduction in UV-254, respectively. This was slightly higher than the 27 percent and 58 percent reductions in DOC and UV-254 by PACl coagulation, respectively. This finding was consistent with a previous study [9], which found that ACH coagulation at 1 percent w/v performed better on UV-254 and DOC reduction than PACl coagulation at 5-6 mg/L. Concerning the capacity of the coagulation process in five raw water sources in Japan, PACl coagulation-filtration reduced DOC and UV-254 by 29 to 65 percent and 63 to 84 percent, respectively [19]. Regarding the findings of this work and previous research, the coagulation process is more effective at reducing DOM with an aromatic character, as indicated by the UV-254 value.

DBPs Formation after Disinfection Process

The DBPFPs after 1 day of chlorination and chloramination is shown in Fig.1. For the raw water (untreated), PACl-treated water, and ACH-treated water after chlorination, THMFP of 171, 63.5, and 53.7 µg/L, were determined, respectively. The levels of I-THMFP, HANFP, and TCNMFP in the raw water (untreated), PACl-treated water, and ACH-treated water were less than 8 µg/L or not detected. In all the chlorinated water samples, TCM was the most prevalent THMs species. TCM distributions of 83, 71, and 56 percent were detected in the raw water, PACl-treated water, and ACH-treated water, respectively. DCIM, BDIM, and TIM were found in the raw water for I-THMs species, but only BDIM was found in the PACl-treated water and only DCIM in the ACH-treated water. For HANs species, TCAN, DCAN, and DBAN were found in the raw water. After PACl and ACH coagulation, only DCAN was detected in both water samples. The raw water and PACl-treated water both produced TCNM, but ACH-treated water did not.

THMFP levels in raw (untreated) water, PACl-treated water, and ACH-treated water were 4.7, 4.8, and 4.4 µg/L for chloramination, respectively. The levels of I-THMFP, HANFP, and HNMFP in the aforementioned water samples were less than 1 µg/L or not detected. (Fig 1). For THM species, only TCM was found in the raw water, PACl-treated water, and ACH-treated water. In the case of I-THM species, DCIM was detected in the water samples after PACl and ACH coagulation but not in the raw water. Only DCAN was found in the raw water for HAN species, but not in the PACl-treated or ACH-treated water. TCNM was found in all the water sample tests.

Table 1 Characterization of raw water and treated water

Parameters	Units	Raw water	Treated water	
			PACl (15 mg/L)	ACH (1 percent W/V)
Turbidity	NTU	31.3±0.5	2.5±0.2	0.97±0.4
Color	Pt-Co	30.6±0.1	3.67±0.07	2.45±0.20
DOC	mg/L	2.52±0.01	1.84±0.06	1.71±0.14
UV-254	cm^{-1}	0.144±0.002	0.061±0.005	0.047±0.011

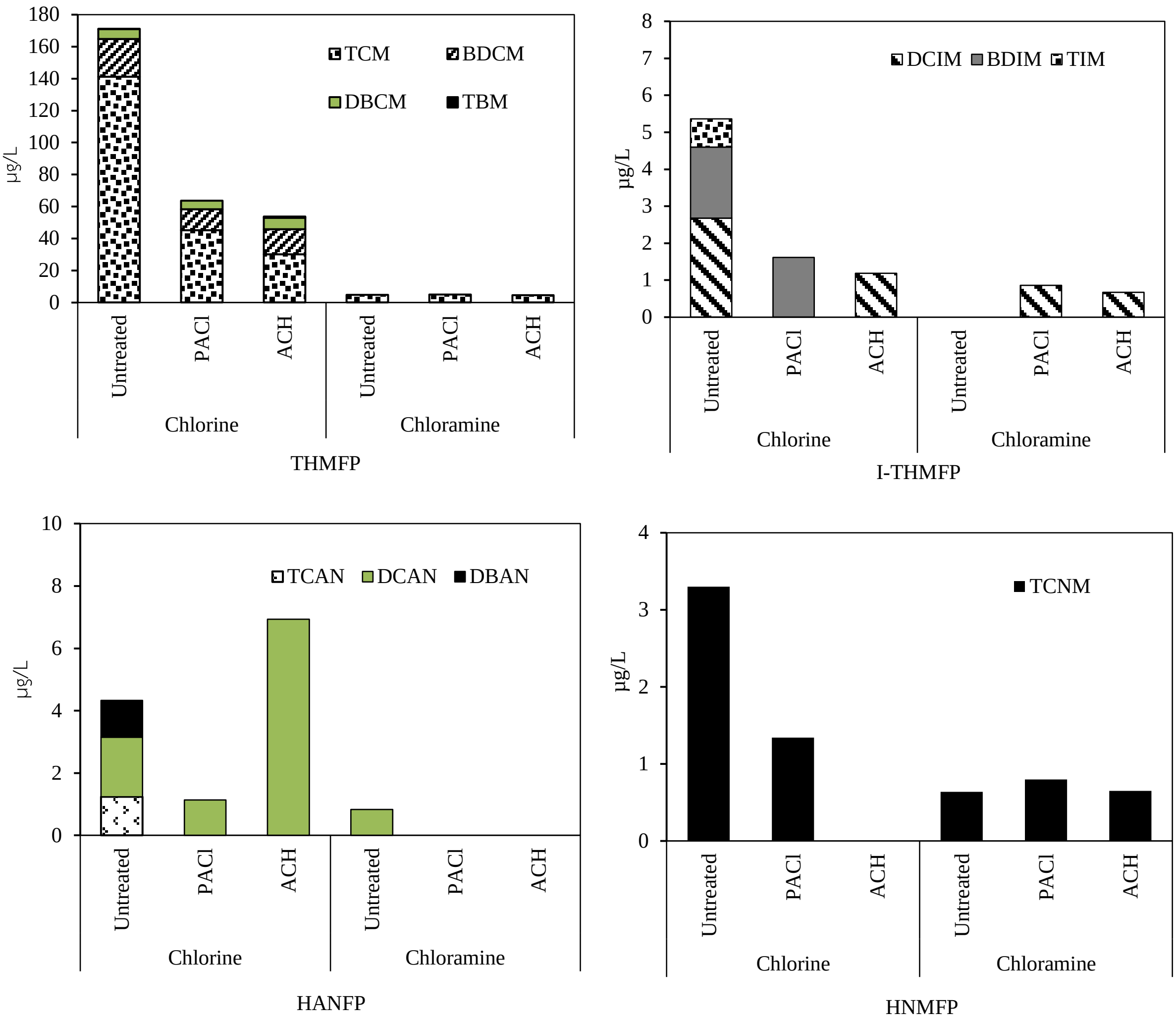

Fig. 1 DBPs formation during chlorination and chloramination after 1-day reaction time

The chlorination affected the formation of DBPs more than chloramination. THM concentrations were 36, 13, and 12 times higher in raw water, PACl-treated water, and ACH-treated water, respectively, than in chloramination with a one-day reaction time. THMFP by chlorination was detected in treated water in Japan using PACl coagulation-filtration with scales ranging from 30 to 150 μg/L, whereas less than 1 to around 5 μg/L of THMFP was produced by chloramination. This result was in accordance with a prior investigation; chloramination significantly decreased the formation potential of THMs [19]. With a one-day reaction time, chlorination produced higher concentrations than chloramination for I-THMs and HANs.

Taking into account the reduction of DBPFP by PACl and ACH coagulation at the day reaction time, after 1 day chlorination, THM and I-THM formation in PACl-treated water was slightly higher than in ACH-treated water. THMs and I-THMs formation were reduced by 63 and 70 percent, and 69 and 78 percent, respectively, when PACl and ACH coagulation were used. The PACl coagulation and filtration process reduced overall total THMFP of five raw water samples in Japan by 46 percent [19]. When using the PACl coagulation, the formation of HANs in PACl-treated water was reduced by 74 percent, while it was detected in higher concentrations than in the raw water when using ACH with chlorination. The formation of TCNM was reduced by 59 and 100 percent in the PACl-treated and ACH-treated waters, respectively. Coagulation can decrease the formation of THMs, I-THMs, HANs, and TCNM. After 1 day of chloramination, a few THMs, HANs, and TCNM were formed. This is similar to the one-day chlorination process, in which the formation of THMs, I-THMs, and TCNM in ACH-treated water was were slightly lower than in the PACl-treated water, whereas HAN formation was not detected in either the PACl-treated water or ACH-treated water.

The DBPFPs of chlorination and chloramination after 7 days of reaction time are shown in Fig.2.Chlorination had a greater effect on the formation of THMs and I-THMs than chloramination, which was similar to the formation of these DBP species after one day. In contrast to the formation of HANs after one day, chloramination had a greater effect on HAN formation than chlorination. At 7-day chlorination, THMFP of 425, 417, and 166 μg/L, I-THMFP of 24.3, 4.4, and 0.66 μg/L, HANFP of 5.1, ND, and 1.3 μg/L, HNMFP of 0.85, 3.7, and 3.8 μg/L were measured in the raw water (untreated), PACl-treated water and ACH-treated water, respectively.

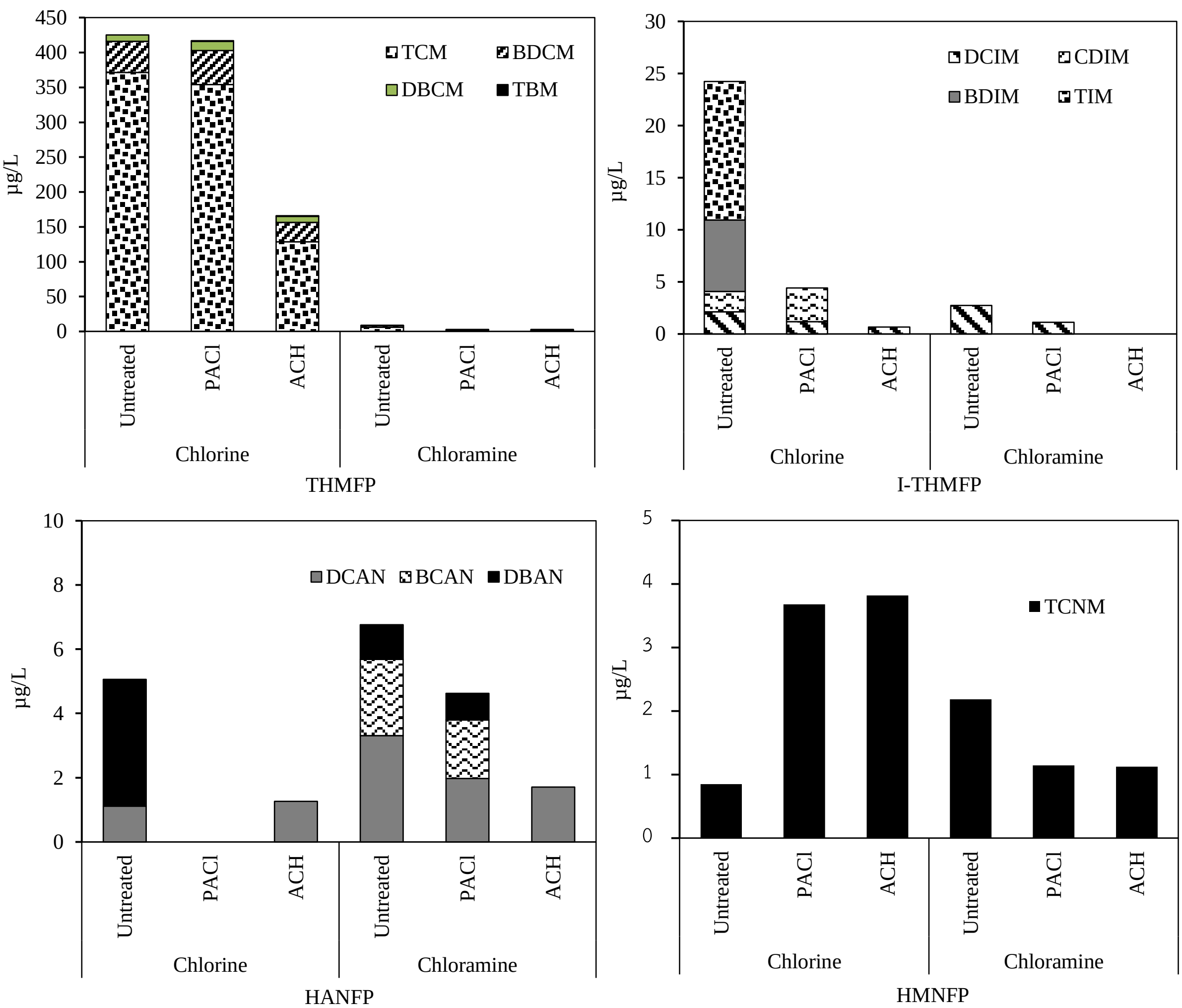

Fig. 2 DBPs formation during chlorination and chloramination after 7-day reaction time

TCM was the major THM species found in all the chlorinated water samples, like these samples after one-day reaction time. TCM distributions of 88, 85, and 78 percent were determined in the raw water, PACl-treated water, and ACH-treated water, respectively. From one day to seven days after chlorination, THMFP levels in the raw water, PACl-treated water, and ACH-treated water increased 2.5, 6.6, and 3.1 times, respectively. DCIM, CDIM, BDIM, and TIM were found in the raw water, CDIM and BDIM were found in the PACl-treated water, and only DCIM was found in the ACH-treated water for I-THMs species. At 7 days of chlorination, CDIM was the only I-THM species found in the raw water and PACl-treated water, but not at one day. TCAN is a HAN species that was detected after one day of chlorination but not after seven days, whereas DCAN was detected at a level that was incomparable to one day and DBAN was detected at a level that was higher than one day of chlorination. DCAN was detected in the ACH-treated water at levels that decreased over time. HAN species were not found in the PACl-treated water. In the PACl-treated water and ACH-treated water, TCNM was detected at a higher level than in one day of chlorination.

At 7 days after starting the reaction, the formation of DBPFPs via the chloramination process was considered. THMFP concentrations of 8.5, 2.8, and 2.6 µg/L, I-THMFP concentrations of 2.8, 1.1, and ND. µg/L, HANFP concentrations of 6.8, 4.6, and 1.7 µg/L, and HNMFP concentrations of 2.2, 1.2, and 1.1 µg/L were determined in the raw water, PACl-treated water, and ACH-treated water, respectively. TCM and BDCM were found in all the samples, while DBCM was found in both the raw and PACl-treated water. TCM in the raw water increased slightly compared to one day, whereas TCM in the PACl-treated water and ACH-treated water decreased compared to one day, while BDCM and DBCM were formed for the first time after 7 days of chloramination. Only DCIM was found in the water samples from I-THM species, as well as in one day of chloramination. More species that could not be detected in one day were formed after 7 days of chloramination in the case of HAN species, including BCAN, and DBAN. TCNM formation was detected at a higher level in all the water samples than in the samples taken one day after chloramination.

After 7 days of reaction time, THMs, and I-THMs could be produced at a higher concentration by chlorination than chloramination. Chlorination of raw water, PACl-treated water, and ACH-treated water produced 50, 149, and 63 times higher THM concentrations than chloramination, respectively. Chlorination formed higher concentrations than chloramination for I-THMs formation with a seven-day reaction time. Interestingly, the amount of HANs produced by chloramination was greater than that produced by chlorination.

After chlorination, THMs and I-THMs were formed at lower levels in the ACH-treated water than in the PACl-treated water. THMFP levels in the PACl-treated and ACH-treated water were reduced by 2 and 61 percent, respectively. I-THMFP levels in the raw water were reduced by 82 percent using PACl coagulation, and I-THMFP could be removed by 97 percent using ACH coagulation. PACl coagulation could completely remove HANs, whereas ACH coagulation was found to reduce 75 percent of HANFPs, respectively.

Considering the reduction of DBPFP by PACl and ACH coagulation after 7 days of chloramination, THMs and I-THMs formation were reduced by 67 and 69 percent, when PACl and ACH coagulation were used, respectively. I-THMFP levels in the raw water were reduced by 59 percent using PACl coagulation. ACH coagulation could completely remove I-THMFP. HANFP levels in the PACl-treated and ACH-treated water were reduced by 46 and 75 percent, respectively. TCNMFP could be reduced by 48 and 49 percent using PACl and ACH coagulation, respectively. In reduced levels of THMs and I-THMFP, ACH coagulation performs better than PACl coagulation.

Conclusion

The turbidity of raw water from U-Tapao, Songkhla, Thailand was found to be 31.3 NTU and the DOC was 2.52 mg/L. Turbidity was reduced to levels below the water supply standard of 4 NTU using PACl of 15 mg/L and ACH of 1 percent w/v. With PACl and ACH, DOC was reduced by 27 and 32 percent, respectively. The most prominent DBPFP found in the chlorinated and chloraminated samples was THMFP. THMFP levels of 171 and 425 µg/L were detected in the chlorinated raw water after 1-day and 7-day reaction times, respectively. In the chloraminated raw water, THMFP of 4.7 and 8.5 µg/L were detected. At 1-day reaction time, the I-THMFP, HANFP, and TCNMFP of the chlorinated raw water were greater than that of the chloraminated raw water. At 7-day response time, I-THMFP, HANFP, and TCNMFP of the chlorinated raw water were 24.3, 5.1, and 0.85 µg/L, respectively, whereas those of the chloraminated raw water were 2.8, 6.8, and 2.2 µg/L. PACl and ACH are capable of lowering DBPFP, particularly THMFP and I-THMFP, in chlorinated raw water and HANFP in chloramined water. ACH coagulation reduced DBPFPs more effectively than PACl coagulation. For treated water at 1-day and 7-day reaction times, chlorination had a greater impact on THMFP and I-THMFP than chloramination. At 7-day reaction time, the TCNMFP of treated water of the chlorinated sample was higher than that of chloraminated sample. The HANFP of the chlorinated samples was higher than that of chloraminated samples after 1-day reaction time, whereas the HANFP of the chloraminated samples was higher than that of the chlorinated samples after 7-day reaction time. Due to the lower level of DBPFP than chlorination, chloramination might be used as the disinfection process of a water treatment plant. The formation of HANs in treated water may be prevented by a one-day reaction period after chloramination.

Acknowledgement

This research was funded by the Center of Excellence on Hazardous Substance Management (HSM), Bangkok, Thailand, under contract number HSM-PJ-CT-18-20. The authors would also like to express their gratitude to the Faculty of Engineering at Prince of Songkla University, Hat Yai Campus for their assistance with the equipment.

References

[1] Wang, Q.F., Shao, Y.S., Gao, N.Y., Liu, S.S., Dong, L., Rao, P.H., Chu, W.H., Xu, B., An, N. and Deng, J. 2020, Impact of zero valent iron/persulfate preoxidation on disinfection by-products through chlorination of alachlor, Chem. Eng. J. 380.

[2] Phatthalung, W.N. and Musikavong, C. 2019, Emerging disinfection by-products' formation potential in raw water, wastewater, and treated wastewater in Thailand, Journal of Environmental Science and Health, Part A, 54(8): 2019. 745-758.

[3] Musikavong, C., Srimuang, K., Tachapattaworakul, T. and Suksaroj, S.C. 2016. Formation of trihalomethanes of dissolved organic matter fractions in reservoir and canal waters. J. Environ. Sci. Health A. 51(9):782-791.

[4] Goslan, E.H., Seigle, C., Purcell, D., Henderson, R., Parsons, S.A., Jefferson, B. and Judd, S.J. 2017. Carbonaceous and nitrogenous disinfection by-product formation from algal organic matter. Chemosphere. 170:1-9.

[5] Zhai, H., He, X., Zhang, Y., Du, T., Adeleye, A.S. and Li, Y. 2017. Disinfection byproduct formation in drinking water sources: A case study of Yuqiao reservoir. Chemosphere. 181: 224-231.

[6] Schwarz. 2005. Directed assistance module no. 4 chloramine disinfection and dbp control.

[7] Poleneni, S.R. 2020. Recent research trends in controlling various types of disinfection by products in drinking water: detection and treatment. Disinfection By-produtcs in Drinking Water. 337-370.

[8] He, J., Wang, F., Zhao, T., Liu, S. and Chu, W. 2020. Characterization of dissolved organic matter derived from atmospheric dry deposition and its DBP Formation. Water Research 171: 115368.

[9] Sitham, K., Choonual, T., Musikavong, C. and Sinyoung, S. 2022. Utilizing Polyaluminum Chloride (PACl) and Aluminum Chlorohydrate (ACH) for Treating Raw Water and DBPs Formation, Suranaree J. Sci Technol, In press.

[10] Musikavong, C. and Wattanachira, S. 2013. Identification of dissolved organic matter in raw water supply from reservoirs and canals as precursors to trihalomethanes formation, Journal of Environmental Science and Health. Part A. 48: 2013. 760-771.

[11] Keawchouy, S. 2021. Treatment of silver nanoparticles microplastic and disinfection by-products in raw water from U-Tapao canal by coagulation and membrane filtration, Master Thesis, Prince of Songkla University.

[12] Zhang, T-Y., Lin, Y-L., Xu, B., Cheng, T., Xia, S-J., Chu, W-H. and Gao, N-Y. 2016. Formation of organic chloramines during chlor (am)ination and UV/chlor(am)ination of algae organic matter in drinking water. Water Research. 103:189-196.

[13] APHA. 1998. Standard Methods for the Examination of Water and Wastewater, 20th Ed.; American Public Health Association, AWWA and WEF: Washington DC. 1998.

[14] Louisiana Department of Health, Chloramination Recommendations For Public Water Systems That Chloraminate : 1-3.

[15] US.EPA. 2003. Determination of chlorination disinfection by-products, chlorinated solvents, and halogenated pesticides/herbicides in drinking water by liquid-liquid extraction and gas chromatography with electron-capture detection, Methods 551.1. Office of research and development, Cincinnati, Ohio 45268. USA.

[16] Song, H., J.W., Addison., Hu, J. and Karanfil, T. 2010. Halonitromethanes formation in wastewater treatment plant effluents. Chemosphere 79: 174-179.

[17] Provincial Waterworks Authority. 2011. Water supply standard according to WHO year 2011.

[18] Jaichuedee, J., Wattanachira, S., Musikavong, C. 2020. Kinetics of the formation and degradation of carbonaceous and nitrogenous disinfection by-products in Bangkok and Songkhla source water. Science of the Total Environment. 708: 134888.

[19] Sakai, H., Tokuhara, S., Murakami, M., Kosaka, K., Oguma, K. and Takizawa, S. 2015. Comparison of chlorination and chloramination in carbonaceous and nitrogenous disinfection byproduct formation potentials with prolonged contact time.

Thai Environmental Engineering Journal

Aims and Scope

Thai Environmental Engineering Journal is published 3 times a year by Environmental Engineering Association of Thailand in aims of provide an interdisciplinary platform for the disseminating recent research work in Environmental field. The journal's scope includes:

- Treatment Processes for Water and Wastewater
- Air Pollution and Control
- Solids and Hazardous Wastes Management
- Site Remediation Technology
- Water Resource Management; Surface water and Groundwater
- Environmental Management Protection and Conservation
- Impact Assessment of Pollution and Pollutants
- All areas of Environmental Engineering and Sciences

Frequency; 3 issues per year, every four months at April, August and December

Information for Authors

Manuscript submitted for publication should be of high academic merit and have never before, in whole or in part, been published elsewhere and will not be published elsewhere, except in abstract form. Manuscripts, parts of which have been previously published in conference proceeding, may be accepted if they contain additional material not previously published and not currently under consideration for publication elsewhere.

Submission of Manuscripts

All manuscripts should be submitted in https://www.tci-thaijo.org/index.php/teej/index

Manuscript Format and Style

Text format

Manuscript should be prepared using a text processing software such as Microsoft Word for windows. A4 size paper is conventionally accepted. Margins set up (in Page set up Menu) are outlined as follow.

Top Margin 3.0 cm., Bottom Margin 3.0 cm.
Left margin 2.5 cm., Right Margin 2.5 cm.

Title, author co-authors, address of correspondence and abstract are included in the first section while the remainder of paper is to appear in the second section. The total pages including figures, tables and references should not exceed 10 pages.

Font, font size & typeface

Times New Roman font type is required for Thai text and English text. Font size [Pica] for various text function are tabulated as follow.

Text functions	Font = Times New Roman	
	Pica Size**	Typeface
Title [English]	16 [CT]	Bold
Author & Co-authors	11 [CT]	Bold
Address of correspondence	11 [CT]	Normal
Abstract heading	12 [LRJ]	Bold
Abstract & Main Texts	11 [LJ]	Normal
Section Heading & Number*	12 [LJ]	Bold
Subsection Heading & Number	11 [LJ]	Bold

* Including "Abstract" "Acknowledgement" and "References"
** CT = Centre Text, LJ = Left Justified, LRJ = Left & Right Justified

Title

All titles of manuscript should be short and precise; long title should be condensed whenever possible (not more than 42 characters). Title should be printed with every first letter of every word capitalized, excluding prepositions and articles. Directly below the title, author should print their full names (first name then family name), address and institution. E-mail of corresponding author and between 3-5 key words should also be provided.

Abstract

Abstract should be provided on separate sheets and be not more than 300 words. International contributor who are unable to provide an abstract in Thai may submit an English abstract alone.

Style Guidelines

Units of measurement should be indicated in SI units throughout.

Tables

Tables and figures should be numbered with Arabic numerals, in order in which they are cited in the text. The table's titular heading should concisely detail the content of the table and include units of measure for all numerical data.

Format of Research Paper

The format of research paper is listed as follows:

1) Title
2) Author
3) Abstract
4) Introduction
5) Materials and Methods
6) Results and Discussion
7) Conclusions
8) References

References

The references section at the end of the manuscript should list all and only the references cited in the text in numberical order, with references given in Thai first and those in English following. In this section, the names of all authors should be provided if more than six, or the first three followed by *et. al.*

Reference to a journal article:

List all authors when six or fewer; when seven or more list only the first three (3) and add *et. al.* Titles of articles from academic journals should be listed in full and begin with a capital letter.

[1] Inthorn, D., Sidtitoon, N., Silapanuntakul, S. and Incharoensakdi, A. 2002. Sorption of mercury, cadmium and lead in aqueous solution by the use of microalgae. Science Asia. 28(3): 253-261.

Reference to article or abstract in a conference proceedings:

[1] Inthorn, D., Singhakarn, C. and Khan, E. Decolorization of reactive dyes by pre-treated Flute reed (phargmites karka (Retz)). At 34th Mid-Atlantic Industrial & Hazardous Conference, Annual Mid Atlantic Industrial and Hazardous Waste Conference at Rugers University, New Jersey, USA on September 20-21, 2002.

Reference to a book:

[1] Polprasert, C. 1996. Organic Waste Recycles. John Wiley & Sons Inc., New York.

Reference to article in a conference proceedings:

[1] Inthorn, D. Heavy metal removal. In: Kojima, H. and Lee, Y.K. Photosynthetic Microorganisms in Environmental Biotechnology, Springer-Verlag, 2001; 111-135.

Reference to an electronic data source:

Use the above format and supply the complete URL as well as the access date.

Subscription Form
Thai Environmental Engineering Journal

Date____________________

Name____

Address____

____

____

____

____

Tel:______________ Fax:______________E-mail:_____________________________

A subscription to the Thai Environmental Engineering Journal is request for_____year (1,000 Baht/year for 3 Volume)

Signature____________________________

(____________________________)

Payment by "Environmental Engineering Association of Thailand"

- ❍ Bank Transfer: Savings Account No. 053-1-24040-3, Bank of Ayudhya Plc., Klong Prapa Branch
- ❍ Bank Transfer: Savings Account No. 056-2-32298-0, Siam Commercial Bank Plc., Aree Sampan Branch

Environmental Engineering Association of Thailand
122/4 Soi Rawadee, Rama VI Rd., Phayathai,
Phayathai, Bangkok 10400
Tel: +66 (0) 2617-1530-1 Fax: +66 (0) 2279-9720
E-mail: teej@eeat.or.th Website: http://www.eeat.or.th

THAI
ENVIRONMENTAL ENGINEERING JOURNAL

Environmental Engineering Association of Thailand (EEAT)

ISSN (PRINT) : 1686 - 2961
ISSN (ONLINE) : 2673 - 0359

Vol. 36 No. 2 May – August 2022